national accelerator laboratory

TM-421
0428

SOME PRELIMINARY CONCEPTS ABOUT THE PROPOSED ENERGY DOUBLER DEVICE FOR THE 200/500 GEV PROTON ACCELERATOR AT THE UNITED STATES NATIONAL ACCELERATOR LABORATORY BATAVIA, ILLINOIS

Edited by:

P. J. Reardon & B. P. Strauss

May, 1973

Operated by Universities Research Association Inc. Under Contract with the United States Atomic Energy Commission

CORRECTION PAGE

Chapter V, Page 3, Line 13

for NbTi d = 40μ, where ξ = density, To = $-Jc(\partial Jc/\partial T) = Tc/2$,

TM-421
0428

Some Preliminary Concepts About The Proposed Energy Doubler Device For the 200/500 GeV Proton Accelerator At The United States National Accelerator Laboratory Batavia, Illinois

Edited By:
P. J. Reardon & B. P. Strauss

CONTRIBUTORS

National Accelerator Laboratory

G. Biallas	M. A. Otavka
R. Cassel	P. J. Reardon
D. A. Edwards	D. E. Richied
W. Fowler	S. Snowden
W. Hanson	B. P. Strauss
H. Hinterberger	D. F. Sutter
W. W. Lee	L. C. Teng
R. McCracken	R. R. Wilson

Cryogenics Consultants, Inc.

H. Daly	P. Vander Arend

Magnetic Corporation of America

Z. J. J. Stekly	R. Thome

TABLE OF CONTENTS

I. Introduction
P. J. Reardon

II. The Doubler As An Accelerator
D. A. Edwards

III. The Doubler As A Storage Ring
L. C. Teng

IV. Magnetic Field Considerations
S. Snowden, K. Lee, P. J. Reardon, Z. J. J. Stekly

V. Wire Selection For Present Energy Doubler Dipole
B. P. Strauss, P. J. Reardon

VI. Dipole Construction
G. Biallas, W. Hanson, H. Hinterberger,
J. O'Meara, R. McCracken

VII. The Cryogenic System For the Proposed NAL Energy Doubler
W. Fowler, P. Vander Arend

VIII. Tests Of The First Energy Doubler Prototype Models
B. P. Strauss, P. J. Reardon, D. Sutter,
R. McCracken, D. Richied, M. A. Otavka

IX. Power Supply Considerations
R. Cassel, P. J. Reardon

AI. Excerpt Of A Statement By Robert R. Wilson, Director, National Accelerator Laboratory, Before The Joint Committee On Atomic Energy

AII. Computations In Support Of Design Effort On Mark II Dipoles: S4B and P6C
Z. J. J. Stekly, R. J. Thome

AIII. Cryogenic Cooling Of Superconducting Magnets For The NAL Energy Doubler System
P. C. Vander Arend, H. F. Daley, Jr.

AIV. Pressure Drops In The Magnet System Of The NAL Energy Doubler System
P. C. Vander Arend, H. F. Daley, Jr.

AV. Heat Transfer Between High Pressure And Low Pressure Boiling Helium Streams Of The NAL Energy Doubler System
P. C. Vander Arend, H. F. Daley, Jr.

Chapter I

INTRODUCTION

P. J. Reardon

R. R. Wilson, from the earliest days of the project to design and construct the now operating 200/500 GeV U.S. National Accelerator, at Batavia, Illinois, decided that in the final design of the enclosure, the structural support system for the 200/500 GeV synchrotron magnet, and the lay-out of the service buildings which contain the power supplies and cooling system for the magnets, provision be made for the later addition of a ring of superconducting magnets and the refrigeration system to cool them. The initial concept for this device was that it would consist of an accelerator using superconducting magnets which would be placed in the same enclosure as our present 200/500 GeV accelerator and that it would raise the energy of the protons from 500 GeV to 1,000 GeV, thereby placing the NAL accelerator in the forefront of high energy physics research for the indefinite future. We are now also considering the use of the device as a storage ring and as an alternate to the provision of energy storage equipment which might otherwise need to be added to our present power supply for operation above 300 GeV. As originally intended, this new ring would be placed into our four mile line Main Ring enclosure and may work in the dc mode as a storage ring

at magnetic fields of 9 kG to 45 kG or as an accelerator where the energy of the beam would be increased from 200 GeV to a top energy of 1,000 GeV. In this latter case, the pulse rate of any intermediate energy between 200 and 1,000 GeV, i.e., 9 kG, would be no faster than one pulse per minute.

The present features of the installed synchrotron reflect this earlier decision; adequate space is available to add a ring of superconducting magnets with a circular cross-section of about 12 inches above or below the present ring of conventional magnets (with modification to the Injection, Extraction, Experimental, and RF equipment in the long straight sections) or at the top of or near the top side of the enclosure (see Figure 1) and to add liquid helium refrigeration and transfer systems in the present service buildings. (Figure 2) This decision having been implemented (even to the extent of leaving a foundation for the new ring on the present magnet structure) and the announcement by R. R. Wilson of his intention to request authorization to build such a device within the $250 million authorized for the project should funds be remaining at the completion of the present facilities, in his testimony before the United States Joint Congressional Committee on Atomic Energy during the hearings on the proposed FY 72 Budget for the High Energy Physics Program by the AEC's Division of Research - (Appendix I) no experimental work, (apart from a conceptual model of a superconducting quadrupole magnet with a 1" bore and a gradient of 10 kG inch constructed by R. Oram, R. Sheldon, and B. Strauss) on the energy doubler device was done until the Fall of 1972.

On September 1, 1972, R. R. Wilson established an informal working group to consider the various technical questions which would have to be resolved in order to develop the energy doubler concept. This group of about ten people met twice a week throughout the Fall of 1972 and through their efforts the fabrication of the first two models which have now been tested was begun and the work to set up a test loop of the proposed refrigeration system to be located in the old Protomain Service Building in the Village was started. On December 21, 1972, after detailed discussions with URA and approval by URA of the concept, NAL requested that they be authorized by the AEC to proceed with a definitive design effort that would include the construction and testing of prototype magnet systems to be located in the Protomain Tunnel in the NAL Village, in order that a report on the design and feasibility tests would be available in the early Spring of 1974. The AEC formally approved this concept in February, 1973. In the meantime on January 5, 1973 R. R. Wilson authorized the establishment of a small (10 people) Energy Doubler Group to be headed by P. J. Reardon as part of the existing Accelerator Section. This group would be responsible for the coordination of the design, the installation and tests of the prototype magnets including their refrigeration system and the preparation of the report mentioned above. The accelerator physics and system questions would be done by the existing Accelerator Section and the engineering and fabrication of the magnets and their support system would be done by the Technical Services Section both on a part time basis and at a level of activity that would not jeopardize the

much more pressing goals of the project, namely, to operate the accelerator at a higher degree of reliability, to improve the intensity and to conduct the comprehensive research program underway with greater efficiency. The effort would be augmented by outside consultants as required in order to keep the effort of the NAL Staff at a level consistent with their other responsibilities. The consultants used so far are Cryogenic Consultants, Inc., working with W. Fowler of the NAL Bubble Chamber group, the Magnetic Corporation of America working with S. Snowden of Accelerator Theory Group, and John Purcell of Argonne National Laboratory. Other Consultants may be used in the future depending on the needs and the status of other work at NAL.

The design effort is proceeding at NAL with the full understanding that the Doubler is not a critical project and has a low priority and that other more important activities take precedence wherever the needs arise. In fact, as a potentially more important early goal the group is now considering the construction of beam transport magnets designed and built along the embryonic ideas being developed for the Doubler. Should these ideas prove fruitful the first application of the technology being developed by the group will be in the experimental areas as a part of the continuing program to upgrade the research facilities of NAL in support of the physics which can be done with the higher proton energies of 300 and 400 GeV which have already been achieved.

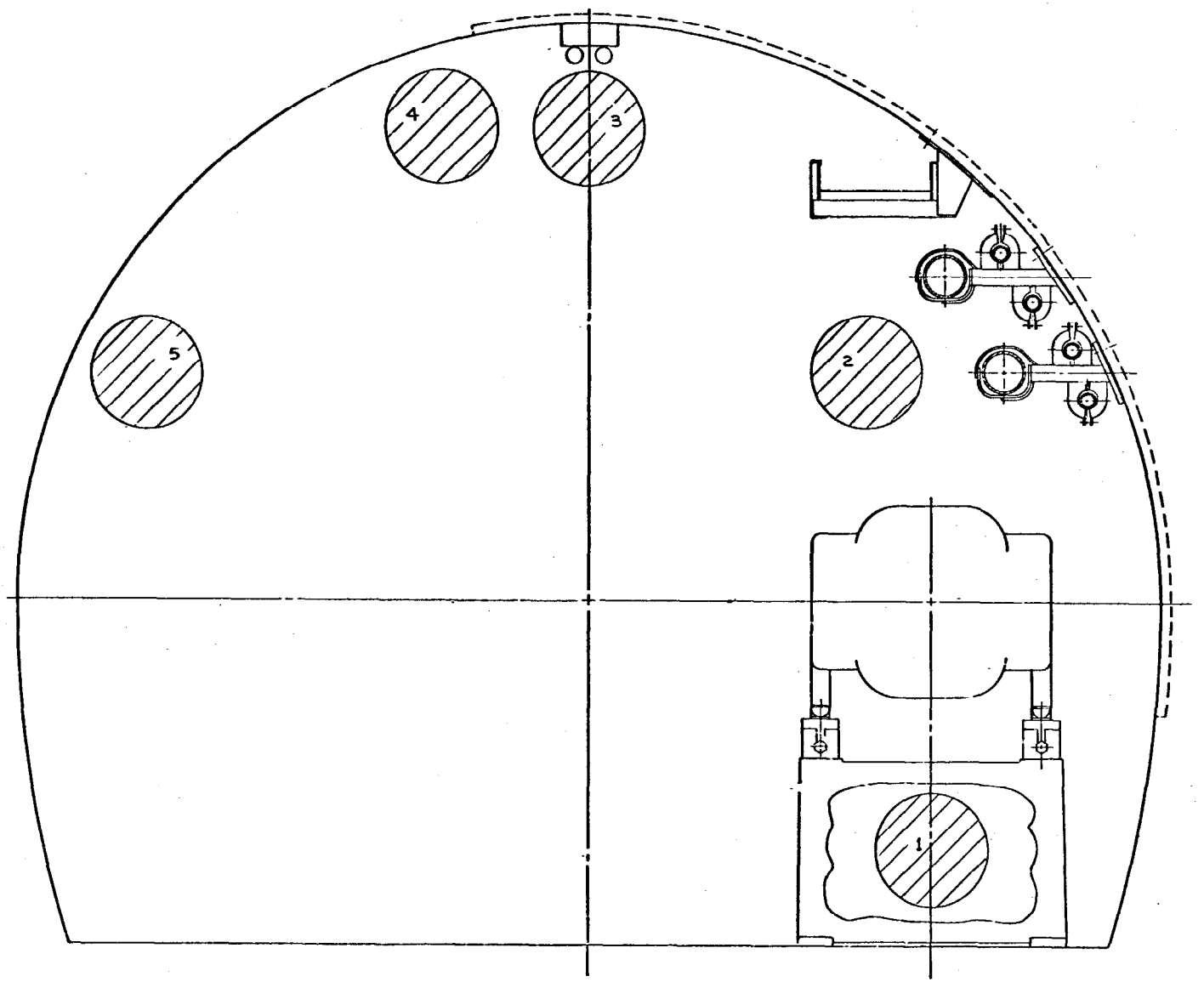

Figure 1

NATIONAL ACCELERATOR LABORATORY
U.S. ATOMIC ENERGY COMMISSION
ENERGY DOUBLER
POSSIBLE LOCATIONS OF NEW BLDG
1:4
0428-LE-53064

TM-421

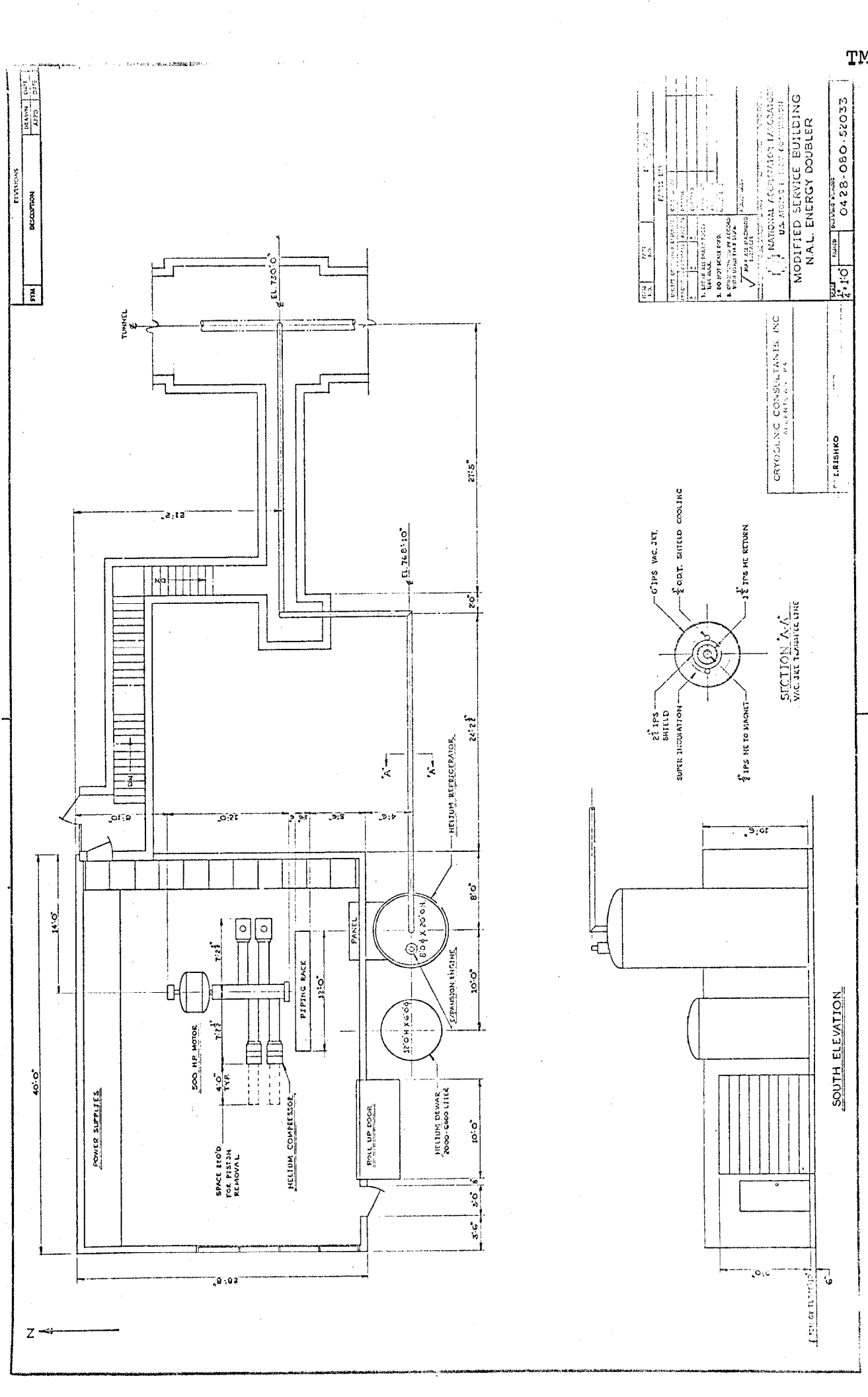
MODIFIED SERVICE BUILDING
N.A.L. ENERGY DOUBLER
0428-080-52033
CRYOGENIC CONSULTANTS, INC
NATIONAL ACCELERATOR LABORATORY
U.S. ATOMIC ENERGY COMMISSION
TUNNEL
EL. 730'-0"
EL. 768'-10"
HELIUM REFRIGERATOR
EXPANSION ENGINE
PANEL
PIPING RACK
500 HP MOTOR
HELIUM COMPRESSOR
SPACE RESVD FOR PISTON REMOVAL
POWER SUPPLIES
ROLL UP DOOR
HELIUM DEWAR 2000-6000 LITER
SECTION 'A-A'
VAC JKT TUNNEL LINE
6" IPS VAC. JKT.
4" O.D.T. SHIELD COOLING
2" IPS HE RETURN
2½" IPS SHIELD
SUPER INSULATION
2" IPS HE TO MAGNET
SOUTH ELEVATION

Chapter II

THE DOUBLER AS AN ACCELERATOR

D. A. Edwards

1. Introduction

For the last twenty years or so, the design process for cyclic accelerators has taken as initial input a familiar magnet technology based on steel. The doubler design study represents a departure from that tradition in that it is assumed from the outset that the guide fields will be provided by superconducting magnets. Accordingly, the principal focus of the present effort is on cryogenic magnet development, for until an appreciation is gained of such factors as achievable field quality, magnet-to-magnet variations arising from production techniques, and magnet-to-magnet tracking under pulsed conditions (not to mention cost considerations), a detailed accelerator design would be premature. The purpose of this section is simply to provide a rough overall sketch of the doubler as an accelerator and to recall a few of the basic aperture considerations for an accelerator of this scale.

We should clarify the sense in which this device is called an "energy doubler." The peak energy which may be achieved by the existing main accelerator at NAL is 500 GeV; the doubler is intended to attain a peak energy of 1000 GeV. However, for a variety of reasons, including the potential of a large reduction in operating costs for power by operating the doubler for physics research at energies above 300 GeV rather than the present accelerator, it would be desirable to inject into the doubler at an energy considerably below 500 GeV. The injection energy would probably not be

lower than 200 GeV to avoid problems associated with trapped flux at fields below 0.9 Tesla.

2. Magnet Location and Distribution

The doubler is visualized as sharing the same tunnel as the main accelerator. In order to provide access to both rings with a minimum of interference, it is now proposed that the doubler magnets would be placed near the apex of the tunnel; the doubler orbit would then be some 3 feet inside of and 4 feet above the main ring beam trajectory.

If the doubler is to be located just under the high point in the enclosure cross section, the bend centers of the guide field magnets must correspond with those of the main accelerator. Of course, some deviation from this condition is possible and will likely be desirable; however, at this stage, let us assume that we duplicate the main accelerator bend for bend.

At a later stage in this design study, it may be appropriate to reexamine the separated function-combined function question. For the present, given the flexibility of the separated function concept and the stage of cryogenic magnet development, we will assume a separated function design; in particular, to have a definite model, we will adopt the main accelerator magnet lattice for this discussion.

The magnet complement for the doubler would then be 774 dipoles, each 20 feet in length with a peak field of 4.5 Tesla, 192 normal cell quadrupoles, and 48 long straight section matching quadrupoles. If the tune of the doubler is to be the same as that of the main

accelerator (this need not be the case), the product of field gradient and length for the normal cell quadrupole would be 133 Tesla at 1000 GeV, and just over 60% of that figure for the matching quads.

3. Aperture Considerations

The selection of an aperture for a synchrotron can be based on clear-cut quantitative matters only up to a point. Ultimately, a judgement must be made between the risk of degraded performance, particularly in the initial stages of operation, for a smaller aperture and the increased costs associated with a larger aperture.

The quantitative side of the process can be divided into three parts: allowances for (i) beam size and orbit curvature in perfect magnets, (ii) orbit distortions arising from magnetic field and placement errors, and (iii) orbit manipulation during extraction.

(i) Beam Size and Orbit Curvature. The sagitta of the orbit in a 20-foot straight dipole magnet is 1/4 inch. At 200 GeV, the beam size of the injected beam would require about 3/8" radially and 1/4" vertically. Thus, in an "ideal" machine, the beam should circulate in an area 5/8" radially by 1/4" vertically.

(ii) Orbit Distortions. At this stage in the design process, it is conventional to consider field and placement errors as random from magnet to magnet and characterize them by suitable rms deviations. For example, suppose that the dipole magnets differ one from another in effective length, and we denote by $\Delta L/L$ the rms value of the distribution of effective length fractional differences. Then, for an ensemble of synchrotrons of the variety that we are

discussing, 25% of them will exhibit an orbit distortion in the radial direction of amplitude larger than 800 ($\Delta L/L$) inches. At this writing, it appears unlikely that it will be possible to control magnet to magnet variation in effective length of superconducting magnets with the precision of conventional magnets. If we take $\Delta L/L = 10^{-3}$, then the aperture required to accommodate the orbit distortion defined in the sense above would be 1.6 inches.

Supposing for the moment that 0.1% is indeed the sort of variation in effective lengths that production magnets will exhibit, then one must provide a means of compensating the deviations from ideal, for a 1.6 inch peak-to-peak orbit distortion is unreasonably large. For instance, if the effective lengths are measured to a precision of 0.01% say, then dipoles can be inserted into positions around the accelerator so that length variations in effect cancel one another and thereby reduce the aperture requirement arising from this source by an order of magnitude or so. If, however, the effective length variations are time dependent, then one has a more difficult problem.

The other sources of orbit distortion under this heading are field placement errors. A rotation of the dipole fields about the beam direction produces a radial field component, hence a vertical orbit distortion, of amplitude (still in the sense defined in the preceding paragraph) 800 θ inches, where θ is the rms angle of rotation in radians. For $\theta = 0.5 \times 10^{-3}$, one would therefore estimate a 0.4 inch peak-to-peak distortion. Placement errors in the quadrupole field produce both radial and vertical orbit distortions, estimation of which depends somewhat on the survey method to be used. If one uses the Wilson method of surveying the magnets in

place using the beam itself as the survey instrument, the value of θ may be made very small. For the present, we will take 60 δ for the amplitude of the distortion in either plane of motion, where δ is the rms survey error in that plane. A very good survey, with δ = 0.004 inches, would be necessary to hold our estimate of peak-to-peak orbit distortion to 1/2 inch in each plane. In practice, the orbit distortion arising from misalignment tends to be larger in the radial direction than in the vertical.

In this category, it is perhaps better to speak of "aperture allowances" rather than "aperture requirements." Given suitable trim magnets to assist in obtaining a circulating beam at injection energy and diagnostic equipment to measure beam position one can deduce a set of transverse displacements of the quadrupoles to compensate the sources of orbit distortion. It is here that the judgement alluded to at the outset of this discussion must be exercised.

(iii) Extraction. In (i) above, the basic aperture required for beam geometry was rather small. In (ii), though one may estimate the peak-to-peak orbit distortions to be larger, it is possible to imagine ways of avoiding making correspondingly large apertures. The situation is different when we turn to extraction, for here we have an aperture requirement, rather than an allowance, and it is large. In a resonant extraction scheme, the aperture has to be large enough to permit a betatron oscillation of sufficient amplitude to develop so that the amplitude-dependent step size becomes sufficient to jump an extraction septum with high efficiency.

The extraction system currently in use on the main accelerator uses about a 2-inch aperture in which the unstable betatron oscillation

builds up and another 3/4 inch space for the particles that will enter the extraction channel upon encountering the septum at the proper phase of their oscillation. The main accelerator system is now operating at an extraction efficiency in the neighborhood of 90% in what should be considered an early stage of its development. As the doubler design study progresses, the optimization of the main accelerator extraction system will yield a better appreciation of the dependence of attainable efficiency on aperture and of the extraction system modifications which may improve the ratio of these two quantities. At this point, however, it would appear imprudent to assign less than 2 inches of aperture (including beam size) in the extraction plane to the process of bringing the beam out of the machine.

As we suggested at the beginning of this discussion, a conclusion cannot be drawn from the foregoing by simply adding up some numbers. For the purposes of this summary, let us ignore the geometric considerations of (i), for the aperture requirements implied by that section are relatively small. The effects of section (ii) indicate a bias toward larger aperture in the radial plane than in the vertical. The extraction process, as noted above, imposes an aperture extension in the extraction plane. Therefore, if radial extraction is to be employed, one is led to an aperture larger in the radial direction than in the vertical by a factor of two or more. This would be the natural choice if one were using conventional steel magnets. The overlapping circle picture of superconducting coils suggests an interesting option, however, in that, though one may find it difficult to obtain a

large aspect ratio for the good field region, a balance can be found between the radial orbit distortion allowance and the extraction requirement by selecting the vertical direction as the extraction plane. One of the tasks of the design study will be to examine the advantages of vertical extraction, for it is clear that a near-circular aperture is more reasonable for the magnet designs under consideration than an aperture with a large radial-to-vertical aspect ratio. In order to propose a specific model for study, we suggest a circular aperture in which the good field region, as defined by a 0.1% tolerance, extends to a radius of 1 inch and for which the clear bore is 2.5 inches in diameter.

4. Other Aspects of the Doubler

As indicated in the introduction, our main purpose here was to introduce some aperture considerations as a basis for further study. We close with a few comments on other problems.

Of the various methods being investigated for fast extraction from the main accelerator, a single-turn process is preferable for injection into the doubler. For then, by reversing the polarity of the kicker magnets which cause the beam to leave the main ring, the beam can be brought out of the main accelerator on the inside at the present extraction straight section. Of course, new septa will be needed on the inside of the ring corresponding to those now used to extract to the outside, but this procedure enables the doubler to benefit from existing main accelerator extraction equipment and the associated lore. The lower the energy at which the transfer from main ring to doubler can be made the better, for a lesser space will be occupied by the transport system.

Further study--especially field measurements on prototype doubler magnets--is necessary in order to reveal the appropriate balance between the convenience of a low injection energy noted above and the disadvantages associated with it, such as "remanent" field effects in the doubler magnets and the increased thermal load on the cooling system implied by a larger acceleration range.

Finally, we note that the radiofrequency system requirements for the doubler are rather modest. Acceleration is to take place on a leisurely time scale of the order of a minute. An energy increase from 200 GeV to 1000 GeV in one minute implies an energy gain of some 1/3 MeV per turn--an order of magnitude less than that of which the present main accelerator system is capable. Of course, bucket size considerations raise the requirement on radiofrequency system voltage somewhat, but the scale of the system is already clear from the foregoing.

Chapter III

THE DOUBLER AS A STORAGE RING

L. C. Teng

The use of superconducting magnets which produce high fields without power consumption makes it possible to operate the "energy doubler" as a storage ring. It can be used to store high-intensity beams at energies up to 1000 GeV. To obtain stored beams at energies above the top energy of the main ring the doubler will have to be operated as a storage accelerator. In this mode of operation a high-intensity beam is first stacked in the doubler at some energy easily attainable by the main ring (say, 200 GeV) and, then, accelerated slowly over many minutes to the desired storage energy (say, 1000 GeV). The additional requirements to enable operating the doubler as a storage accelerator are (1) a beam-stacking system must be added, (2) the rf system must be capable of accelerating many amperes of beam, and (3) the vacuum must be better than 10^{-10} Torr. These are all modest requirements. It is, therefore, reasonable to consider incorporating this capability in the design of the doubler.

The principal purpose of storing high-intensity beams is to obtain the colliding-beam interaction in which the available center-of-mass energy is many orders of magnitude higher than that for the interaction of a beam on stationary target. There are several ways to provide a second beam and achieve collisions between the beams.

(1) The second (oppositely directed) beam could be provided also in the main-ring tunnel by either a second doubler ring or the main ring itself and made to intersect the first beam in long straight-sections. In either case, the main ring must be modified to accelerate beams in opposite directions.

These arrangements are not quite satisfactory because the 50m straight-section length is inadequate and because setting up experiments directly in the main-ring tunnel is rather disruptive.

2) To avoid setting up experiments in the main-ring tunnel a beam by-pass with an extra long straight-section can be added to the doubler. The doubler beam can, then, intersect the second beam (whatever its source) in the by-pass.

It is premature to explore and evaluate all these possibilities at this time. Here we will only examine the feasibility and capability of the doubler as specified for storing a single high-intensity beam. As a model we shall assume that the bending and focusing properties of the doubler to be the same as those of the main ring.

A. Beam Intensity Limitation

The long-term stability of a stored beam is limited by the self-induced non-linear field. This "stochasticity limit" can be expressed in terms of an upper limit for the incoherent tune-shift caused by the self-field. One immediate consequence of this consideration is that it favors a circular ring aperture for which the incoherent tune-shift is smallest. For a circular superconducting aperture of radius a the tune-shift is

$$\delta\nu \cong -\frac{r_p}{10}\,\frac{R^2}{\nu}\,\frac{\varepsilon}{a^2}\,\frac{\lambda}{\gamma}$$

where

r_p = classifical proton radius = 1.535×10^{-18}m

R = radius of ring = 10^3m

ν = unshifted tune = 20.25

γ = beam total energy in mc^2 unit = 214 (at 200 GeV)

λ = linear density of beam

ε = geometric parameter of order unity.

Empirically, it has been verified that for long-term stability $|\delta\nu| \leq 0.02$. Thus, we get for the maximum λ or the equivalent maximum current I

$$I = ec\lambda = \left(\frac{2.7}{\varepsilon}\ A/cm^2\right)\ a^2.$$

With a 2-1/2" coil bore, a = 3.17 cm and

$$I = \frac{27}{\varepsilon}\ A.$$

To get a feeling for the magnitude of this current we note that the luminosity per unit length $\frac{L}{\ell}$ of the head-on collision of two beams of linear densities λ_1 and λ_2 and identical cross-section is

$$\frac{L}{\ell} = 2c\ \frac{\lambda_1\lambda_2}{S}$$

where S is the cross-sectional area of the beams. This shows that for high luminosity S must be small (hence the low-β insertions). For two identical beams having the maximum current given above and cross-sectional area of π mm^2 we get

$$\frac{L}{\ell} = \frac{0.6 \times 10^{34}}{\varepsilon^2}\ cm^{-2}\ sec^{-1}/m.$$

It is interesting to note that the luminosity is proportional to a^4. A little increase in aperture means a great deal in luminosity.

B. Beam Stacking

The tried-and-true scheme of beam stacking in the momentum space as used in the CERN ISR can be employed here. The bunched

momentum spread of the main ring beam at 200 GeV is about 2×10^{-4}. When properly debunched this should go down to $\frac{\delta p}{p} \cong 10^{-5}$. At the location of maximum dispersion $x_p \cong 5$ m, this corresponds to a radial momentum width of .05 mm. Assuming that 100 main-ring pulses are stacked in the doubler we will need a beam current of 270 mA per main-ring pulse to achieve the stochasticity limited stored beam current of 27A. The beam current of 270 mA is somewhat lower than the design value of the main-ring current. The beam stack, then, has a momentum spread of $\frac{\delta p}{p} \sim 10^{-3}$ and a momentum width of 5 mm. The radial betatron width of the main-ring beam at 200 GeV is also ~5 mm giving a total beam stack width of ~1 cm. With a good field aperture of 2 inches this should leave adequate radial spacing for necessary injection and stacking manipulations and allowance for field and alignment errors.

The rf required for beam stacking is minimal. All it has to do is to accelerate (or decelerate) the injected beam by a maximum Δx of ~5 cm which corresponds to $\frac{\Delta p}{p} \sim 1\%$ or $\Delta E \sim 2$ GeV. The acceleration time can be rather long, say, 1 sec. This requires an rf voltage of only ~100 kV per turn. The rf system for acceleration can easily be used also for stacking.

Two conclusions may be drawn from these consideration.

(1) Assuming reasonable performance of the main ring the aperture of the doubler when used as a storage ring is indeed dictated by the desired intensity of the stored beam and not by the space necessary for injection and stacking manipulations. This is only true, of course, provided that the allowance required for errors in field and alignment is not excessively large.

(2) It may be desirable even when using the doubler as an accelerator to inject and stack tens of main-ring pulses before accelerating the entire stack to the final energy. If the acceleration time in the doubler is 1 minute and the main ring is running at 200 GeV at 1 pulse every 3 seconds, the optimal stack size is ~20 main-ring pulses.

C. Vacuum System

With cold-bore superconducting magnets it is natural to use cryosorption pumping. Experience gained on the CERN ISR shows that with proper care in surface treatment and bake-out there should be no difficulty in obtaining a vacuum of 10^{-10} Torr or better.

D. Radiofrequency System

For the rf system of the doubler we shall assume a frequency equal to that of the main ring, namely a harmonic number of ~1113. As expected, the storage accelerator mode of operation imposes the heaviest demand on the rf system. However, since, even for this mode the requirement is rather modest we shall assume that only one rf system is provided which will be used for all modes of operation. If a higher harmonic number is used, we could use fewer cavities but at a higher voltage.

The longitudinal phase-space area occupied by one main-ring pulse at 200 GeV is $(\delta\phi)\left(\frac{\delta p}{p}\right) \cong 2\pi \times 10^{-5}$. For a beam stack of 100 main-ring pulses this area is $\sim 2\pi \times 10^{-3} = 6.28 \times 10^{-3}$. To provide rf buckets of this area at 200 GeV we need a minimum voltage of 560 kV/turn. With the voltage for acceleration included the total rf voltage required is ~750 kV/turn. Operating at a synchronous

phase angle of ϕ_s = 177° (measured from the rising-zero point) the area of the rf bucket at 200 GeV is 6.44×10^{-3} just adequate for containing the beam stack. The rate of acceleration will be 750 (sin 3°) kV/turn = 39 kV/turn. Acceleration of the beam stack from 200 GeV to 1000 GeV will take ~7 min.

For the accelerator mode of operation we want to accelerate the beam from 200 GeV to 1000 GeV in 60 sec. This corresponds to an energy gain of 280 keV/turn and we must lower the synchronous phase to ϕ_s = 158°. The rf bucket area is, now 3.33×10^{-3} more than adequate to contain the beam stack of 20 main-ring pulses which has a phase-space area of $\sim 0.4\pi \times 10^{-3} = 1.26 \times 10^{-3}$. The momentum width of the rf bucket is 1.82×10^{-3} which is ample for containing the bunched momentum spread of 2×10^{-4} of the main-ring beam when a single undebunched pulse is injected into the doubler for synchronous capture by the doubler rf.

These considerations indicate that even for the storage accelerator mode of operation the rf system is not extravagant and the same rf system will serve well for all other operating modes. For the storage accelerator mode, however, aside from the voltage consideration in view of the very high beam current (~27A), hence the very heavy beam loading on the cavities it is most important that the beam-cavity interaction be carefully controlled throughout the acceleration cycle.

Chapter IV

MAGNETIC FIELD CONSIDERATIONS

S. Snowden, W W Lee, P. J. Reardon, Z. J. J. Stekly

After a review of the types of magnets that we feel were applicable to our goals, we have concentrated on two types of dipoles, one of which we call the pancake type and the other, the shell type. We have considered two different bore diameters; a 2 inch bore and a 1-1/2 inch bore and for our first two models we have built one of each bore size. Our next two models will have a bore of 2.16 inches. Later we will consider a 2.5 inch bore magnet which appears to be more appropriate for an accelerator which can provide external proton beams and for using the doubler as a storage ring. We also considered two different effective current densities in the coils, 20,000 amperes per sq. cm. and 30,000 amperes per sq. cm. Finally, power supplies for the ring which would operate at 2,000 amperes or at 5,000 amperes were earlier contemplated. For the 2.5 inch bore models we will concentrate on coil designs where the peak current is about 2,500 amperes, the effective current density is about 32,000 ampers/cm^2, the number of turns is about 160 and the current density in the wire slightly greater than 40,000 amperes/cm^2.

We are designing the magnets to operate at a pulse rate of one per minute (.01Hz) or one every other minute and we do not intend to inject into the doubler at fields less than about 0.5T and typically we would inject at 200 GeV, about 0.9T, which would allow us to operate the present accelerator at a faster pulse rate that it does presently when running at 300 or 400 GeV. All of the magnets we have considered so far have cooling passages built into the coils and the inner bore of the vacuum tube is sized to just encompass the "good field" region when the "good field" is defined as that region where the field varies no more than 1 part in a 1,000 from the central field value. The space between this diameter and the diameter of the inner-coil circle is alternately used both for cooling passages and support structures along the length of the vacuum tube. At one point we considered using an elliptical bore with an aspect ratio of about 2 to 1 radial to vertical in order to provide for extraction of the beam in the radial plane (in fact the P6A model now under construction is slightly elliptical) but it now appears that a circular model would be easier and less costly to construct and more appropriate for vertical extraction and beam stacking associated with storage ring applications.

Complex variable methods have been employed to obtain expressions for the magnetic field due to a rectangular block of uniform current density located parallel to a horizontal plane and within a circular shield of infinite permeability. Superposition of the results from many blocks is used to provide

the magnetic field of the pancake design.

This method is extended to a shell design by locating four blocks of current such that they touch in symmetrical pairs above and below the median plane. Subsequent rotation of coordinates gives the field for one pair of conductors located on a circular shell. Superposition of the results for many conductors provides the magnetic field of the shell design. A slight modification permits the individual conductors to be keystoned instead of rectangular if desired.

In order to find suitable locations for the various pancakes or shells, one first finds an expression for the energy within a bore radius. Subsequent minimization of the difference between this energy and the energy obtained assuming a uniform field yields the proper conductor placement. Generally speaking, it is possible to find conductor locations such that the field within 75% of the conductor aperture is within $\pm$.05%. The pancake or shell location accuracy corresponding to this field uniformity is +.001 inch.

Tables I and II give the approximate requirements for the bending magnets and focusing magnets required for the doubler lattice. These requirements are based on using the present Main Ring lattice. The peak fields may be lower if the lattice is changed such that all space between magnets, such as mini-straights, is filled. Tables III and IV give the design specifications for the first two models of the pancake coil design. In Mark I no attempt was made to provide the desired field or field uniformity. Mark II design attempts to correct these deficiencies. Tables V and VI provide the design specifications for the first two models

of the shell design. Again, for Mark I, no attempt was made to provide the proper magnitude of uniformity of field. Table VII presents a tentative design for the first quadrupole.

Table I

PRELIMINARY REQUIREMENTS FOR BENDING MAGNET
ASSUMING THE PRESENT M.R. LATTICE

Field Strength (1000 GeV)	45 kG
Good Field Width	1.5 in.
Field Tolerance	±.05%
Position Tolerance for Layers or Shells	±.001 in.
Coil Aperture (roughly circular)	2.0 in. dia.
Lamination Bore Diameter	6.0 in.
Lamination Thickness (warm)	.0625 in.
Magnet Length	240 in.
Magnet Cross Section	14 in. by 12 in.

Table II

PRELIMINARY REQUIREMENTS FOR FOCUSING MAGNET
ASSUMING THE PRESENT M.R. LATTICE

Gradient Strength (1000 GeV)	16 kG/in.
Good Field Width	1.5 in.
Gradient Tolerance	±.2%
Coil Aperture (roughly circular)	2.0 in. dia.
Lamination Bore Diameter	6.0 in.
Lamination Thickness (warm)	.0625 in.
Magnet Length	84 in.
Magnet Cross Section	14 in. by 12 in.

Table III

DESIGN DATA FOR MARK I PANCAKE MAGNET

Field Strength (no shield)	20 kG
Field Tolerance (1.5 in. width)	±.5%
Coil Aperture	1.930 in.
Effective Magnet Length	40 in.
Conductor Size (MCA 360)	.112 in. by .056 in.
Formvar Coating Thickness	.002 in.
Effective Current Density	22 kA/cm^2
Max. Current Density in Wire	40 kA/cm^2
Turns	208
Peak Current Expected	1500 amps
Transfer Constant (no shield)	18.6 G/A
Transfer Constant (6" i.d. shield)	22.3 G/A
Inductance (no shield)	18.3 mHy
(with shield)	32.6 mHy

Location of Pancakes in First Quadrant (with Insulation)

Blk.	Turns/Layer	X1(in)	X2(in)	Y1(in)	Y2(in)
1	13	.9650	1.7150	.020	.170
2	13	.9650	1.7150	.170	.320
3	13	.8743	1.6243	.360	.510
4	13	.8743	1.6243	.510	.660
5	13	.6563	1.4063	.700	.850
6	13	.6563	1.4063	.850	1.000
7	13	.2586	1.0086	1.040	1.190
8	13	.2586	1.0086	1.190	1.340

Table IV

DESIGN DATA FOR MARK II PANCAKE MAGNET

Field Strength (6 in. i.d. shield)	45 kG
Field Tolerance (1.5 in. Width)	±.035%
Coil Aperture	2.274 in.
Effective Magnet Length	40 in.
Conductor Size (MCA 1300)	.150 in. by .075 in.
Formvar Coating Thickness	.002 in.
Effective Current Density	34.8 kA/cm^2
Current Density in Wire	51.4 kA/cm^2
Turns	156
Peak Current Expected	1800 A
Transfer Constant (no shield)	14.8 G/A
Transfer Constant (6 in. i.d. shield)	17.8 G/A
Inductance (no shield)	8.5 mHy
(with shield)	15.2 mHy

Location of Pancakes in First Quadrant (with Insulation)

Blk.	Turns/Layer	X1(in)	X2(in)	Y1(in)	Y2(in)
1	13	1.136	2.111	.020	.170
2	13	1.091	2.066	.170	.320
3	13	.977	1.952	.360	.510
4	13	.857	1.832	.510	.660
5	13	.600	1.575	.700	.850
6	13	.232	1.207	.850	1.000

Table V

DESIGN DATA FOR MARK I SHELL MAGNET

Field Strength (no shield)	25 kG
Field Tolerance (1.125 in. width)	±3%
Coil Aperture	1.5 in.
Effective Magnet Length	12.in.
Conductor Size (MCA 1300)	.112 in. by .056 in.
Formvar Coating Thickness	.002 in.
Effective Current Density	27.7 kA/cm^2
Max. Current Density in Wire	40.0 kA/cm^2
Turns	176
Peak Current Expected	1400 A
Transfer Constant (no shield)	22.3 G/A
Inductance (no shield)	4.7 mHy

Location of Shells in First Quadrant (with Insulation)

Shell	Turns/Quadrant	R1(in)	R2(in)
1	22	.7500	.8625
2	22	.8625	.9745
3	22	1.0045	1.1180
4	22	1.1180	1.2300

Table VI

DESIGN DATA FOR MARK II SHELL MAGNET

Field Strength (6 in. i.d. shield)	45 kG
Field Tolerance (1.5 in. width)	±.04%
Coil Aperture	2.0 in.
Effective Magnet Length	16 in.
Inner Conductor Size (MCA 1300)	.150 in. by .075 in.
Outer Conductor Size (MCA 1300)	.150 in. by .050 in.
Formvar Coating Thickness	.002 in.
Maximum Effective Current Density (inner conductor)	32.4 kA/cm^2
Maximum Effective Current Density (outer conductor)	48.6 kA/cm^2
Transfer Constant (no shield)	15.9 G/A
(with shield)	19.1 G/A
Peak Current	2500 A
Inductance (no shield)	4.9 mHy
(with shield)	8.7 mHy

Location of Shells in First Quadrant (with Insulation)

Shell	Turns/Quadrant	R1(in)	R2(in)
1	18	1.000	1.150
2	20	1.150	1.300
3	20	1.325	1.475
4	20	1.475	1.625

Table VII

DESIGN DATA FOR MARK I QUADRUPOLE

Gradient Strength (6 in. i.d. shield)	10 kG/in.
Gradient Tolerance	±.5%
Coil Aperture	2.0 in.
Effective Magnet Length	28 in.
Conductor Size (MCA 1300)	.150 in. by .075 in.
Formvar Coating Thickness	.002 in.
Turns per Coil	53
No. Coils	4
Transfer Constant (no shield)	∿.014 kG/in/A
Transfer Constant (with shield)	.017 kG/in/A
Inductance (no shield)	8 mHy
(with shield)	∿14 mHy

To date in the effort related to an understanding of the structural problem associated with the two types of dipoles we are considering, we have emphasized the calculation of deflections and shear stresses to determine whether motion might occur within the windings which would induce a quench of the superconductor.

In order to do this it was necessary to compute the magnetic fields within the windings. This was done by using stick models for the windings in a three dimensional magnetic field computation.

This calculation was set up for two coil configurations proposed for the Mark II dipole models, the P6B (a pancake configuration) and the S4B (a shell type configuration).

The basic calculations were performed for air core windings. The concentration factor of magnetic field in an air core configuration (defined as the maximum field at the windings divided by the central field) was 1.19 for the P6B configuration, which had end windings which were spread out axially versus 1.29 for the more concentrated windings which were assumed for the S4B.

It can be concluded from the work accomplished so far that future designs should be made with spread out ends.

Also since the iron contribution to the magnetic field in the central region is in the neighborhood of 0.8T, the iron should be terminated well before the end turns cross over in order that the fields in the end windings do not exceed those in the center of the magnet.

Table VIII summarizes the geometry and magnetic fields computed for the two coil configurations.

In order to have an experimentally obtained value of minimum shear stress with proposed coil bonding systems to compare calculated shear stress with, four specimens of bonded winding were tested in liquid nitrogen up to failure of the bond between the conductors. The values of the maximum shear at failure raised from 4270 psi to 9810 psi. In all cases failure was between the conductor itself and its insulation and not in the epoxy system which formed the bond between the series. This would indicate that in the future for a production run of wire, the wire manufacturer should improve the bonding of the formvar to the copper which should not be too difficult a task.

Table IX summarizes the more important results from the deflection and stress analysis.

The deflections were computed for the long straight sections and are for the point in the winding which sees the largest deflection.

For the P6C two deflections were computed, one with the bore tube and bonding bonded to the winding, the second for the case where these are unbonded. (High pretension in the strap has the same effect as the bonding since it allows shear to be transmitted between the bore tube, the winding and the bonding.)

The preliminary computations of the additional shear at the ends shows that for this design there is not a large shear stress.

Comparing the 4260 psi shear for the S4B, however, (at

4.5T central field) to the lowest value of 4270 psi obtained for the shear stress at failure in the specimens tested, we conclude that these values are uncomfortably close and that further effort is required to improve the bonding of the wire insulation to the wire.

Also, the value of shear stress can be lowered readily by increasing the bonding thickness or the bore tube thickness, or both, therefore, there does not seem to be a major problem in this regard provided these factors are taken into account before finish prototype magnets are built.

The test coils (Mark I P8A and Mark I S4A) that have operated so far have had lower field levels so that we would not expect any problems with them.

Also shown in Table IX are the estimated values of the magnetic force spring constant for vertical and horizontal motion of the magnet.

1. Quench computations

Calculation of the quench currents, voltages and temperatures will be performed for two proposed configurations. One configuration has uniform current density, the other has windings with two current densities.

Calculations will be performed at the peak operating field of 4.5T, however, results will be generated for various operating currents to allow checking with experimental data.

2. Magnetization Effects on Magnetic Field & A. C. Losses

The object of this task is to examine the effect of wire

geometry (size, no. of strands, and twist rate) on the ac loss and the magnetic field generated on a functions of injection field, peak field, rate of rise of field, and pulse rate. The magnetization and ac loss will be computed for wires of various sizes, number of strands and twist rates.

A computer program will be set up and used to compute the magnetic fields in the straight section of the coils taking into account the magnetization of the wire.

3. Preliminary Investigation of Reproducibility

The problem of reproducibility of magnetic field will be examined in a preliminary fashion to determine what effects the ability to exactly reproduce the same magnetic field from magnet to magnet. Variables that will be considered are: placement of the conductor, placement of the iron, magnetization of the conductor, variable iron properties. Estimates of the magnitude of these effects will be made for each variable.

Table VIII

MAGNETIC FIELDS
(AIR CORE ONLY)

	P6C	S4B
NI	3.95×10^5	3.95×10^5
Winding Inner Radius (in.)	1.136	4.04×10^5
Winding Outer Radius (in.)	2.111	1.625
Central Field (kG) (no iron)	37.5	43.5
Ratio of Max. B to Central B.	1.19	1.29
End Geometry	Spaced Out	Concentrated

Table IX

SUMMARY OF CALCULATIVE DEFLECTIONS

	P6C	S4B
Deflection (in.)		
All Bonds Good	1.93×10^{-4}	1.61×10^{-3}
Unbonded	1.22×10^{-3}	--------
Max. Shear (Lateral psi)	2820	4260
Max. Stress in strap (psi)	7490	22,500
End Shear (psi)	605	1080
Effective Spring Const.		
Vertical (lb/in^2)	1594	1130
Horizontal (lb/in^2)	3188	1738

Chapter V

WIRE SELECTION FOR PRESENT ENERGY DOUBLER DIPOLE

B. P. Strauss & P. J. Reardon

In view of the high cost for the superconducting magnet wire for approximately 1,000 magnets, we are interested in obtaining a high current density wire which will operate at a reasonably high overall current. We would expect to attain this goal, however, only if the wire could be reliably and economically produced and if the splicing problems for higher currents can be solved economically. Should present design concepts persist, we have a requirement for about 6,000,000 feet of superconducting wire. We expect that for these lengths of conductor production economics of scale should set in and cost should come down to some asymptotic level that may be substantially less than half of present costs. In addition the cost difference between a relatively sophisticated small filament cable and a larger filament wire should also be small and in fact the cost difference, if any, may be wiped out by the savings in refrigeration. Needless to say, an order of this size will have a major impact on the superconductor industry and our price assumptions above are based somewhat on this perturbation. Figure 1 shows our expected cost per foot as a function of total length.

Our initial request for proposal for stablized superconducting wire was based on a 2 inch bore magnet using approximately 240 turns or a 1-1/2 inch bore magnet using approximately 200 turns both operating at 2000 amperes and an effective current density of 20,000 amp/cm^2. Our present designs are for 160 turn 2.5 inch bore magnets which operate at about 2,500 amperes peak, an effective current density of about 30,000 amps/cm^2. All of our designs so far are for magnets which pulse at a rate of one per minute or one every other minute. As a result of the first RFP, two wires from two manufacturers were chosen.

CONDUCTOR CHARACTERISTICS

Although superconductors at dc are lossless, that is they have zero resistivity, movement of flux throught the winding may cause high thermal losses. Even worse, these losses or heat fluctuations caused by mechanical movement might cause the conductor to revert to the normal state. We are faced with the problem then that the severe heat transfer restrictions and the difficulty of restraining the conductor motion will lead to a reduction of the maximum current density obtainable.

A brief discussion of stability follows. Methods of stability can be classified into the foll wing three categories:

1) Cryogenic Stabilization, which in essence is the provision of an alternate path for the current to shunt the superconductor. This path must be large enough to limit the temperature rise to less than 0.5°K, the pool boiling limit.

2) Enthalpy Stabilization, the heat capacity and/or stored energy in the individual strand and its surroundings are such

that a normal front may not occur.

3) Dynamic Stabilization, which is obtained by the presence of enough low or intermediate resistance filler to impede flux flow, thus dampening magnetic instabilities that might exist.

Due to the high overall current densities that are required by superconducting synchrotoron dipoles, the first method is of very little interest. This method, however, is well understood and has been utilized and proven in many large magnet systems, particularly bubble chambers.

The second criteria may be expressed as an upper limit on filament size

$$d \leq \pi \sqrt{(3\xi C_p T_o/2\mu_o)}\ /J_c$$

for NbTi d = 40μ, where ξ = density, To = $-Jc(\partial Jc/\partial T) = Tc/2$, and Cp is the specific heat of the conductor.

For conductors used in a time varying magnetic field we will now consider the heat loss due to magnetization currents. If the individual filaments are in an insulator then all magnetization currents will be confined to the individual strands. For a low resistivity matrix a given $\dot{H}$ can drive magnetization currents into the substrate thus producing I^2R losses. These conductors will occupy a finite length of the conductor. It can be shown that this length, ℓ_c, is

$$\ell_c^2 \simeq 10^8 \lambda\, J_c d\rho/\dot{H}$$

where d = filament size, Jc = critical current, ρ = the substrate resistivity and λ = a space factor $\simeq$ 1. Then if the conductor length is less than ℓc the currents can be made to flow in the filaments by twisting the conductor so that the twist pitch is about ℓc/2 or about 1 to 2 twists per inch. With twisting, the

adjacent voltages in each loop will cancel and each filament will act independently.

In our first specifications for the wire, it was also assumed that the magnets would be operated in subcooled liquid helium at about a temperature of 4.6 to 4.9°K. This imposes a degradation on the conductor performance of about 40%. It was also assumed that the conductor would be operated at 80% of the short sample current for a given ambient temperature and field. Our latest concepts for refrigeration indicate that it may be possible for us to operate at temperatures of 3.8 to 4.2°K. It is for this reason that we consider it possible for us to talk about operating the superconducting wire at current densities of 40,000 A/cm^2, thereby getting an effective current density in the coil that will approximate 30,000A/cm^2.

Care must be given in the choice of wire in order to minimize the ac losses which are proportional to the diameter of the individual filaments, the twist length, the peak field, the ramp rate and the overall conductor size. The losses are also inversely proportional to the effective resistance of the composite which depends on the resistivity of the normal metal matrix as well as other construction, metallurgical, and geometrical factors.

In choosing a conductor several facts which are ultimately related to cost performance and reliability should be considered. While one would like to reduce the filament size as much as possible in order to reduce ac losses, the limit on this reduction is dependent on the quality control employed as well as

metallurgical considerations. A tight twist is desirable in order to reduce coupling between filaments as well as reducing ac losses. However, it is found that the effective current density is reduced because of geometry. Other attempts at increasing ℓc by using an effectively higher resistivity matrix have their disadvantages. For example, experience with conductors having strands separated by organic insulation shows low ac losses and very low stability. Other composites using only cupro-nickle as a high resistivity matrix show very little stability because of the high magnetic diffusivity in the matrix. We are planning to respecify the conductor after some experience with the present models.

Because of the parameters of the "doubler" some of the requirements on the ac performance of the conductor are not so stringent. Magnetization and trapped flux problems are reduced by the high field at injection into the magnets as well as the low ramp rate. A review of the literature indicates that we may have been a bit brash in our initial choice of filament size, 40μ, if we are to keep our ac losses below 1W/m. We realized this, of course, at the outset and recognize that we can always go to more sophisticated conductors if necessary. In fact, the cable conductor we ordered as a back up wire more nearly fits the criteria for low ac losses and we believe it or something like it could be produced almost as economically in a long production run. We also felt that the more important criteria to establish first was the attainability of the high

current density and that later industry could develop a wire similar to our 40 micron filament wire but with a filament size close to 20 microns which should enable us to achieve the ac loss rate we need. Further work in obtaining a more optimum twist rate is also required.

Table I contains the specifications for the conductor used for our Mark I test models P8A and S4A. Table II lists the parameters of the wire to be used for our Mark I P6C and S3C. Table III lists the specifications for the conductor to be used in the last two types of 1 - meter D models and the 6 - meter prototype dipoles. All of the above conductors prototypes were supplied by Magnetic Corporation of America.

Table IV lists the parameters of a cable conductor to be supplied by Supercon, Inc. This conductor has the same short sample properties as the conductor in Table III, but is a cable composed of seven three component composite wires. As mentioned above, since the individual filaments of the superconductors are less than 20 microns, this wire and others similar to it may be more favorable for our ultimate application. Also, it is a three component wire which has cupro-nickel next to each filament. We will probably build one or more one meter models as well as some six meter prototypes from this wire as well. As a result of our model test program we intend to resolicit all manufacturers on the basis of a new wire specification. One of the basic requirements of the model test program is to experimentally establish the ac losses in the superconductor as a function of the type wire used.

Table I

CONDUCTOR FOR FIRST MODELS

Manufacturer	MCA - Kryoconductor
Size	0.112 x 0.056 inches
Asub/As.c.	1. 25/1
No of Filaments	361
Filament Size	.003 inches (77μ)
Twist	1 per inch
S.C. Alloy	NbTi
Substrate	Copper
R300/R4.2	>100
Insulation	Formvar (6 Mil. - total build)
Minimum Short Sample	1250 A. @ 5T; 1580 A @ 4T

Note: This conductor was used to build dipoles MK-I/P8A and MK-I/S4A.

Table II

INTERMEDIATE CONDUCTOR

Manufacturer	MCA
Size	0.075 x 0.150 inches
Asub/As.c.	2:1
No. of Filaments	1345
Filament Size	1.88 mils.(47μ)
Twist	1 per inch
S.C. Alloy	NbTi
Substrate	Copper
R300/R4.2	>100
Insulation	Formvar (Bondable)
Minimum Short Sample	2250 @ 5T and 4.2° K

Note: This conductor is to be used for dipole magnets MKII/P6C and MKII/S3C. In the latter case, to test the variable density concept, the outer shells will be fabricated from the wire listed in Table I.

Table III

CONDUCTOR TO BE USED FOR FULL FIELD 1 M MODELS
AND FIRST 6 M PROTOTYPE MODELS

Manufacturer	MCA, Inc.
Size 1	.150 x .075 inches overall
Size 2*	.150 x .050 inches overall
Asub/Asc	2/1
# of Filaments	2300
Filament Size	35μ
Twist	1 per inch
S. C. Alloy	NbTi
Substrate	Copper
R300/R4.2	>100
Insulation	Self bonding Polyvinyl Formal (Formvar)
Minimum Short Sample	3500 @ 5T and 4.2°K
NAL Specification	0428-090-52500

*This smaller cross section wire will be obtained by drawing down the Size 1 wire bringing about an approximately 30% reduction in filament size.

Table IV

CABLE CONDUCTOR FOR FULI FIELD
1 Meter and 6 Meter Prototype Models

Manufacturer	Supercon, Inc. Natick, Mass.
Type	Cable of 7 - 0.036 strands solder filled and rolled .150 x 0.075 inches overall
Asub/Asc	2/1
# of Filaments	160/strand
Filament Size	20μ (0.0008 in.)
Twist	2/inch (strand)
S.C. Alloy	NbTi
Substrate	Copper and Cupro Nickel
R300/R4.2	>100
Insulation	Wrapped Mylar
Minimum Short Sample	3500A @ 5T and 4.2°K
NAL Specification	As ordered under Subcontract No. 80110 dated 12/6/72

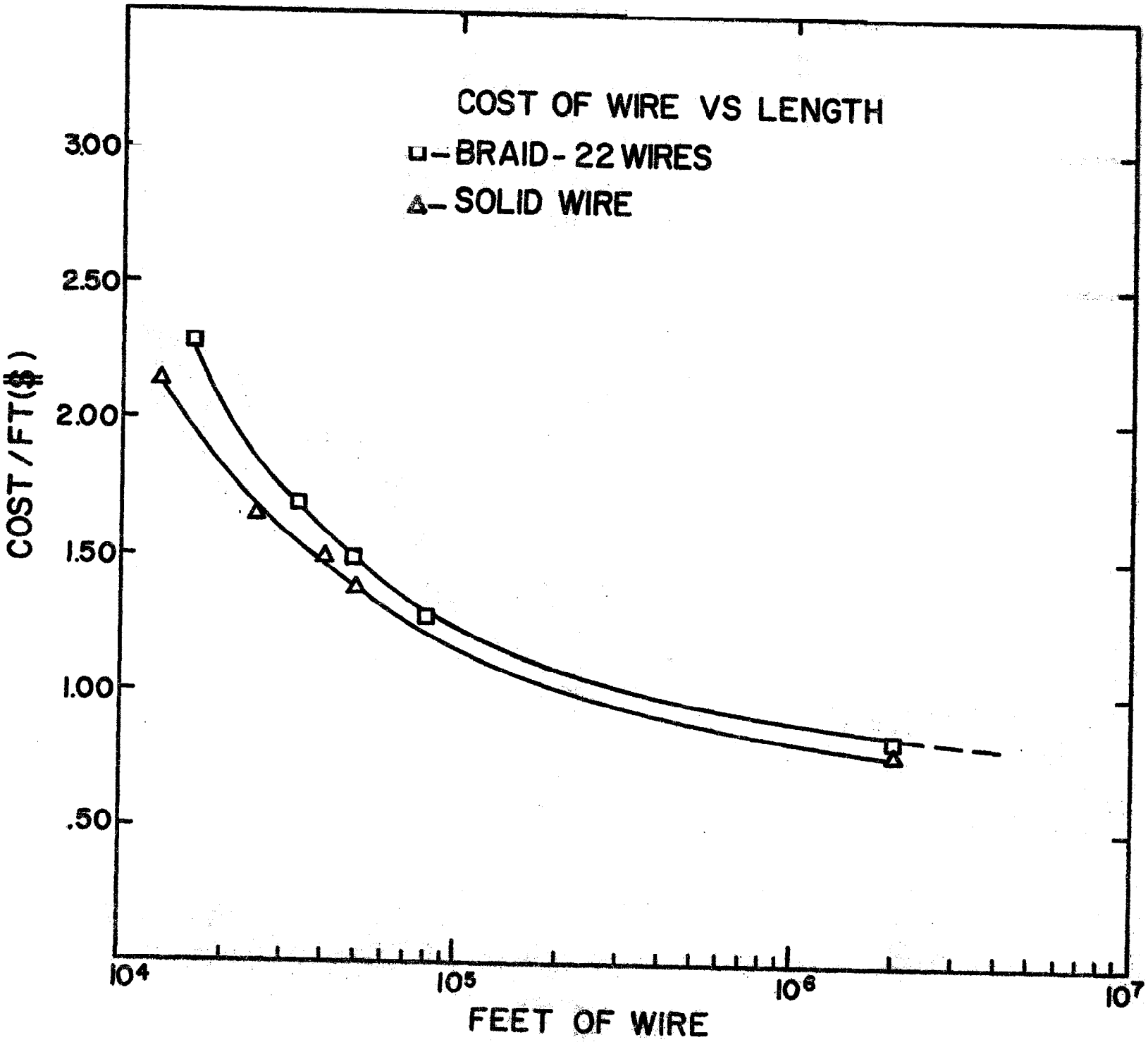
COST OF WIRE VS LENGTH
□ – BRAID - 22 WIRES
△ – SOLID WIRE
COST / FT ($)
3.00
2.50
2.00
1.50
1.00
.50
10⁴
10⁵
10⁶
10⁷
FEET OF WIRE

FIGURE 1

Chapter VI

DIPOLE CONSTRUCTION

G. Biallas, W. Hanson, H. Hinterberger
J. O'Meara, B. McCracken

As mentioned earlier we are, at this time, considering two methods of dipole magnet construction which we call the shell type and the pancake type.

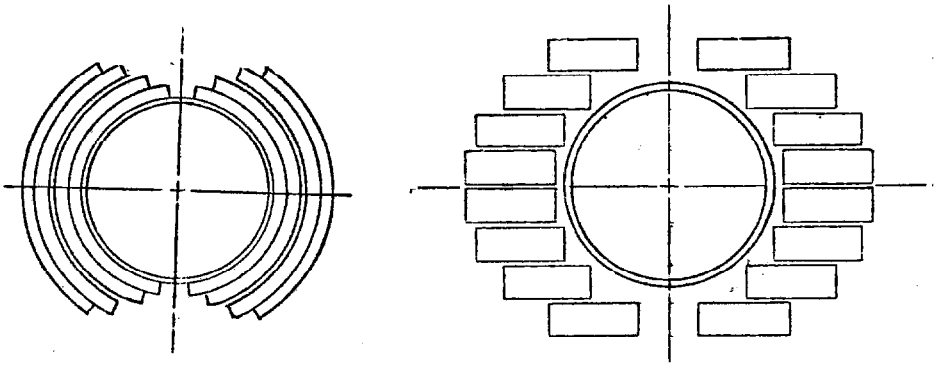

Shell Type Pancake Type

The pancake style was at first thought to be easier to fabricate; however, on the basis of our experience in fabricating one of each type, Mark I - P8A and Mark I - S4A, we now feel that the difference in fabrication cost may be minimal. The horizontal width of the shell type is less than that of the pancake type, due to a higher packing factor for the shell. This is due to the fact that less of the cross sectional area is taken up by cooling passages in the shell, and there is no waste space at the corners (see sketch above). There is, however, a school of thought that the pancake coils can be placed more accurately, and that the pancake coils are more adaptable to present winding

techniques that industrial firms use. We now believe, however, that with adequate tooling design, the shell type would also present few difficulties to industrial coil firms.

Another apparent advantage of the pancake design is that all coils for the dipole could be wound in series with a single length of wire of the same cross section. This is probably true for the shell as well but not as obvious. The shell design, on the other hand, appears to be well suited for building dipoles with variable current density, each shell being wound with different wire in order to save on the overall cost of the superconductor. It also is possible to build pancakes using the variable density techniques.

Our present thinking is to use a warm iron configuration. There are two arguments for warm iron. Firstly, the time required to cool down and warm up a cold iron magnet was considered to be prohibitive. In an operating synchrotron, particularly during initial startup, one must anticipate a certain number of magnet failures. If each failure requires a week for warmup and cooldown, then the whole startup process becomes excruciatingly difficult. Secondly, we wish to have the steel far enough away from the coil to prevent saturation in parts of the steel. In practice, this means something like a 3/4" space between the O.D. of the coils and the I.D. of the steel. Obviously, this space can be put to good use for the coil superinsulation. Now, it is certainly true that one can use cold iron with the same 3/4" space to prevent saturation being filled with a rigid nonmagnetic material. However, in addition to the previous

objections, one must consider the cost of the additional refrigeration required by the larger surface area of the superinsulation around the outside of the steel. Being about triple the surface area of the superinsulation in the warm iron design, refrigeration required would increase from about one watt to about three watts per meter (assuming no intermediate heat shield). The best argument in favor of a cold iron configuration is that the iron may be used to resist the forces which act horizontally outward on the coils when they carry current. We propose to use banding to accomplish this task.

Various types of banding to restrain the coils have been considered. The MARK I pancake model P8A has phosphor bronze bands about 3/8" wide woumd very tightly around a fully impregnated assembly of coils and G-10 spacers. These bands are spaced about 3/16" apart to permit liquid helium access to the small passages that permeate the assembly. The MARK I shell model, S4A, is not impregnated. Rather, the coil shells are placed directly against an alumina tube and held in place with bands of tightly wound Mylar. In both these designs, the intent is to use a banding material with a higher coefficient of contraction than that of the combination of bore tube and superconducting coil. Thus, the banding would become tighter at low temperatures. Various other banding materials have been suggested and are being considered.

The procedure for fabricating the Mark I P8A (See Fig. 1, Chapter 8) pancake type magnet consisted of winding each double pancake on

a flat mandrel using a wet epoxy layup procedure. The mandrel size was accurately controlled to bring the finished coil to an overall tolerance of within 1 mil. The wet layup compensated for minute variations in the wire size, thus hydrostatically spacing the individual conductors in the total pack. The coils were cured in the winding fixture, and the ends bent up after curing.

Cooling passages were provided between double pancakes so that each conductor would be cured from one edge. The curing passages were 1/4" wide with 3/8" support in between. Rubber bands were positioned to form the curing passages. Fiberglass tape was provided to tie the coil assembly to the vacuum tube, which acted as a center core. Fiberglass was also wrapped around the entire assembly and it was then vacuum impregnated. The rubber bands were pulled out to form the passages. The potted assembly was placed in a lathe and heavily tensioned. Phosphor Bronze banding was wrapped around the assembly to counter the outward coil loads. Eight mil by 3/8" wide banding was built up to a thickness of 3/16". The banding was circumferentially wound to prevent introducing twist and the ends soldered in place.

In the procedure followed for the Fabrication of the MARK I S4A Shell type Dipole (See Fig. 5, chapter 8) the coils were wound on a curved mandrel. The individual conductor was tapered as part of the winding procedure so that the conductors would position themselves in a radial manner. Each double layer shell was bonded with epoxy and cured in the winding fixture.

A rigid ceramic vacuum tube provided the core for this

magnet. Its outside diameter was grooved to form the cooling passages. The two coil assemblies were spaced 1/32 inches apart to provide curing passages so that each conductor was cured on one edge. The entire assembly was then tightly wrapped with 1 mil mylar banding built up to a total thickness of 3/16 inches. The banding was 1/4" wide with 1/8" space to allow for conductor cooling.

The bore tube should, ideally, be made of a strong, rigid, nonmagnetic insulating material (except for a thin inner bore liner of a conducting material to prevent charge build-up), so we do not have to provide insulation between it and the coil. One of the problems we are concerned with for a 20 foot long magnet is that the banding exerts a high compressive force on the coil, which causes high frictional forces between the coil and the bore tube. Because of the longer length of the 20 foot coil, these friction forces increase proportionately, to the point where one begins to worry about failure of the coil or bore tube due to longitudinal forces caused by the different coefficients of contraction of the materials involved. A design which we propose to test consists of a thin stainless steel inner tube over which is wound a fiberglass monofilament tape in a helical pattern. Alternate layers would have helices of opposite hand. The stainless steel tube would provide a vacuum tight jacket which is easily weldable to the rest of the cryostat. By varying the heliax angle of the fiberglass prepreg tape, we believe we can adjust the longitudinal coefficient of contraction of the tube to match that of the superconductor. The fabrication technique would be to wind the fiberglass tape directly onto the

stainless tube after coating the tube with a mold release agent. Thus, at low temperatures the stainless tube, having a higher coefficient of contraction than the transverse coefficient of contraction of the fiberglass tube, would break away from it and not see any longitudinal friction forces. The fiberglass tube would be built up to a wall thickness of perhaps 1/8", providing adequate strength to resist the compressive forces of the banding, and good electrical insulation. The circumferential helium fluid passages required at the inside surface of the coil would be built into the fiberglass bore tube by a final wrap of fiberglass tape of an appropriate width, thickness, and helix angle. This construction method is equally well applicable to bores of elliptical or circular cross section.

The method of providing fluid passages throughout the coil is not settled. In the fully impregnated type of coil, several methods are under consideration. One method consists of placing rubber bands wherever passages are required. These are then pulsed out after impregnation. This works well for passages of simple geometry, but tends to fail when the passages are of too tortuous a geometry. Another method consists of placing Woods metal alloy or wax in the coil of the same shape as the network of fluid passages. These materials would have a melting point slightly higher than the cure temperature of the epoxy, but not so high that one would be concerned about damage to the epoxy or Formvar used on the superconductor. The removal of the molten materials may have to be assisted by centrifugal force produced by spinning the coil. In coil designs which are not fully impregnated, provision of fluid passages is a much simpler matter.

In the first shell model, the fluid passages are provided by grinding grooves in the bore tube, placing a mylar spacer between the two shells, and leaving space between the bands.

It became obvious when we wound the first shell type coil that a rectangular wire shape was not well suited to this geometry. Along the length of the coil, the wires touched only at the corners, leaving small triangular gaps which reduced the packing factor. Also, any forces between turns would result in high localized stress levels where the corners of the wires touched. At the ends, where the wires saddle over the bore tube, the wires keystoned and again touched only at the corners. Happily, we found that keystoning the wire before winding solved both problems. Along the length of the coil, the sides of the wires touch, and at the ends the initial keystoning counteracts the keystoning resulting from saddling over the bore tube, resulting in the rectangular cross section of the original wire. This situation will not be quite so happy if we use an elliptical bore, but we believe that some average keystoning shape will result in an acceptable coil in both the circular and elliptical bores.

Since the permissible current level in a superconducting wire is a strong function of the magnetic field surrounding the wire, it is, of course, tempting to use different size wires for the high field and the low field portions of the coil. We decided to limit ourselves to two wire sizes in order to limit the problems and costs of procurement of the wire. Working from a detailed calculation of the field distribution throughout the coil cross section, we found that it was very easy to design a shell type coil with the two inner layers made of a large wire and the two

outer layers made of a small wire. The area ratio of the large to the small wire can be about 1.8 to 1 if the small wire sees a magnetic field not in excess of 25 kG. At the ends of the coil, one must be careful to place the small wire in a low field region. We are attempting to apply the same principle to pancake coil designs, with somewhat more difficulty.

A major problem with a warm iron dipole design is that any error in centering the coil in the iron bore results in a large force in a direction to further displace the coil. Thus, if the suspension which holds the coil in the iron bore has a spring constant which is lower than this magnetic displacement force, the system is unstable in the sense that the displacement of the coil will increase without limit. Therefore, the suspension must be designed under the dual constraints of high spring constant and low thermal losses. One design that has evolved consists of two concentric rings with fiberglass nomofilament prepreg ribbon wrapped around both rings. The outer ring, which is made of stainless steel, would be spot welded to the outer vacuum tube. The inner ring, made of aluminum, would be dimensioned to slide on the inner vacuum tube at room temperature. Since the aluminum has a higher coefficient of contraction than the stainless steel vacuum tube, it can be dimensioned to seize on the stainless tube just before the final operating temperature is reached. The assembly is thereby firm and without play, while at the same time permitting the large longitudinal contraction of the inner vacuum tube and coil. Another design which has been proposed consists of thin columns of stainless steel tubing or ceramic tubing supporting the forces in compression. These tubes would be fastened to the inner vacuum

tube and slide on the outer vacuum tube. Either of these designs could be used with or without an intermediate heat shield. This is a tube in the space between the inner and outer vacuum tube which would be cooled to about 15^{o} to 20^{o}K by means of separate connections to the refrigerators. All designs, of course, use superinsulation in the vacuum space for the primary thermal insulation.

We consider the outer mild steel core to be the main structural element.

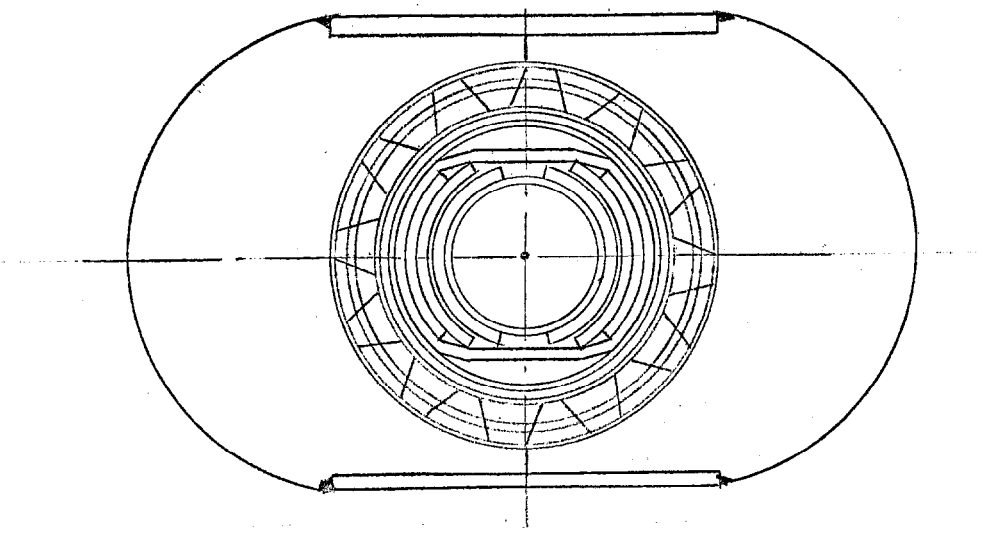

Shell Dipole Cross Section

It will consist of low carbon steel laminations bonded together with epoxy. A flat steel plate at the top and bottom will provide the required structural strength. The steel core will also have an upward chamber built into it during fabrication. This will be of such a magnitude that when the magnet is supported at the ends, the core will sag to a perfectly flat shape.

In the present concept, the dipoles will be suspended from the ceiling of the main ring tunnel, perhaps from the existing

Unistruts. It is planned to have them remotely adjustable in elevation, radius, and tilt. The details of this system have not yet been designed, but it will be similar to that developed by R. R. Wilson and his colleagues at Cornell University.

The vacuum system has not yet been designed. We would expect it to be similar in concept to the main ring magnet system, with roughing pumps located in the service buildings, booster pumps in the tunnel below the service buildings, and pumps at intervals around the main ring. Whether the ion pumps will be on every dipole, or spaced at longer intervals, is not yet clear. The vacuum required to start is that at which the superinsulation begins to function with low heat loss, so that cooldown of the coil can proceed. After that, the system can be considered as cryopumped. We assume, at this time, that the bore vacuum and the superinsulation vacuum are interconnected.

Chapter VII

THE CRYOGENIC SYSTEM FOR THE PROPOSED NAL ENERGY DOUBLER

W. Fowler, P. Vander Arend*

As in the case of the initial concept of the energy doubler, the proposed refrigeration system for the superconducting magnets is highly influenced by the utilization of existing facilities at NAL; i.e., the tunnel, the service buildings, the connecting passages from the service buildings to the main ring tunnel and the utilities. Several schemes have been looked at for cooling the 20,000 feet of superconducting accelerator magnets to liquid helium temperature ($\simeq$4.2°K).

Since there are twenty-four service buildings located at approximately 800 foot intervals around the accelerator, and these buildings are only partly occupied with equipment, we have considered locating the cryogenic refrigerators or liquefiers in these buildings and have investigated the feasibility that each liquefier or refrigerator will service at least 800 feet of energy doubler magnets. Depending on refrigeration requirements and the size of equipment it may be feasible to reduce the number of refrigerators to twelve.

Other design parameters chosen at the start of the project were the following:

* Cryogenic Consultants, Inc.

a) The magnets will be constructed with warm iron located outside the vacuum shell of the magnet dewar.

b) Total refrigeration requirements were selected to be 5 watts per meter. This number was chosen on the basis of information given in papers by P. F. Smith and Bronca et. al.

In particular, in the second reference for a rise time of 33 sec, the total losses were given as 4.4 watt/meter for a warm iron magnet similar to energy doubler magnets. The static losses were estimated as 3.5 watts/meter, leaving 0.9 watts/meter for the ac losses. We, therefore, began our studies by using the following division of the refrigerator loads:

ac losses in the magnet	1 watt/meter
heat gain through insulation and supports of the magnet	2 watt/meter
miscellaneous	2 watt/meter

The total amount of refrigeration to be provided served primarily as a guide in order to be able to develop concepts for the refrigeration system. As noted in Chapter II, the 1 watt/meter is affected strongly by the filament diameter of the superconductor and that an initial choices may have to be modified to achieve the projected one watt/meter.

The cryogenic development work has been carried out along two main avenues as follows:

a) Conceptual design of the magnet dewar and support systems.

b) Transport of the required refrigeration from the

service building into the tunnel and along the system of magnets.

The use of warm iron makes it necessary to use a rigid support system between the magnet and the iron. The spring constant of this support system needs to be high to reduce deflections from out of center location of the magnet relative to the iron. At the same time it is necessary to realize a low heat leak and reasonable cost and ease of installation.

Calculations of magnetic forces indicated that the force moving the coil in horizontal direction is 600 lbs per running foot and 200 lbs per running foot in the vertical direction of a misalignment of .010" from the center of the iron.

Two support systems are under development; Figure 1 shows the schematic arrangement of a support system consisting of pins which carry the forces directly from magnet to iron through the various shells of the magnet system. The frequency of the support system is determined by the beam properties of the magnet and the bore tube. It appears that support pins located at intervals of one foot will carry the load adequately.

When the magnet system is warm, the assembly as shown in Figure 1 is held rigidly, relative to the vacuum jacket of approximately 6" diameter which in turn is locked into the iron. During cooling of the magnet, the system shrinks and only the two lower supports touch the outside vacuum shell. The magnet is in stable position as long as the resultant forces are directed downward and in between the two pin supports. In order to satisfy this requirement, certain tolerances cannot be exceeded

during the assembly of the magnet.

A different support system is shown schematically in Figure 2. The supports are located at one foot intervals along the length of the tube by dual rings held together by means of fiberglass tape. This system is discussed in more detail in Chapter VI.

Both support systems are reasonable from a standpoint of heat leak between the outer vacuum vessel and the magnet dewar.

Magnet cooling has been investigated. One of the important requirements is the removal of ac heat from the windings of the coils. Some calculations were carried out which indicate that channels spaced in between pancakes or shells will allow circulation of liquid helium through the coil at a rate sufficiently high to maintain the coil temperature within .1 or .2°K of the bulk helium temperature. The removal of heat is based on the generation of convective currents in the helium. These currents are generated through density differences in the liquid and cooling of the bulk fluid outside the coil. The cross sections of the channels need to be large enough to allow sufficient flow based on the available driving forces. It appears that a high current density in the magnet is compatible with sufficient flow of helium through the channels.

It should be noted that the channels discussed above are located in a plane parallel with a cross section of the magnet. The channels do not serve to carry liquid helium in longitudinal direction necessary to transport heat back to the refrigerator

located at the service building.

A considerable amount of work was carried out to devise a system suitable to carry heat from the magnets to the refrigerator. The distance can be great since the magnet located halfway between adjacent service buildings is 400 feet from the nearest refrigerator.

Cooling of bulk helium surrounding the magnet coils may be carried out either by vaporization of liquid or by flowing super critical helium.

The use of boiling helium, if carried out in the conventional way, represents a number of problems as follows:

a) It will be very difficult to maintain in accurate liquid level in each magnet dewar.

b) An expensive distribution system is required for carrying the right amount of liquid to, and to remove the vapor from, each magnet.

The use of super critical helium requires flow through the magnet system from service station to service station. Heat is removed by the flowing helium. In order to remove this heat, the temperature of the liquid needs to rise. This phenomenon sets requirements on minimum flow rate, maximum permissible temperature rise, minimum allowable cross sections for flow to maintain tolerable pressure drop, etc.

After some detailed analysis of both approaches to magnet cooling, a concept of magnet cooling was developed which appears to have many advantages of the single and two phase cooling systems. Figure 3 shows the basic flow schematic of the system.

Liquid helium from the reservoir in the liquefier is pumped to a pressure of 10-15 psig by a reciprocating or centrifugal pump. The liquid flows throught the magnet dewars for a distance of at least 400 feet. At this point the pressure of the liquid is reduced by flowing through a throttle valve. The liquid now becomes boiling liquid. The two phase stream returns through an annulus surrounding the magnet dewar to the refrigerator. Remaining liquid is separated from the gas in the refrigerator. The gas is then processed by the refrigerator and recondensed.

One of the features of the system is that the liquid helium flowing through the magnet is cooled by the boiling liquid helium surrounding the magnet vessel. Calculations show that removal of the ac heat from the magnet reservoir may be accomplished with a very small termperature difference between the two streams. Also, the temperature of the liquid helium in all magnet reservoirs is the same and only a function of the temperature of the boiling helium surrounding the magnet vessels.

The temperature at which the magnets are maintained is controlled by the pressure of the boiling liquid helium in the annulus surrounding the magnet vessel. It is relatively easy and inexpensive to reduce the temperature level of the magnet by reducing the vapor pressure of the boiling liquid helium. This may be done by adding a vacuum pump or extra stage to the compressor of the helium liquefier. Not all of the flow circulating in the helium liquefier will be processed by the vacuum pump, but only that part which is vaporized in the magnet cooling system. The increase in cost and required horsepower is

relatively small. By this technique it would be possible to optimize the operating temperature of the magnet between a minimum of 3.6°K and a maximum of 5°K. This could be a very important cost factor due to the increased current density in the conductor at lower operating temperatures.

Figure 1 also shows a modification of the basic magnet system. The modification consists of a cooled shield which is located between magnet reservoir (with return annulus) and the warm outer shell. The purpose of the shield is to intercept practically all heat flowing in from the warm environment through radiation and conduction. By maintaining the shield temperature in the range of 15-20°K it is possible to remove a large part of the heat at a fairly high temperature level. The removal of heat is easily accomplished through flow of high pressure helium through tubes located on the shield. The helium leaves the refrigerator as cold helium and returns to the same refrigerator at a slightly higher temperature and somewhat lower pressure. Calculations show that pressure drops are reasonable when helium of a pressure of 20 atm is used. Also, the power requirements necessary to provide refrigeration at the higher temperature level are approximately 1/3 of those required at 4.5°K. Furthermore, it is easy to incorporate the refrigeration at 15-20°K. The magnet support systems discussed earlier both lend themselves to use with the cooled radiation shield.

The concept of single phase liquid helium flow one way with boiling liquid helium the other way uses the magnet system

itself for transport of the cold fluids. It is not necessary to provide the very expensive extra vacuum jacketed piping running in parallel with the accelerator which would otherwise be needed. Also the distribution of liquid helium to individual magnets is solved. The number of valves required to operate the system is minimal and so far everything points to a system which may be built at a reasonable cost.

The overall cryogenic system is based on the present state of the art components. The refrigerators may be built by industry. The amount of transfer line necessary to carry the liquid and gaseous helium between service buildings and tunnel is minimal and of small size. The component with least amount of experience is the liquid helium pump. However, pumping liquid helium under the conditions required for the proposed system is well within the state of the art.

In order to gain experience at an early date with various facets of the cryogenic system, a pump loop of rather large scale will be installed in the near future. The pump loop will employ a liquid helium pump of the required capacity for the ultimate system. A helium liquefier with a capacity of 150-200 liters per hour has been acquired and is presently being installed at the site of the pump loop. It is planned to install as much as 400 ft of liquid helium piping in a configuration which resembles the magnet dewar arrangements. At the end of the 400 ft a valve will be used to reduce the pressure of the liquid helium

in the line. The condition of a stream of two phase fluid surrounding the single phase layout will be simulated.

The pump loop will be a "field" installed facility and it will be possible to remove sections of the loop and insert dewars with or without magnets.

The pump loop will be used to gain experience with a large system of the type to be used for the energy doubler. It will be possible to carry out tests of various types in the loop. For instance, the loop will be used to study the effects of a magnet going normal. Also heat transfer can be evaluated and heat going through various types of insulation. Non-steady state conditions such as cooldown of a section of 400 ft of magnets will be simulated.

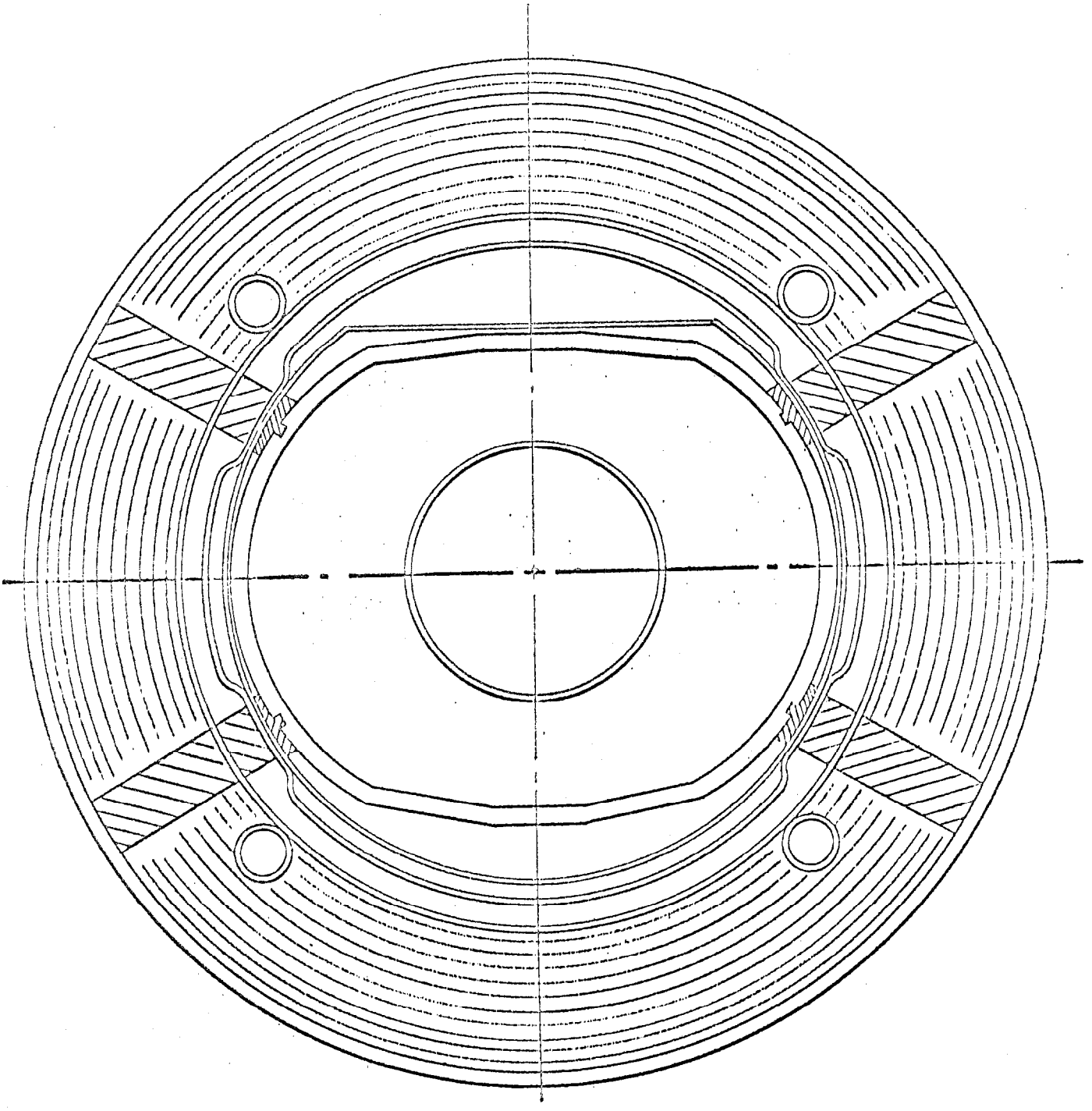

FIG. 1 - PROPOSED RIGID POST MAGNET SUPPORT SYSTEM

REVISIONS			
SYM	DESCRIPTION	DRAWN / APPD.	DATE

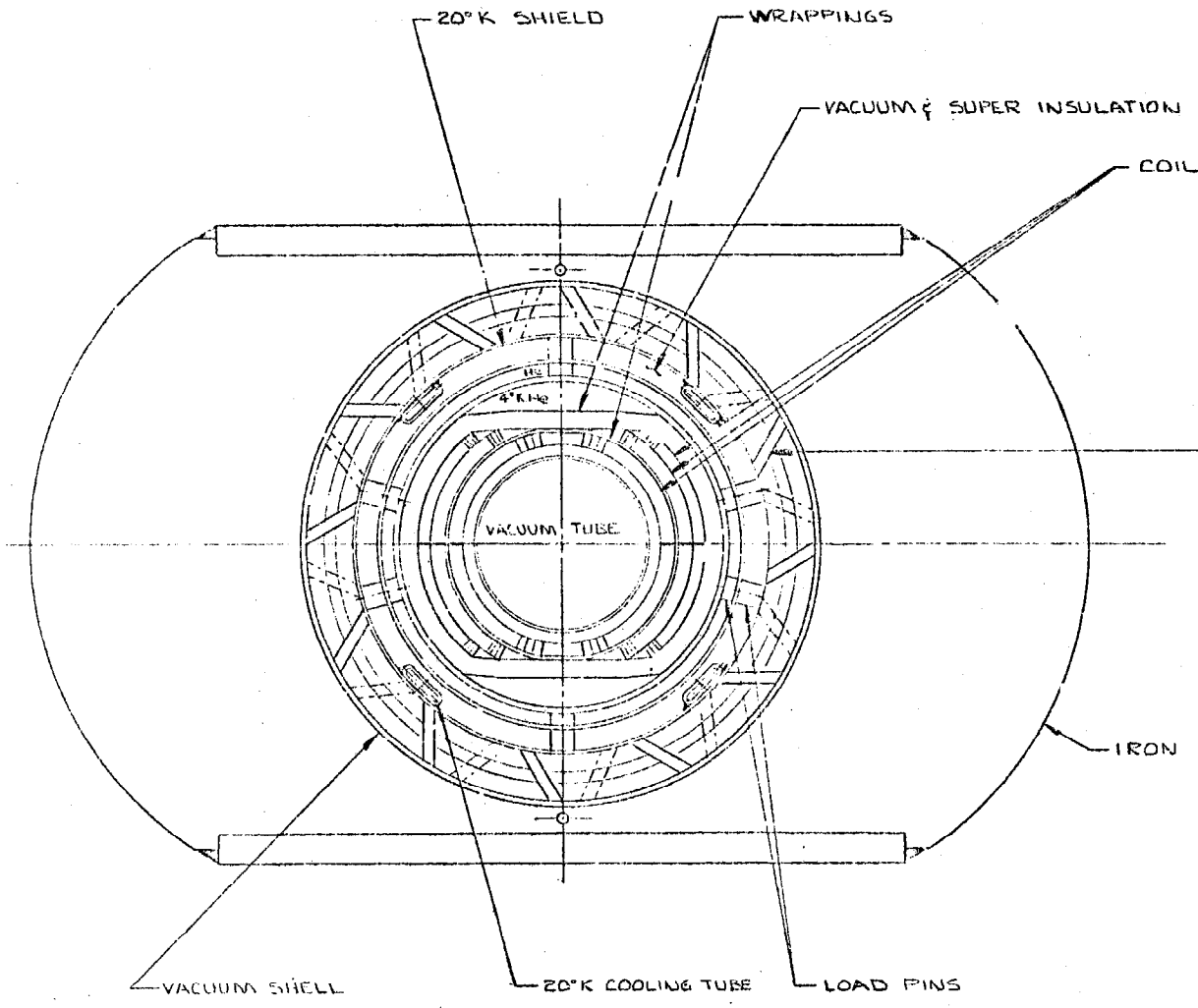

ITEM NO.	PART NO.	DESCRIPTION	QTY. REQ.

PARTS LIST

UNLESS OTHERWISE SPECIFIED			ORIGINATOR		
FRACTIONS	DECIMALS	ANGLES	DRAWN	D OLSON	1-30-73
±	±	±	CHECKED		
1. BREAK ALL SHARP EDGES 1/64 MAX.			APPROVED		
2. DO NOT SCALE DWG.			APPROVED		
3. DIMENSIONING IN ACCORD WITH USASI Y14.5 STD'S.			USED ON		
√ MAX. ALL MACHINED SURFACES			MATERIAL-		

NATIONAL ACCELERATOR LABORATORY
U.S. ATOMIC ENERGY COMMISSION

ENERGY DOUBLER
S3A COIL WITH HEAT SHIELD
CROSS SECTION

SCALE	FILMED	DRAWING NUMBER	REV.
FULL		0428-MC-53049	

TM-421

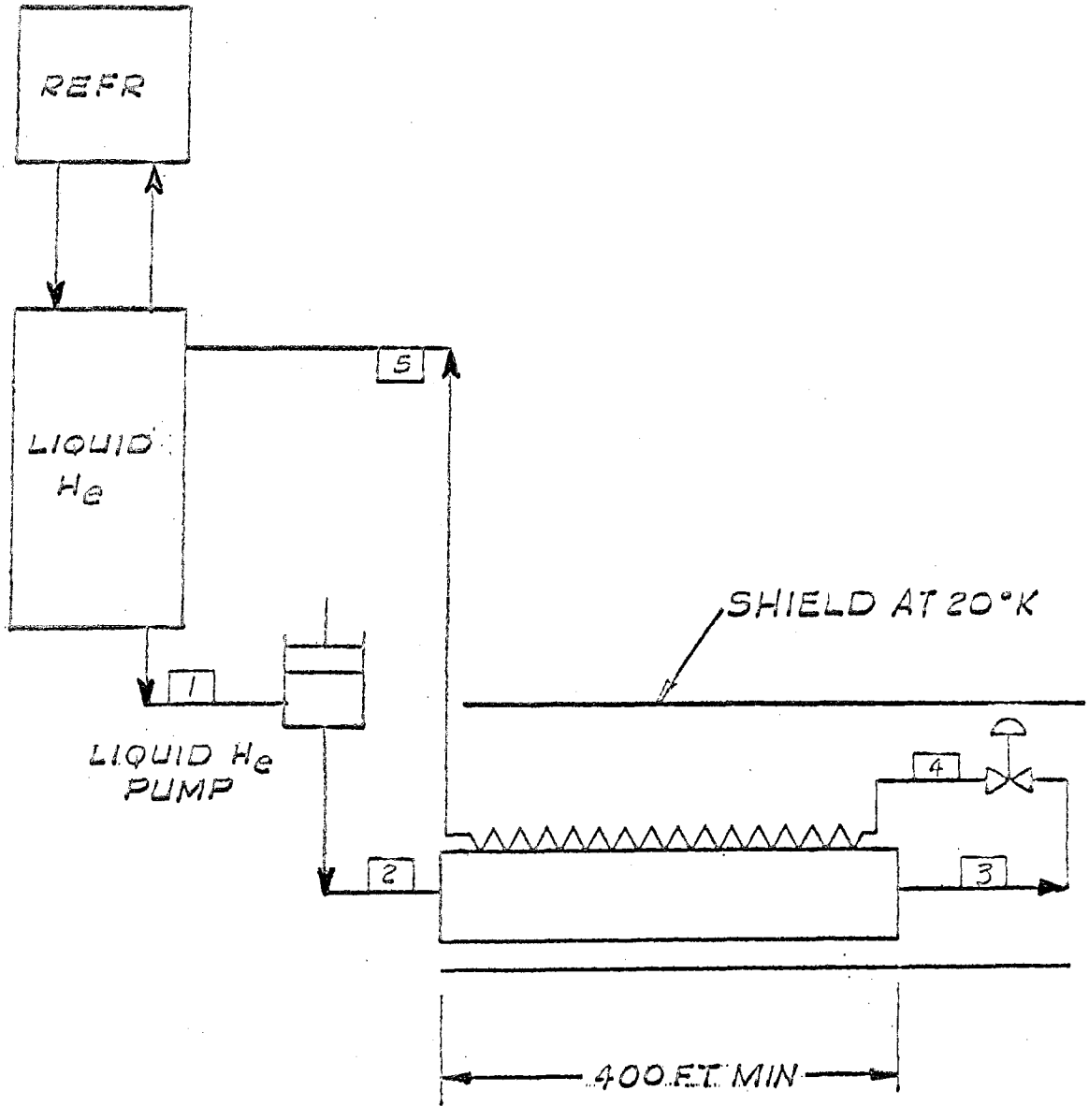

FIG. 3 - MAGNET COOLING SCHEMATIC

Chapter VIII

TESTS OF THE FIRST ENERGY DOUBLER PROTOTYPE MODELS

B. P. Strauss, P. J. Reardon, D. F. Sutter,
R. McCracken, D. E. Richied, M. A. Otavka

The first two model magnets, the Mark I Pancake (P8A) and the Mark I Shell (S4A), were constructed from the 361 filament wire purchased off the shelf from Magnetic Corporation of America. They were, therefore, not expected to perform as well as later models using more suitable wire. The main purpose for building these two magnets was to test theoretical models for design of the magnets, concepts of fabrication for both types of magnets, adequacy of the rather innovative cooling concepts, difficulties that might be encountered in achieving the higher current densities, and to gain some experience on testing pulsed superconducting magnets. Two other pancake models were also constructed and tested. Both had the same design as far as location of the windings, but each had a different method of clamping. The first used an impregnated epoxy clamping method and the second used windings of mylar and fiberglass to retain the coils.

A brief description of tests and the results obtained with these magnets follows. They were tested under dc and pulsed conditions in both vertical and horizontal dewars. In the horizontal dewar a warm iron shield was added and its effects were determined. In the tests completed so far, results from the dc tests were most encouraging as the magnets achieved the maximum current density

expected and operated at higher fields than anticipated. A note of caution, however, these higher current densities were obtained at fields less than would be experienced in the final design and the coil clamping system withstood considerably less force than it will be required to do in that design.

GENERAL PROCEDURE

A general block diagram of the test system is shown in Figure 1. A number of supplies other than the Transrex 500-5 were used. The first supply used was a reconditioned electro-plating supply consisting of a six phase transformer and copper oxide rectifier system controlled by a three phase Variac on the input side of the transformer. There was no other regulation of filtering. Ramping was not done with this supply.

For the first ramping tests, an HP 6464A power supply operating in the remote programmed, current regulation mode was used instead of the Transrex 500-5. The HP 6464A is an SCR controlled type and suffers from severe turn-on transients when operated with the SCR's phased back for low level output. Damped vibrations in the coil were observed at turn-on and several times during some ramps. In the second version of this system, the 6464A supply was replaced by the Transrex 500-5 supply which is used in the NAL experimental areas. In all cases, safety circuit, consisting of a precision voltage comparator and relay driver, was installed across the output of the power supply and automatically shut off the supply whenever the onslought of a quench caused the voltage across the coil to exceed a preset value. This let the coil back emf forward bias a normally reverse biased diode and dump the stored energy into a special load resistor constructed of stainless steel tubing.

During all power tests, x-y recorder plots were made of coil voltage vs. current. In addition, voltages across the power supply as well as other portions of the apparatus were monitored.

An automatic liquid helium filling system was used to maintain liquid level. This consisted of a voltage comparator looking at the voltage across a superconducting liquid level gauge. On low level the comparator would trigger an NAL design in-line valve[1] for a set filling time after the set point was passed.

In all tests the magnets were precooled with liquid Nitrogen which was purged before the introduction of the liquid helium. The magnet itself was its own thermometer; its resistance was measured continuously during cooldown and the resistance ratio was compared to that of OFHC copper to find the temperature. Normally, cooldown was accomplished within three hours.

DC POWER TESTS

Before the cooldown, each of the coils was subjected to a ringing test for shorts, an inductance test, a dc resistance measurement, and a megger test. The ringing, inductance, and megger tests were repeated at both liquid Nitrogen and liquid Helium temperatures.

TESTS ON THE MK I-P8A DIPOLE

The unshielded Mark I Pancake model was tested in a vertical position in a pool of boiling Helium, suspended from a flange by an extension of the main beam tube. The test assembly was fitted with a pair of American Magnetics model L-2000 counter-cooled current leads. Voltage leads were placed at the top of the cooled

---

[1] M.A. Otavka, B.P. Strauss, and R.W. Fast, "A Magnetically Operated Cryogenic Valve," Advances in Cryogenic Engineering, Vol. 16.

leads, at the junction of the cooled leads and the magnet leads, and at the magnet just before the potting.

On the first runs the MK-I (P8A) magnet (Figure 2) could not be energized above 825 amps. Training was evident and was thought to be from movement of the leads. The test assembly was removed from the cryostat and lead separation was found. This was repaired and all parts of the current lead assembly were reinforced by potting with epoxy. On subsequently energizing the coil it was found that the quench current could be "trained" to ~1500 amps which corresponds to a field of 2.7T in the center of the two inch bore. This occurred in about 100 amp steps during repeated cycling of the magnet. As expected, the quenches showed no evidence of current sharing because of the high current density in the wire as well as the low copper to superconductor ratio. An average quench consumed about three to five liters of Helium since the stored energy was low. It should be noted that the wire is not intrinsically stable since the filament size is large, the copper to superconductor ratio small, the the twist length ℓ_c is relatively large.

A copy of the operating curve of the P8A magnet is shown in Figure 3.

Preliminary field plots for this MK I-P8A Pancake Magnet were obtained with a Rawson probe, and confirmed that the calculated transfer constant was correct. Measurements taken along the axis of the magnet show a small rise in field in the ends of about 1% and then a fall to zero in about eight inches. (Figure 4)

A series of current ramps were run on the MK I-P8A magnet. Although the statistics are far from complete, it can be inferred

that the coil showed severe ramp rate sensitivity. To some extent this was expected. The filament size is twice as large as that required for intrinsic stability at the ramp used. The twist rate is too low to provide decoupling of the filaments, and there is an extra coating of epoxy on the coils further limiting heat transfer.

Some other characteristics of the quenches are interesting. All occurred after at least one cycle, and many showed current sharing in the conductor as evidenced by an IR voltage drop in addition to the inductive voltage drop. This seems to indicate an increase of magnet temperature with time. This current sharing can be expected for this conductor at the low maximum current attained in this test.

The MK I-P8A Pancake was later tested in a horizontal cryostat of NAL design. Due to the lack of a vapor bleed chimney at the far end of the cryostat, cooldown was somewhat complicated since there was poor heat transfer between the vapor and magnet. During the run there was some difficulty in maintaining liquid level in the cryostat due to accumulated gas bubbles over the windings. As a result, the highest current we were able to attain in this cryostat was only 700 amps. No ramp tests were run in this magnet configuration.

THE MK I-S4A DIPOLE

The MK I-S4A magnet (Figure 5) was tested in the vertical cryostat using the same procedure as for the pancake magnet. This magnet showed very little training and reached a peak current of 1500 amps after only two quenches. This corresponds to a magnetic field of 3 Tesla in the center of the 1.5 inch bore. The dc performance curve is shown in Figure 6. Figure 7 shows the magnetic field curve measured with the Rawson probe along the axis which, as for the P8A dipole, shows a 1% rise and then a fall to zero in 5 inches.

This magnet was not sensitive to ramp rate and could not be driven normal even when subjected to peak ramp voltage of 10 volts or 100 A/second. These tests were run repeatedly up to the maximum critical current found in the dc tests by presetting the plating supply to the desired current and pushing the "ON" button. A second test of this magnet was run with the Hewlett-Packard supply described previously. The magnet was pulsed at many different rates of rise and ultimately at a 6 second repetition rate to a field of about 1.7T for over an hour from a low field of 0.2T. This corresponds to the maximum current output of the 6464A supply which was 850 amps, which is equivalent to an energy level of 400 GeV in the present NAL machine.

The MK I-S4A magnet was then fitted into the horizontal cryostat which was previously modified with a vapor bleed stack at the far end. Even with this stack, liquid level instrumentation showed large variations in liquid during ramping. The magnet operated to the same dc critical field as measured vertically. The warm iron flux return shield was subsequently fitted around the dewar. The iron enhancement factor was 1.18 to the highest fields measured, indicating that we had not reached saturation. A "pulse" test was performed using the 100 second repetition rate suggested for the Doubler. This test was performed with an injection current of 200 amps (121 GeV), a peak current of 1410 amps, a 20 second flat top, an "injection" period of 20 seconds, and a ramp rate corresponding to a $\dot{B}$ of 800 G/s. The peak field under these circumstances was 3.8T which is equivalent to 845 GeV. It should be noted that during the pulse test the magnet operated to 98% of its dc quench point in the horizontal cryostat. Within 0.5% accuracy of measurement, the magnet was reproducable from pulse to pulse at injection and flat top fields.

In order to determine ramp rate sensitivity of the magnet, the repetition rate was shortened gradually to 16.6 Hz^{-1}. The magnet ran successfully between the same peak and injection current conditions as above. At 13 Hz^{-1} the magnet quenched.

Two identical magnets, except for the method of coil clamping, were constructed from the second order of superconducting wire (Table II Chapter V). The first magnet used the fully impregnated epoxy structure discussed in Chapter VI while the second magnet used a banding method consisting of many individual bands. This second model was constructed in order to eliminate the thin coating of epoxy that was evident over the "open" portions of the windings in the fully impregnated windings. To put things more fully in perspective, it should be noted that these magnets were designed for the forced sub-cooled convertive cooling described in Chapter VI and not for the pool boiling helium in which they were tested. In each version of the structure and in any test configuration, these magnets had small cross section channels of large horizontal extent. This tends to lead to gas accumulation over the windings and poor heat transfer.

Both magnets were run to a maximum current of 1900 amps corresponding to a field of 3.4T in the bore. This was accomplished only after much training and by increasing the current at a very slow rate with a number of rest levels to maintain thermal equilibrium. Attempts were made to cycle the magnets when each was in the vertical dewar. The results for the fully impregnated magnet were not promising. However, the banded magnet was able to be cycled at a 33 second repetition rate from an injection field of .5T to a flat top of 3T or an equivalent energy of 666 GeV. This "ultimate"

repetition rate required a lot of training and could only be attained after increasing the cycle rate from 10^{-3} Hz to 6×10^{-2} Hz. All these tests were without the iron shield.

The fully impregnated model was fitted into a horizontal cryostat. Because of the design, only runs with the iron shield were made. The magnet operated to the same field-current product as without the iron shield. This corresponds to the same stored energy and forces on the conductor.

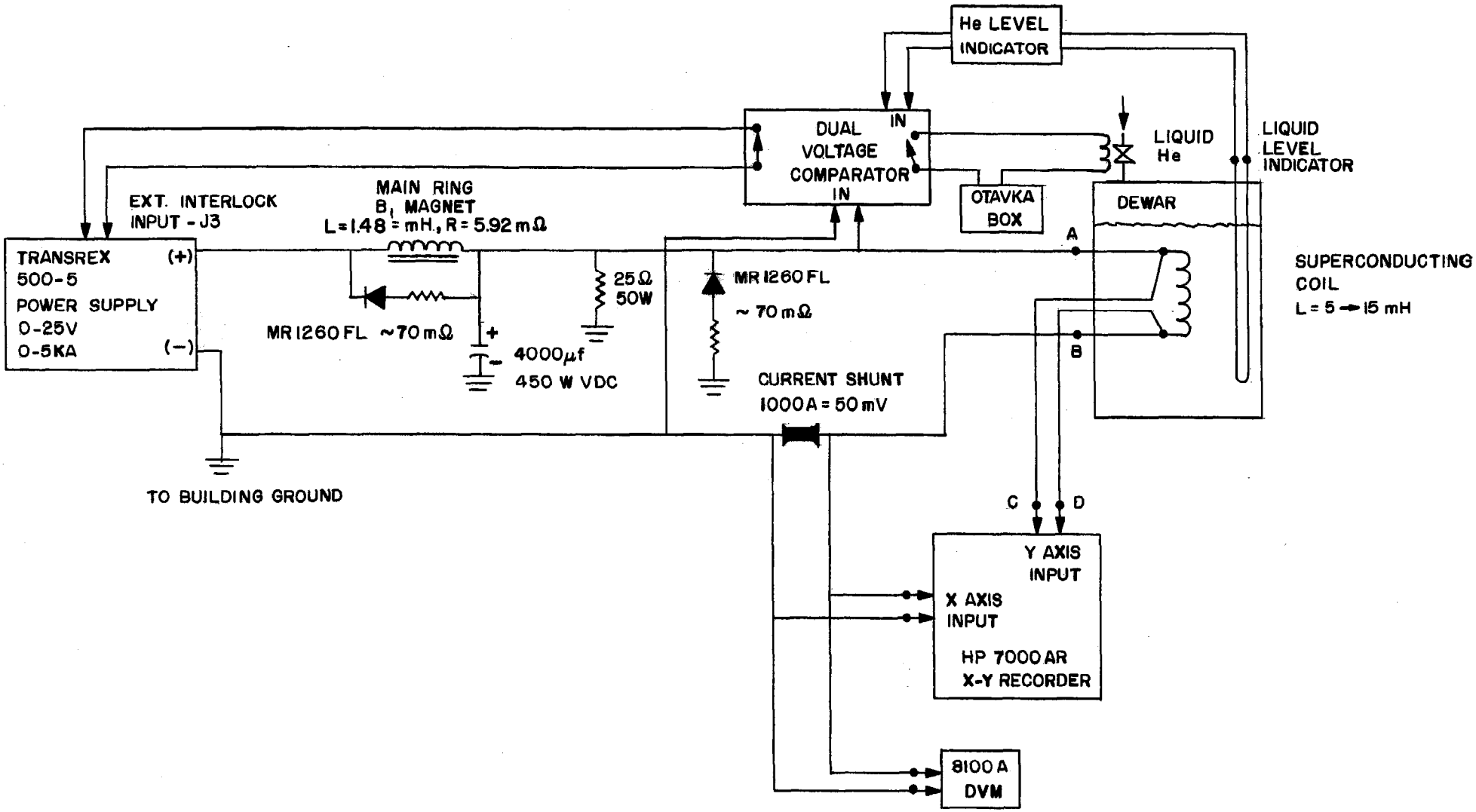
He LEVEL
INDICATOR
DUAL
VOLTAGE
COMPARATOR
IN
IN
LIQUID
He
LIQUID
LEVEL
INDICATOR
OTAVKA
BOX
DEWAR
EXT. INTERLOCK
INPUT - J3
MAIN RING
B1 MAGNET
L=1.48 = mH, R=5.92 mΩ
TRANSREX
500-5
POWER SUPPLY
0-25V
0-5KA
(+)
(−)
MR1260FL ~70mΩ
25Ω
50W
4000μf
450 W VDC
MR1260FL
~ 70 mΩ
CURRENT SHUNT
1000A = 50 mV
A
B
SUPERCONDUCTING
COIL
L = 5 → 15 mH
TO BUILDING GROUND
C
D
Y AXIS
INPUT
X AXIS
INPUT
HP 7000AR
X-Y RECORDER
8100A
DVM

Figure 1

NATIONAL ACCELERATOR LABORATORY ENGINEERING NOTE	SECTION	PROJECT	SERIAL•CATEGORY	PAGE
	Accel.	Energ.Doub.		1

SUBJECT

Design Data Mark I (P8A) Pancake Magnet
Ref: 0428.010-MD-15581 (E)

NAME
B. Strauss

DATE	REVISION DATE
15 Jan 73	14 Feb 73

Type	Intersecting Ellipse
Number of Pancakes	4 per half
Turns per pancake	26
Construction	Coils epoxy potted into place with 12% face cooling channels

Field Strength (no shield)	20 kG
Field Tolerance (1.5 in. width)	±.5%
Coil Aperture	1.930 in.
Effective Magnet Length	40 in.
Actual Peak Current	1500 A
Peak Current Expected	1400 A
Peak Current Density in wire	40 kA/cm^2
Effective Current Density (overall)	22 kA/cm^2
Turns	208
Transfer Constant (no shield)	18.6 G/A
Transfer Constant (6" i.d. shield)	22.3 G/A
Inductance (no shield)	18.3 mHy
(with shield)	32.6 mHy

Conductor

Manufacturer	MCA
Filaments	361
A sub/A sc	1.25/1
Substrate Material	Copper
Filament Size	0.003 inches
Twist	1 per inch
S. C. Alloy	NbTi
Overall Size	0.112 x 0.056 inches
Insulation	Formvar
Minimum short sample	1250A @ 5T; 1580A @ 4T (bare)

Figure 2

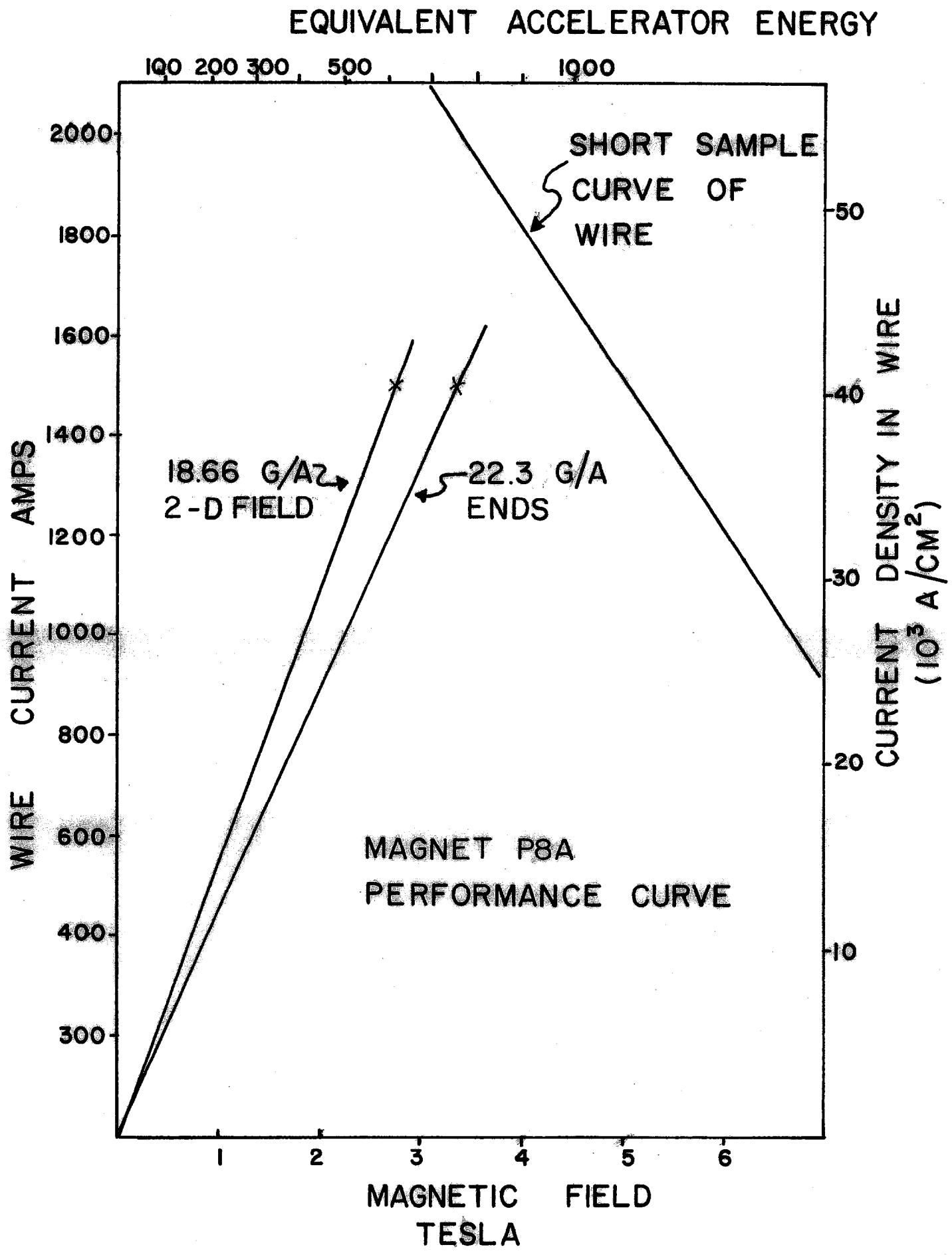
EQUIVALENT ACCELERATOR ENERGY
100 200 300 500 1000
SHORT SAMPLE CURVE OF WIRE
18.66 G/A 2-D FIELD
22.3 G/A ENDS
MAGNET P8A PERFORMANCE CURVE
WIRE CURRENT AMPS
2000
1800
1600
1400
1200
1000
800
600
400
300
CURRENT DENSITY IN WIRE (10^3 A/CM^2)
50
40
30
20
10
1 2 3 4 5 6
MAGNETIC FIELD TESLA

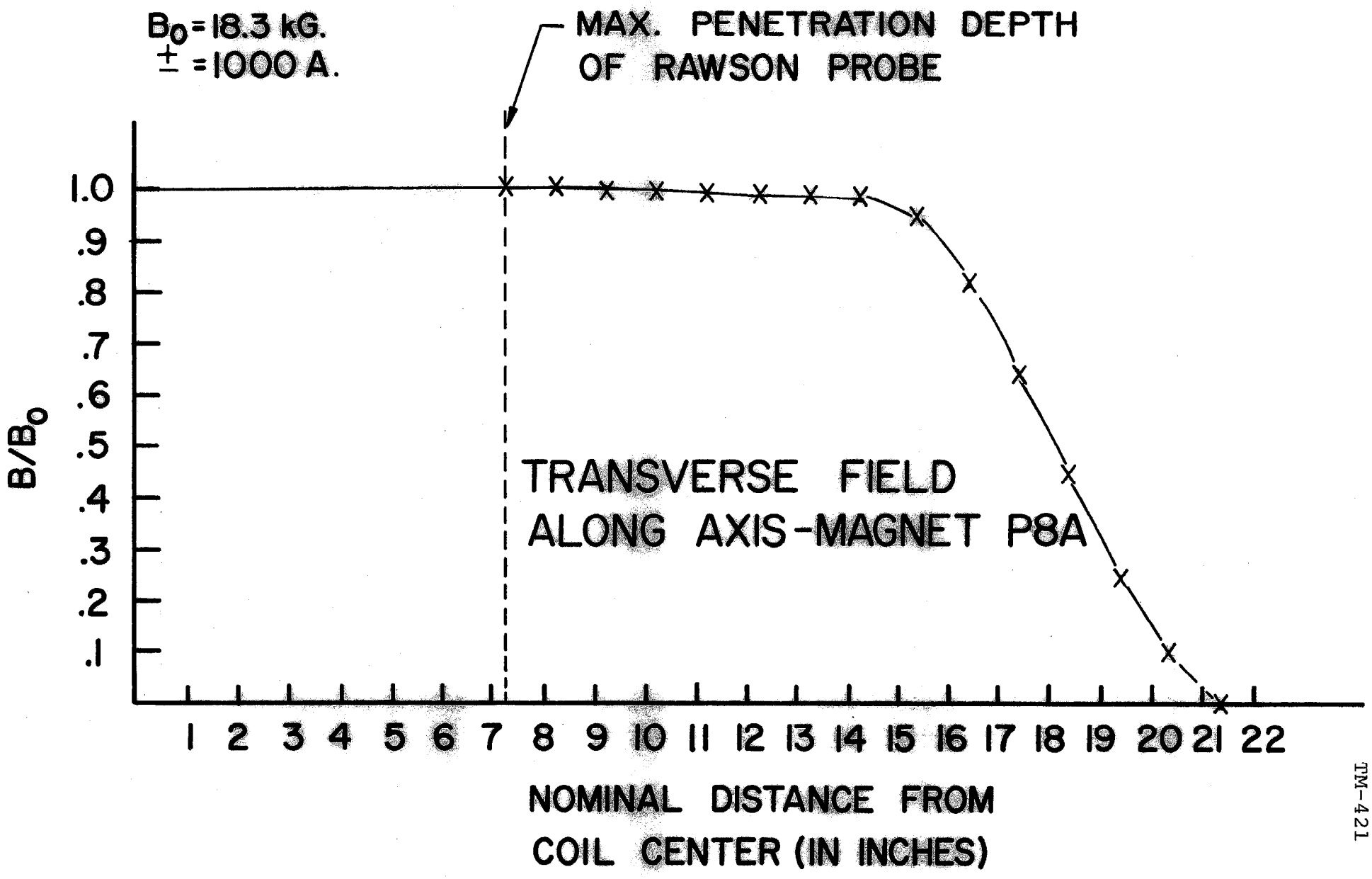
B_0 = 18.3 kG.
± = 1000 A.
MAX. PENETRATION DEPTH
OF RAWSON PROBE
1.0
.9
.8
.7
.6
.5
.4
.3
.2
.1
B/B0
TRANSVERSE FIELD
ALONG AXIS-MAGNET P8A
1 2 3 4 5 6 7 8 9 10 11 12 13 14 15 16 17 18 19 20 21 22
NOMINAL DISTANCE FROM
COIL CENTER (IN INCHES)
TM-421

Figure 4

MARK I S4A SHELL MAGNET PARAMETERS

Field Strength (no shield)	25 kG
Field Tolerance (1.125 in. width)	+3%
Coil Aperture	1.5 in.
Effective Magnet Length	12 in.
Conductor Size	.112 in. by .056 in.
Formvar Coating Thickness	.002 in.
Effective Current Density	27.7 kA/cm^2
Maximum Current Density in Wire	40 kA/cm^2
Peak Current Expected	1400 A
Turns	176
Transfer Constant (no shield)	22.3 G/A
Inductance (no shield)	4.7 mHy
Construction	Coils Epoxy Bonded Mylar wrap for force retention and cooling channels
Location of shells in First Quadrant	(as built)

Shell	Turns/Quadrant	R1(in)	R2(in)
1	22	.800	.916
2	22	.916	1.032
3	22	1.060	1.176
4	22	1.176	1.292

Conductor

Manufacturer	MCA
Filaments	361
A sub/A sc	1.25/1
Substrate Material	Copper
Filament Size	0.003 inches
Twist	1 per inch
S.C. Alloy	NbTi
Overall Size	0.112 x 0.056 inches
Insulation	Formvar
Minimum short sample	1250 A @ 5T; 1580 A @ 4T (bare)

Figure 5

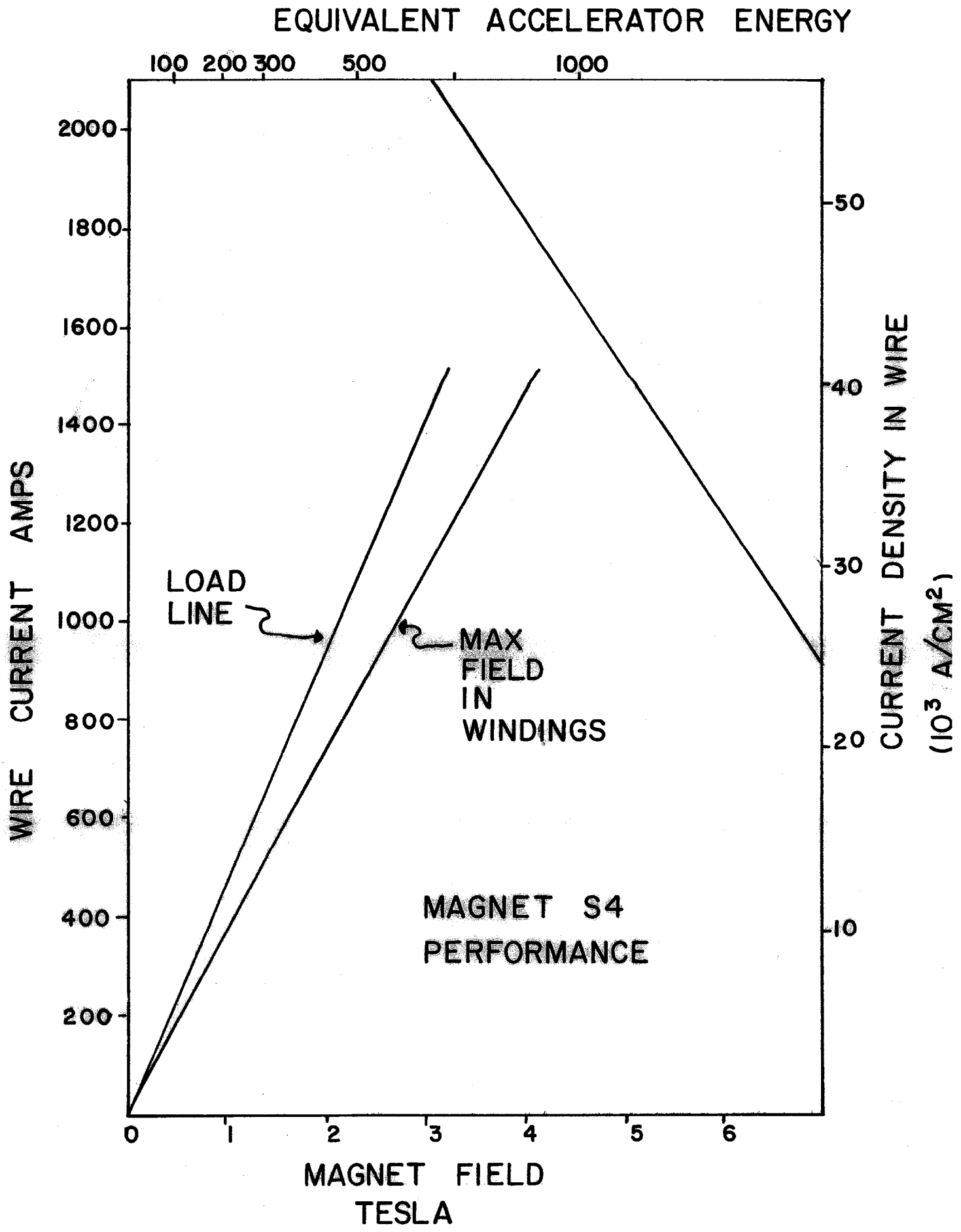
EQUIVALENT ACCELERATOR ENERGY
100 200 300 500 1000
2000
1800
1600
1400
1200
1000
800
600
400
200
WIRE CURRENT AMPS
50
40
30
20
10
CURRENT DENSITY IN WIRE
(10³ A/CM²)
LOAD LINE
MAX FIELD IN WINDINGS
MAGNET S4 PERFORMANCE
0 1 2 3 4 5 6
MAGNET FIELD TESLA

Figure 6

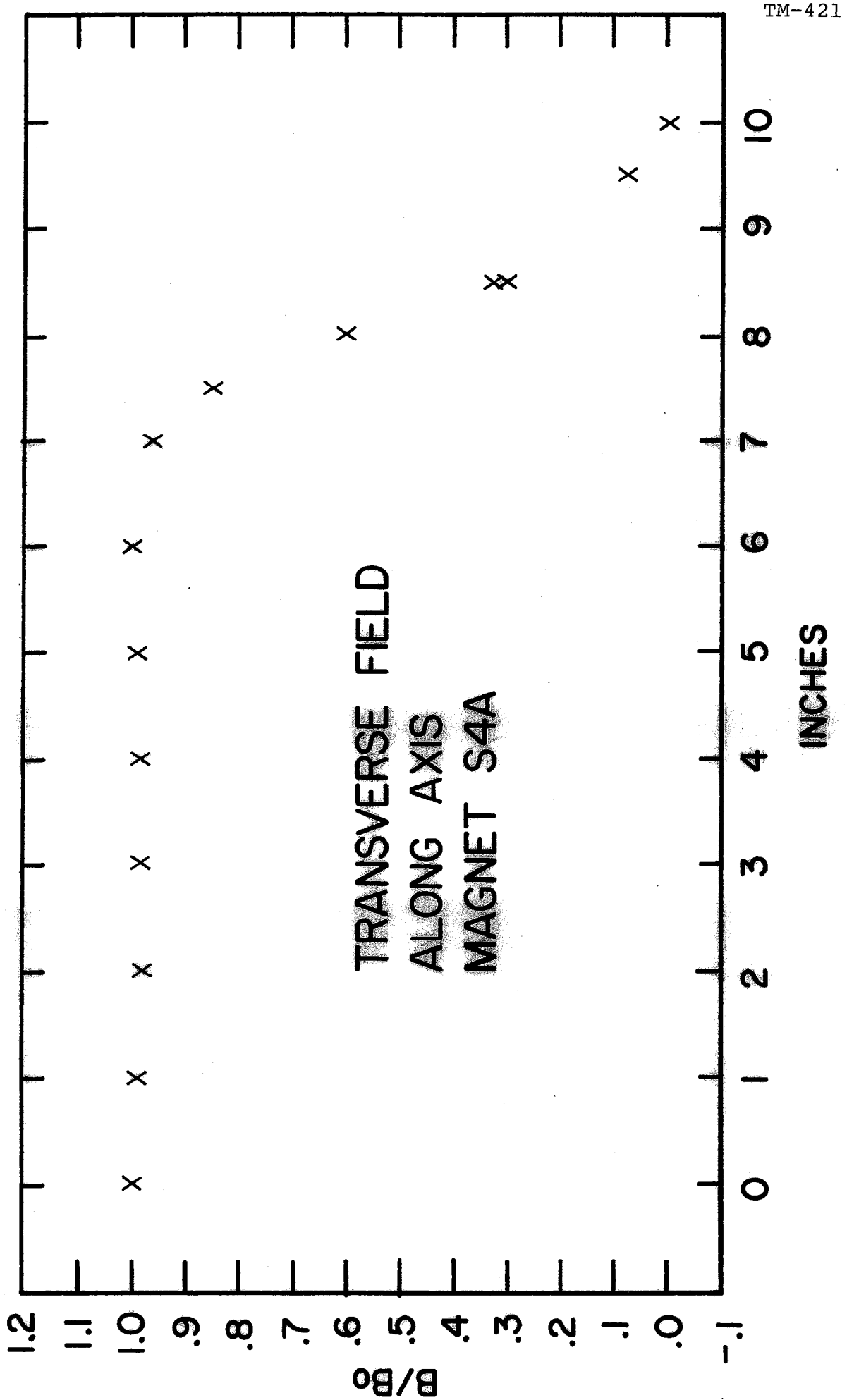
TRANSVERSE FIELD
ALONG AXIS
MAGNET S4A
B/Bo
INCHES
1.2
1.1
1.0
.9
.8
.7
.6
.5
.4
.3
.2
.1
0.
-.1
0
1
2
3
4
5
6
7
8
9
10

Figure 7

Chapter IX

POWER SUPPLY CONSIDERATIONS

R. Cassel, P. J. Reardon

In order to change the field in the superconducting doubler magnets it is necessary to transfer stored energy to or from the magnets. To make the doubler useful for an accelerator, stored energy must be cycled in and out at the desired repetition rate. The present design of the doubler would set its peak stored energy at approximately 300 megajoules. The cyclic energy flow to run the magnet system from 300 GeV to 1000 GeV would be approximately 275 megajoules. On-site storage of this amount of energy in the form of another magnet or capacitor bank would be prohibitively expensive. If, however, the cyclic rate is slow enough, the peak power requirements would be low enough to make it possible to run the doubler directly from the power lines. A plot of power requirements versus repetition rate is given in Figure 1. The peak power requirements for a 60 second repetition rate would be only about 18 megawatts with an RMS power of approximately 8 megawatts. This is in contrast with the present main accelerator running at 300 GeV, which requires a peak power of 112 megawatts and an RMS power of 60 megawatts for a six second repetition rate.

The power required from the power lines is also returned to the power line, resulting in an average power flow of only

approximately 500 kilowatts average. This loss is due to the power supply losses and the losses in the non-superconducting leads.

Static phase back power supplies have the characteristics of being able to supply power to, and put power back into, the line from an inductance stored energy system. The supplies for the doubler could be the same or similar to the existing main accelerator power supplies.

The total voltage required to drive the doubler at a repetition rate of 60 seconds would be approximately 7500 volts. If power supplies and magnets are interlaced, as in the main accelerator, the voltage to ground can be maintained at a low level.

If a maximum of 500 volts to ground were acceptable for the doubler magnets, eight (8) of the presently installed main ring power supplies could be used to drive the doubler. These supplies would not be needed by the main accelerator if it is operated at a 300 GeV or any lower energy level for injection into the doubler. With a small modification to the main ring power supplies, the voltage to ground could be even further reduced, and still allow for operation of the doubler with existing main ring power supplies for injection levels of 300 GeV or lower.

One of the potential advantages of the proposed doubler is the expected savings in power costs for operating the doubler at energies above 200 GeV rather than using the present accelerator for energies up to 500 GeV. At 300 GeV, our nominal operating energy, the average power used by the accelerator is about 30 megawatts for a six second pulse rate with a half second flat top which costs for a 90% duty factor about $2.2 million per year in FY 1973 dollars. Operating the doubler at essentially any

energy up to 1000 GeV above a 300 GeV injection point with a sixty second pulse rate would require about an additional 10 megawatts for refrigeration, magnet power supply and RF, and bring the power bill up to about $2.8 million per year. This is to be contrasted with the calculated bill for 400 GeV on the same basis but with an 8 second repetition rate including a half second flat top of about $4 million per year.

Operation of the present accelerator at 500 GeV with a 12 second repetition rate and no flat top takes 75 megawatts of power which with a 90% duty factor would cost, again in FY 1973 dollars, $5.4 million per year. On the other hand, injection at 200 GeV into the doubler requires no flat top and uses 10 megawatts of power for a 3 second repetition rate which would develop a total cost including the 10 megawatts for the doubler of about $1.25 million per year for a 90% duty factor. The proton energy (admittedly with about a factor of ten reduction in average intensity assuming 2 pulses out of 20 are injected into the doubler with the remaining 200 GeV pulses being used to conduct a low energy research program) would be up to 1000 GeV with as long a flat top as is desirable. In time, and even to a large extent already due to increasing costs for power because of higher fuel costs and lower operating budgets, operation of the present accelerator at 400 GeV and 500 GeV will become cost prohibitive for long runs and, of course, impossible above 500 GeV.

DOUBLER PULSED POWER

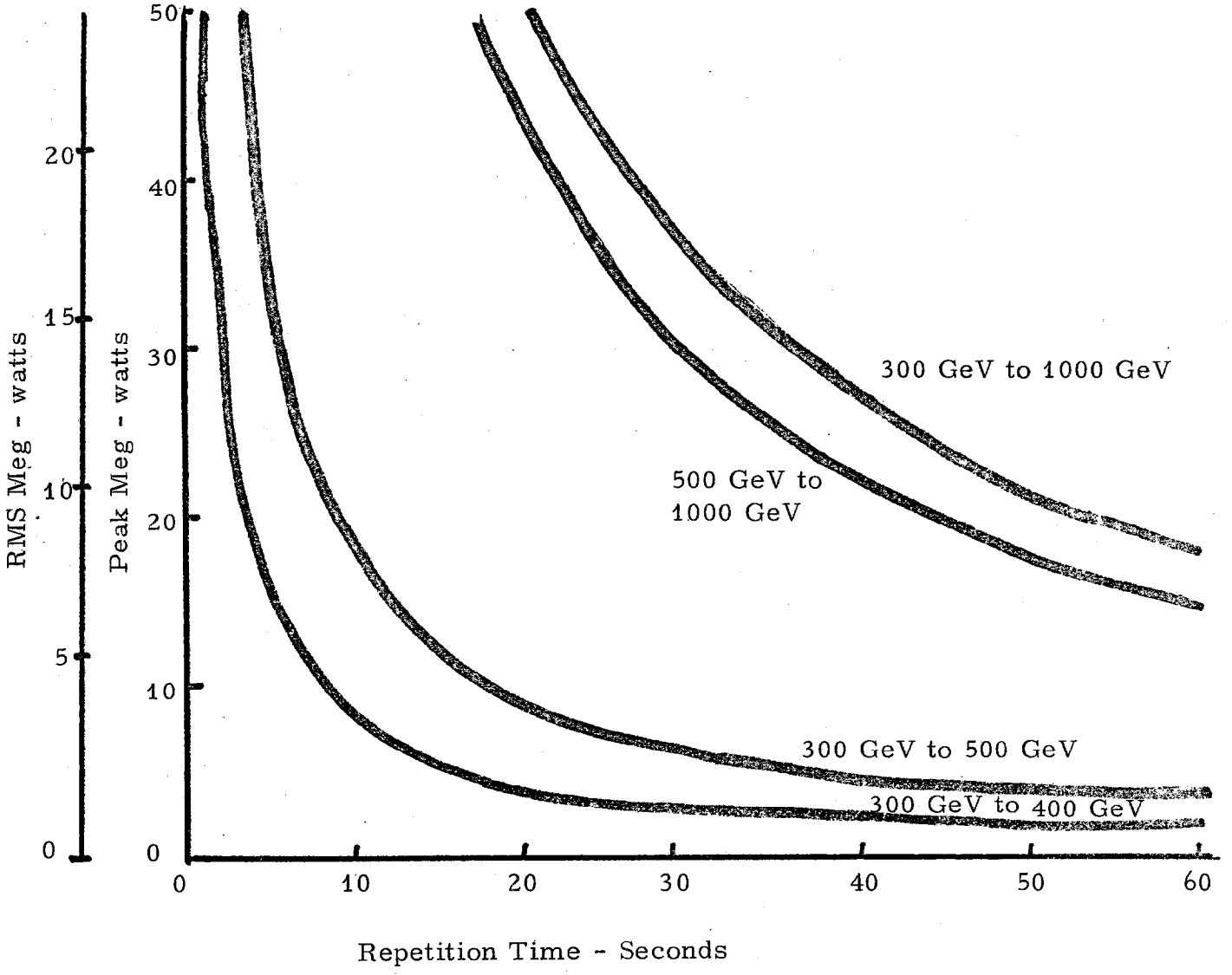

FIGURE 1

Appendix I

EXCERPT OF A STATEMENT BY ROBERT R. WILSON,
DIRECTOR, NATIONAL ACCELERATOR LABORATORY
BEFORE THE JOINT COMMITTEE ON ATOMIC ENERGY
MARCH 9, 1971

...Full operation at 500 BeV would mean an increased power consumption and hence an increased operating cost. Now this eventuality of going to 500 BeV came about, you will remember, because of the recommendation in 1968 of the JCAE Subcommittee on Research, Development and Radiation that we try for a higher energy. They also had advised a continued study of the possibility of achieving a higher energy by the use of superconductivity. It appears now that such a possibility may become feasible in the concept of what I like to call an "energy doubler." It is a small-bore superconducting magnet that can be mounted "pickaback" on the present main ring magnet. If successful, it should be of modest cost and should enable us to achieve higher energies - as much as 1000 BeV. Just as important, though, is that operation above the 200 BeV level would cost much less using the superconducting magnet than it would using out present copper and iron magnets. In fact, a considerable fraction of the cost of the energy doubler might be recovered in the first years by savings in operating costs. It might also forestall the necessity of installing additional water cooling or of installing devices to smooth out our electrical loads on the power lines.

Let me try to give a rough idea of how the energy doubler might work. It would consist of a very small bore superconducting magnet that would be placed just above the main-ring magnets, as shown in the figure. It would also have the same configuration as the main-ring magnets; that is, wherever a main-ring bending or focusing magnet is located, then just above it would be found the same kind of superconducting magnet. The protons, after being accelerated to a particular energy in the Main Ring, would be transferred to the superconducting ring which would have at that time exactly the same magnetic field as the Main Ring. Then the field in the superconducting ring would be raised to twice its initial value, and because the protons would be being accelerated by an oscillating electric field as the magnetic field increased, the energy would be doubled. In a sense, the old Main Ring would become a Booster Accelerator for the New Main Ring, now made of superconductors. The electrical energy for the new ring might also come from the old one. The only thing novel about all this is that the injection field for the new magnet would be very high so that most of the problems encountered up till now in trying to make an accelerator using superconductivity are avoided. In other words, it is only because we have the conventional Main Ring magnet made of copper and steel that we can consider the use of a superconducting magnet at this time.

Because the bore of the new magnets would be so small, because no new tunnel or buildings would have to be constructed, we can hope to be able to build such a device for less than $20

million, possibly even for less than $10 million. All of these considerations, it must be emphasized, are based only on the most preliminary of studies....

Appendix II

COMPUTATIONS IN SUPPORT OF DESIGN EFFORT ON MARK II DIPOLES: S4B & P6C[1]

Z. J. J. Stekly and R. J. Thome

The following is a brief discussion of the results of computations and tests carried out by Magnetic Corporation of America in support of the design effort on the National Accelerator Laboratory superconducting dipole magnets "S4B" and "P6C".

Generally speaking, superconducting windings which operate the dipoles mentioned above, are sensitive to operational perturbations which may be mechanically induced even if the superconductor is intrinsically stable. This arises as a result of local energy dissipation due to friction in the event of sudden relative conductor motion.

As a coil system is charged, the loads of electromagnetic origin deform the winding and supporting structure. If the mechanical characteristics of an epoxy bonded high current density winding structure are such that the bond strength is exceeded at some point in the charge sequence, then a sudden local failure can occur with a corresponding sudden relative conductor motion and stress redistribution. Because of the low specific heat of materials at these temperatures, local energy dissipations of the order of a few tenths of a joule[2] are sufficient to raise the local temperature to the critical level. In windings of this type it is, therefore, particularly important to insure that the shear stress transmitted by the epoxy bond

---

[1]Performed by MCA under subcontract 11306 with NAL work completely supported by USAEC

[2]Z. J. J. Stekly and R. J. Thome, "Mechanically Induced Operational Perturbations in High Current Density Superconducting Coils," to be published.

at each point in the winding bundle is such that local failure is highly unlikely. To analyze these effects in connection with the designs for NAL dipoles S4B and P6C it was necessary to:

1. determine shear strength of the epoxy used in construction.
2. determine loads of electromagnetic origin on the winding.
3. estimate deflections and maximum shear stresses at critical points in the winding.

In addition to the above, the following areas were considered because of their possible design impact:

4. central field, maximum field, and field profile determination (without iron effects) within the bore of the coil systems.
5. estimation of load enhancement due to presence of iron.
6. estimates of forces resulting from an asymmetric location of the dipoles within an iron cavity.
7. estimates of thermally induced stress.

1. Shear Tests

To determine the shear strength of a typical bond a section of winding was obtained from NAL and test specimens were constructed. Each specimen consisted of many adjacent, epoxy bonded conductors. Tests were carried out at liquid nitrogen temperature with specimens mounted in the manner of centrally loaded, simply supported beams. During each test, force versus deflection were continuously recorded. In this configuration, the maximum shear stress occurs at the midplane of the beam and knowledge of the dimensions and load at failure allows determination of the shear stress at failure. Results are summarized in the following table.

TABLE I

MAXIMUM SHEAR STRESS AT FAILURE (78 K)

Sample No.	Shear Stress (psi)
1	4270
2	9810
3	6040
4	6290
	average = 6600 psi

2) Determination of Loads of Electromagnetic Origin

For both dipoles, the loads of electromagnetic origin were initially computed without taking account of iron effects and at the operating current densities as supplied by NAL. Shear stresses and deflections computed with these force distributions were then scaled up to a level corresponding to a central field of 4.5 Wb/m^2 and adjusted to take account in an approximate fashion of load enhancement due to the presence of iron.

The S4B dipole consists of four shells which were modeled for purposes of this calculation by eight current filaments per quadrant of the transverse section. Each quadrant of the end turn region was modeled by twenty-four straight current filaments. Figure 1 shows the force distribution and resultants on a transverse section of the dipole while Figures 2 and 3 show the resultant forces on one half of the magnet end turn region. The resultants on the end turn were determined from the force distribution by computing the forces at two locations per current filament (a total of 48 locations in one quadrant of the end turn region at one end of the coil system.)

3. Maximum Shear Stress and Deflections

For each dipole a transverse section of the magnet far from the end turns was modeled as a composite beam which is exposed to the distributed load of electromagnetic origin and to the equilibrating forces arising from the structure. In addition, an estimate of the maximum shear stress and deflection was computed in each case in the plane at which the straight side sections of the magnet begin to cross over the bore tube. Results are summarized in Figures 7 through 10.

In all cases, the maximum shear stresses are below the average value obtained in the shear test on the epoxy; however, they are substantially lower for the P6C than for the S4B. Results are approximate because of the simplifying assumptions necessary, but may be expected to be of the proper order. In view of the test results it may be desirable to increase the thickness of the inconel strap in each of the designs to assure that the maximum shear stress experienced is below the minimum obtained in the shear tests.

4. Field Calculations

Computations of magnetic field were carried out with current filament models which were composed of 16 and 24 filaments respectively for one quadrant of a transverse section of the S4B and P6C dipoles. In the end turn regions of the S4B and P6C, 48 filaments and 96 filaments respectively were used in a quadrant of the end turn region. Central fields were computed and field concentration ratios for each geometry were found without taking iron effects into consideration. Results are summarized in Table II.

TABLE II

CENTRAL FIELDS AND FIELD CONCENTRATION RATIOS

Dipole	Current Density (kA/cm^2)	Central Field (Wb/m^2)	Field Concentration Ratio
S4B	38.2 (inner) 52.5 (outer)	4.3	1.29
P6C	34.8	3.75	1.19

In addition, field profiles (no iron) were computed along lines in the end turn region and parallel to the bore axis at three locations in the bore for each dipole. Results are given in Figures 11 through 16. Computed results giving coordinates, field components and net field along these lines are appended to the end of this discussion.

5. Load Enhancement Due to Iron

The placement of the dipole windings within an iron cavity will lead to an alteration in load distribution and magnitude. To gain an insight into this effect a simplified model was considered and the results are shown in Figure 17. In this case, the transverse force, F, is the repulsive force between the windings on each side of the bore. The ordinate is the ratio of the transverse force with iron present to the transverse force without iron and the abscissa is the ratio of the dipole diameter to the cavity diameter. Two cases are shown, one for constant current in the dipole and the other for constant central field. The case of interest is the latter and the graph indicates a force enhancement ratio of 1.2 for the S4B and 1.35 for the P6C. A six inch diameter cavity was assumed in each case. Though the model is approximate, the implication is that the effect is not negligible;

consequently, these factors were utilized in scaling the previously discussed results on stresses and deflections.

6. Asymmetric Location of the Dipoles in an Iron Cavity

If a dipole is symmetrically located in a cylindrical cavity in permeable material, no net transverse force will result. However, in practice, a degree of eccentricity is unavoidable; consequently, a net force results which must be considered in the design of the supports for the inner helium container. Estimates of the magnitude of these forces were computed for the S4B and P6C dipoles and are given in Figures 18 through 21.

7. Thermally Induced Stress

The most severe thermal contraction in each dipole will occur in the axial direction; consequently, estimates of thermally induced stress were performed based on a coil length of ten feet. Results are summarized in the following table and indicate moderate stress levels which should not be a source of difficulty. Effects due to asymmetry were not considered.

TABLE III

AXIAL THERMAL CONTRACTION FOR S4B & P6C

	P6C	S4B
Net contraction of winding & bore tube (in.)	0.324	0.325
Ave. compressive stress in winding (psi)	930	1015
Ave. tensile stress in bore tube (psi)	8850	8600
Ave. shear stress in epoxy (psi)	4.6	4.5

NAL dipole S48

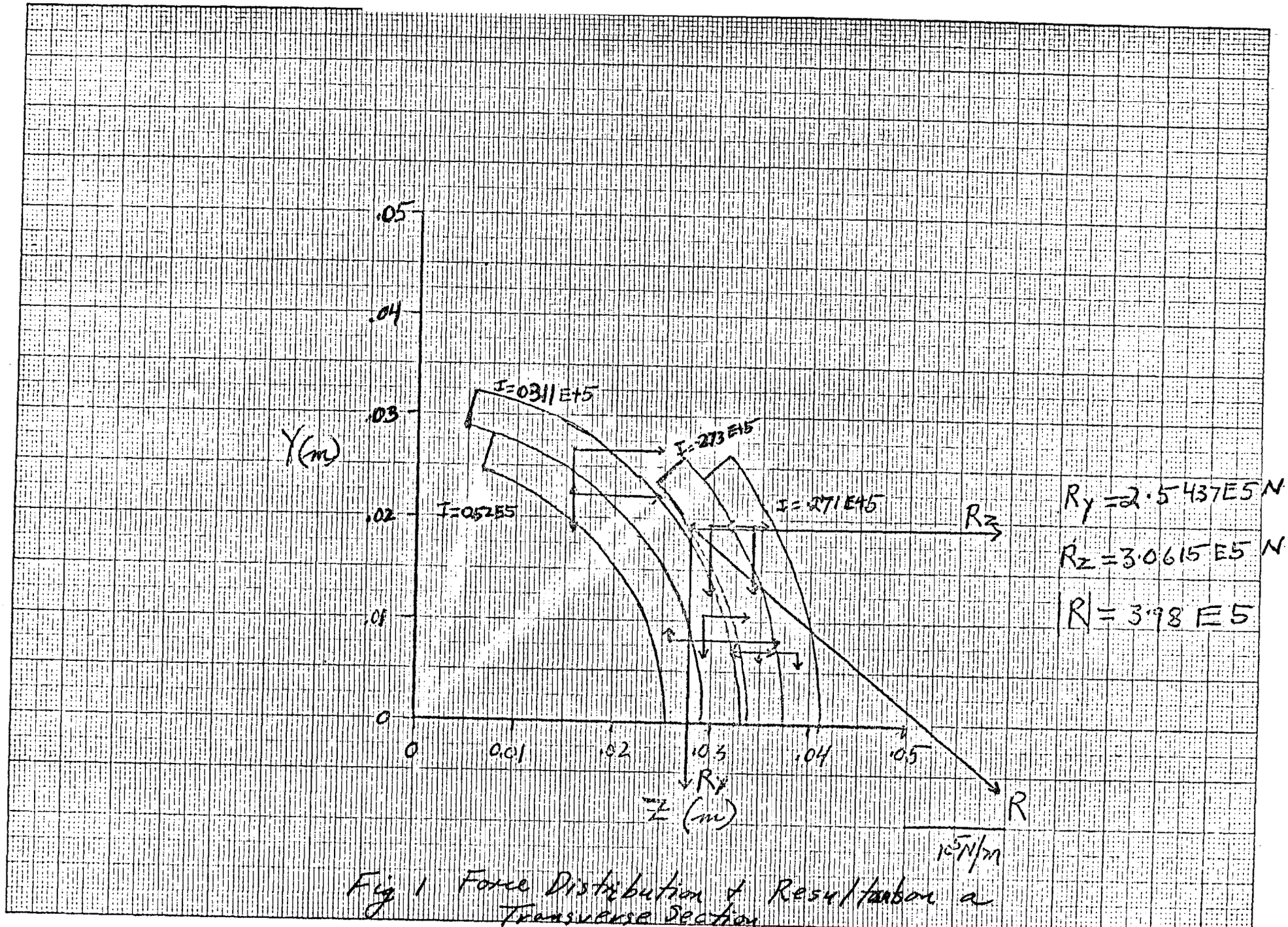

$R_Y = 2.5437E5\ N$

$R_Z = 3.0615\ E5\ N$

$R = 3.98\ E5$

Fig 1 Force Distribution & Resultant on a Transverse Section

NAL Dipole CAR

INAL-T 070 [illegible]

J (inner 2 coils) = 3.82 X 10^8 A/m2

J (outer 2 coils) = 5.25 X 10^8 A/m2

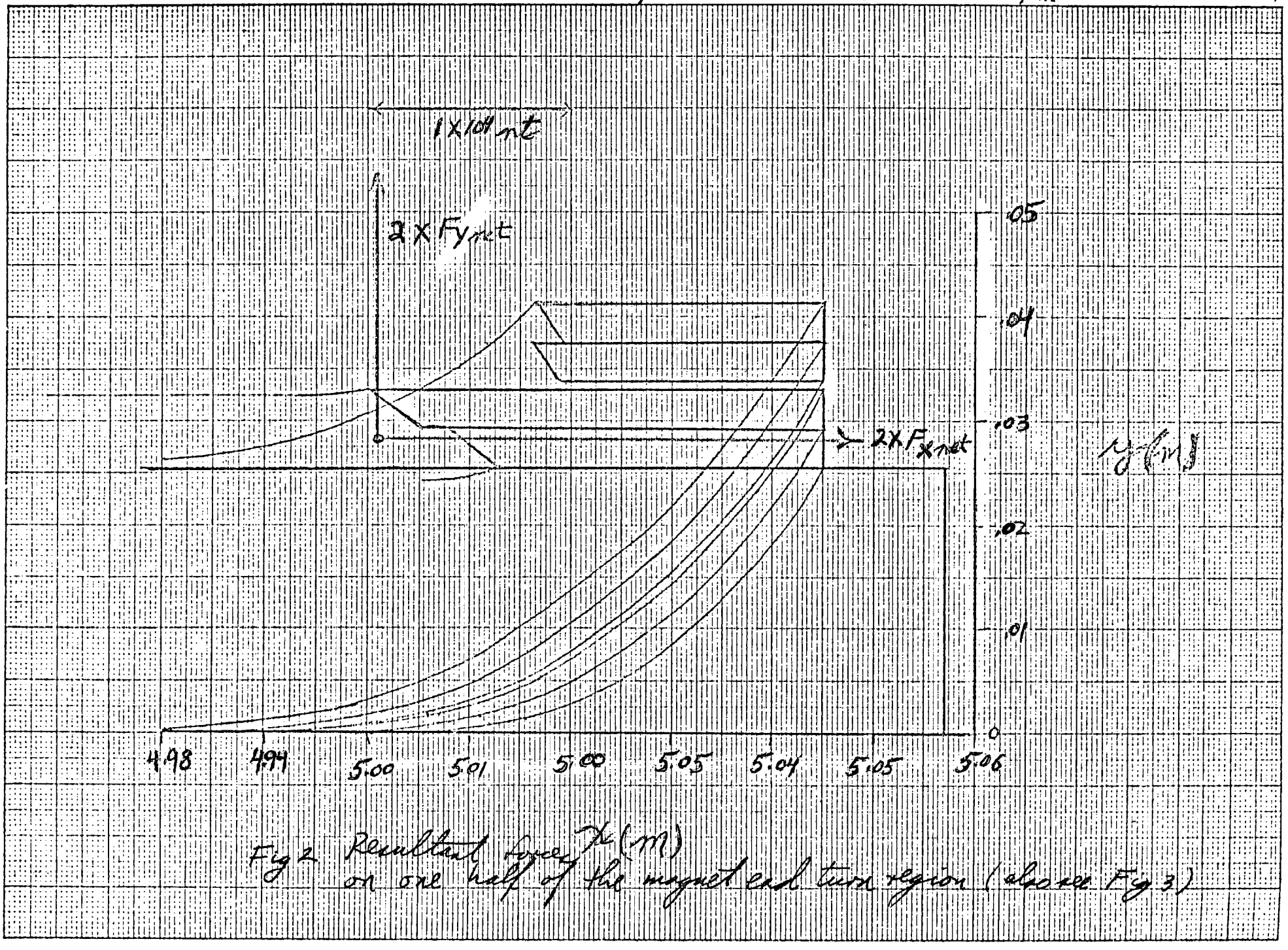

Fig 2 Resultant forces on one half of the magnet end turn region (also see Fig 3)

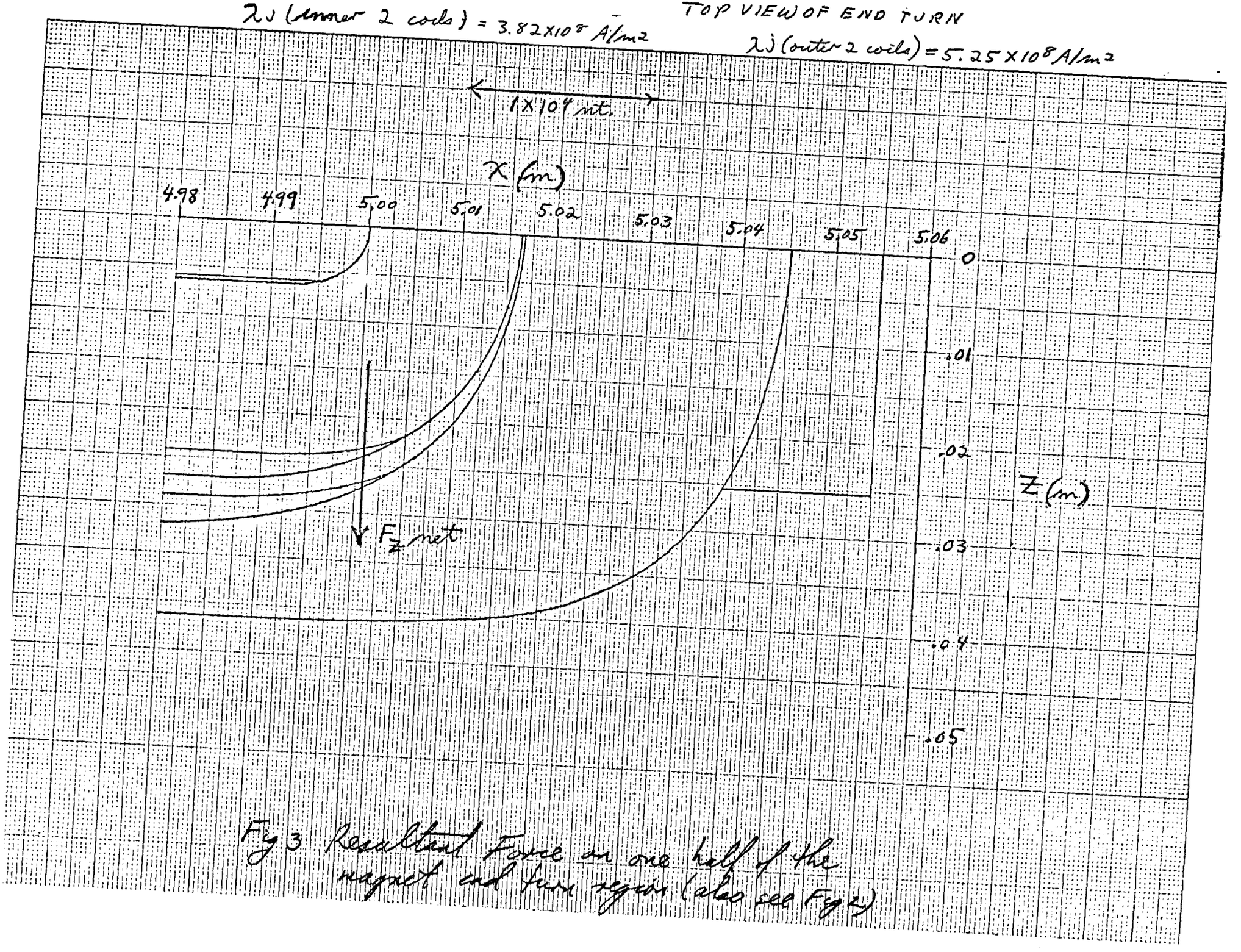

Fig 3 Resultant Force on one half of the magnet end turn region (also see Fig 4)

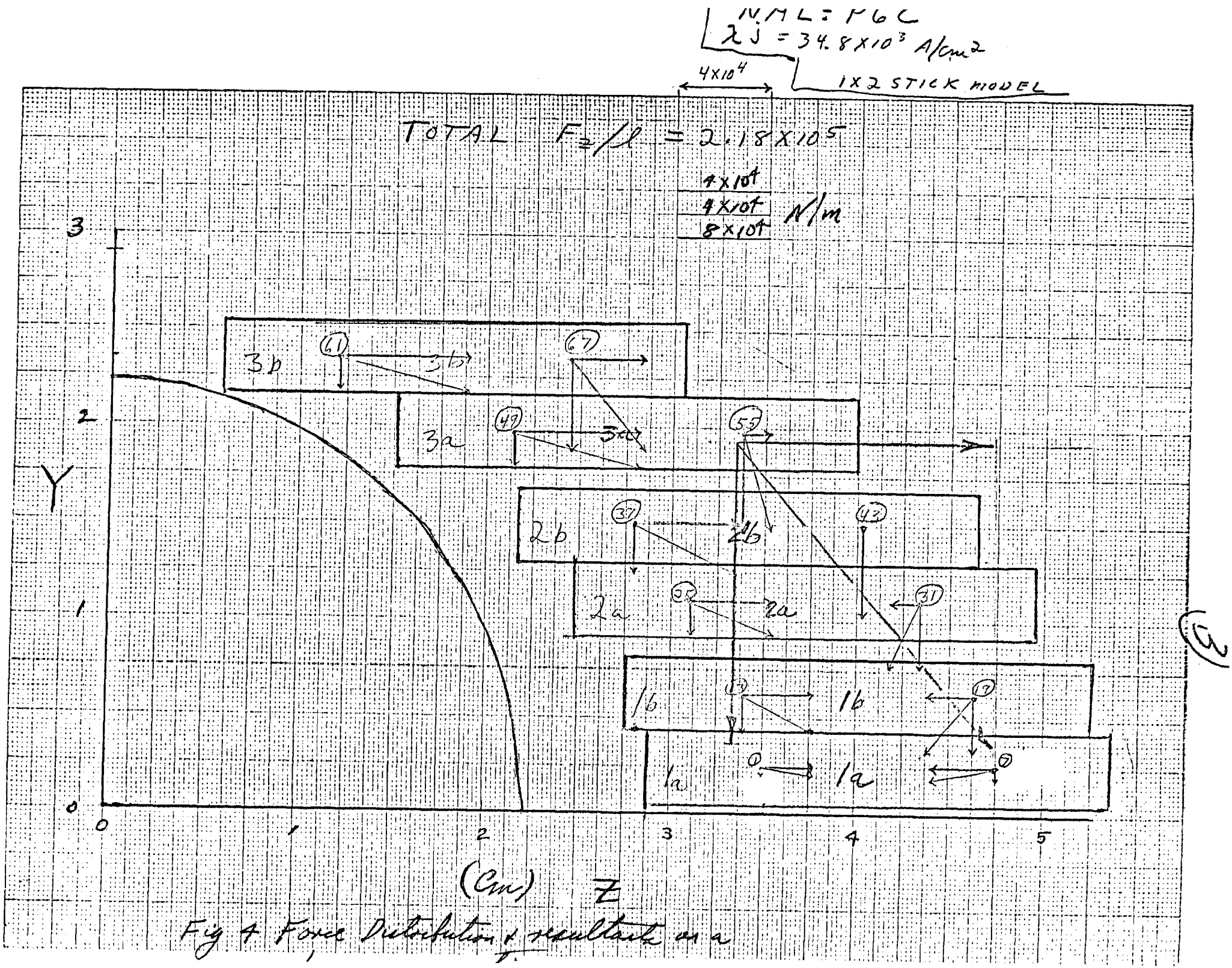

Fig 4 Force distribution & resultant on a

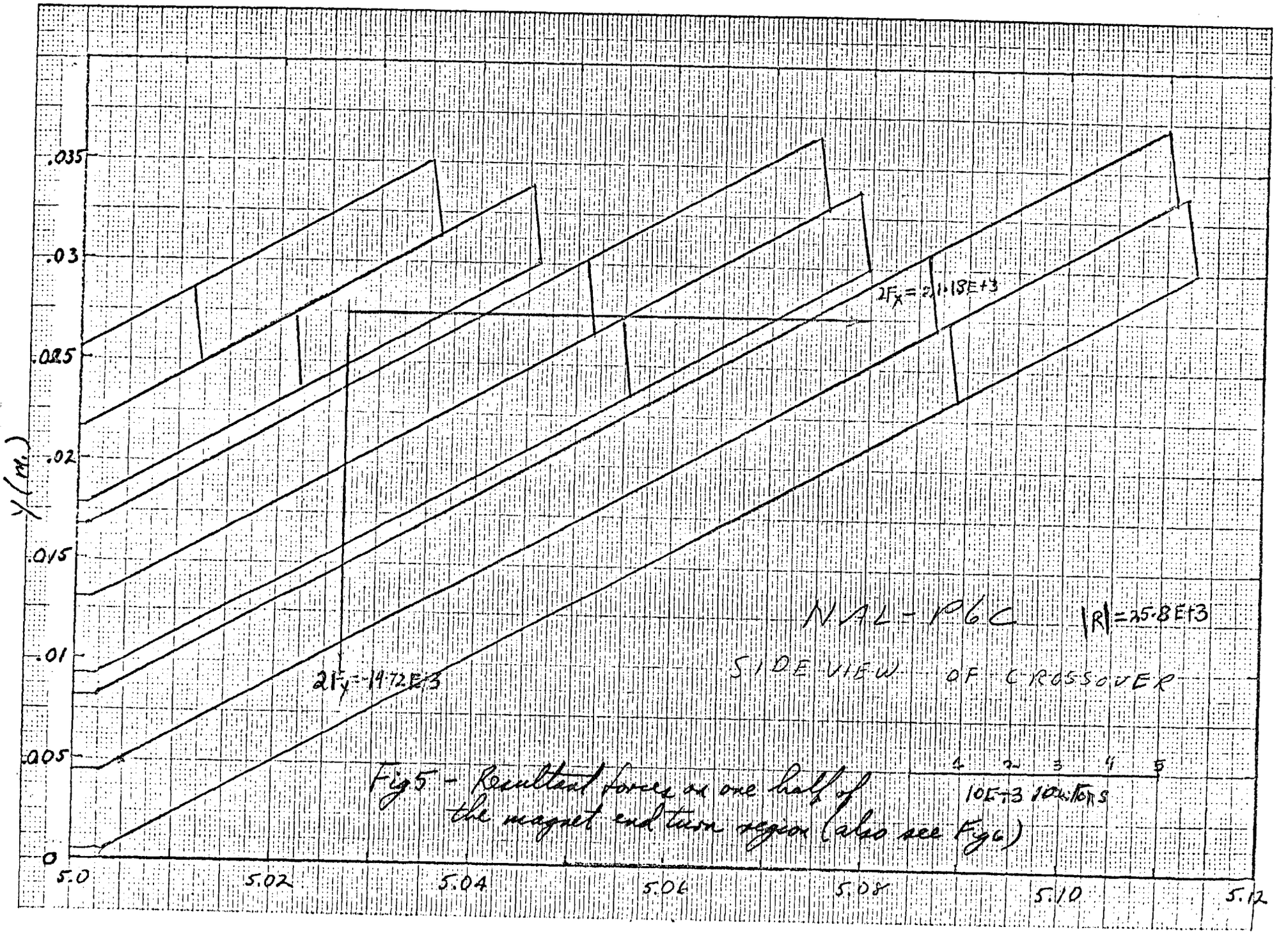

Fig 5 - Resultant forces on one half of the magnet end turn region (also see Fig 6)

NAL-4 P6C

TOP VIEW OF END TURNS -

$\lambda j = 3.48 \times 10^8$ A/m²

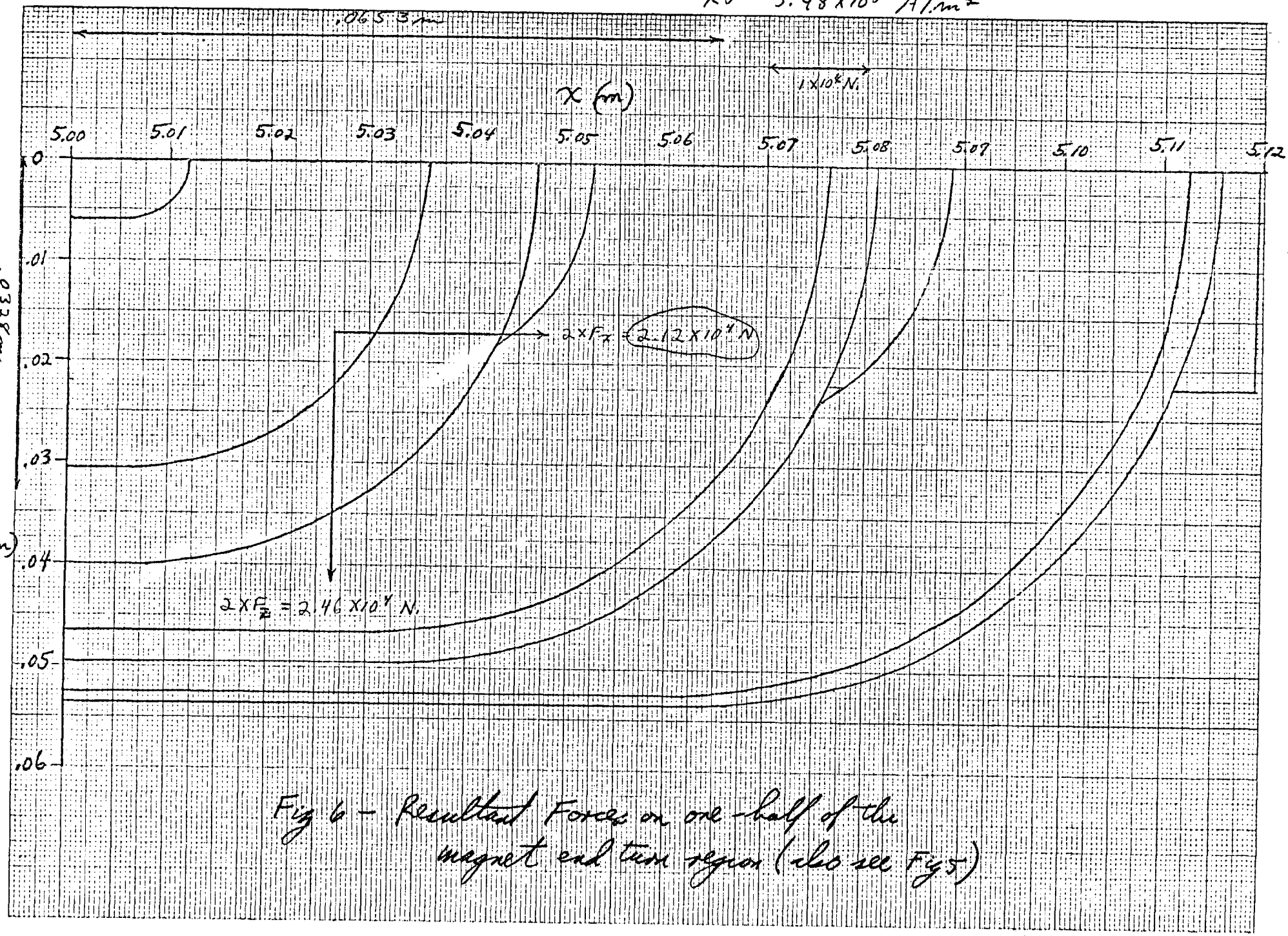

Fig 6 - Resultant Forces on one-half of the magnet end turn region (also see Fig 5)

Fig 7-

Transverse Deflection Far From End Turns for S4B

transverse section:

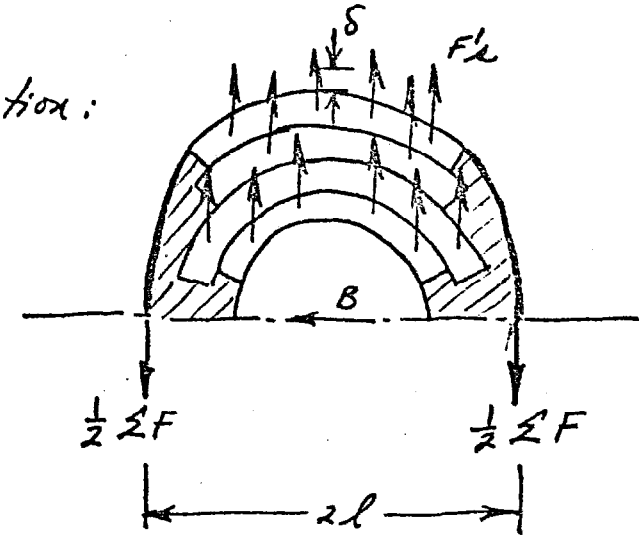

model: composite cantilever with distributed load

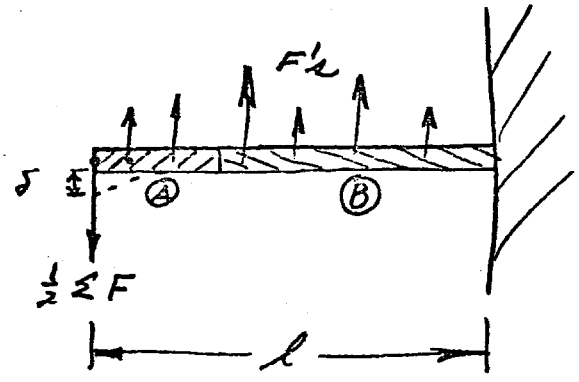

beam composition, section (A):

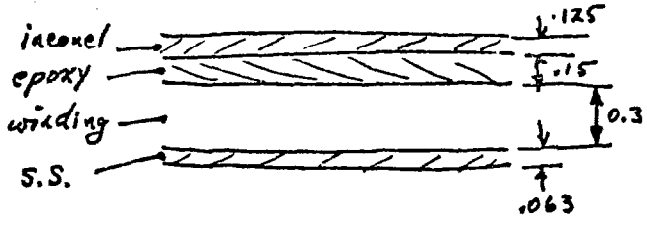

beam composition, section (B)

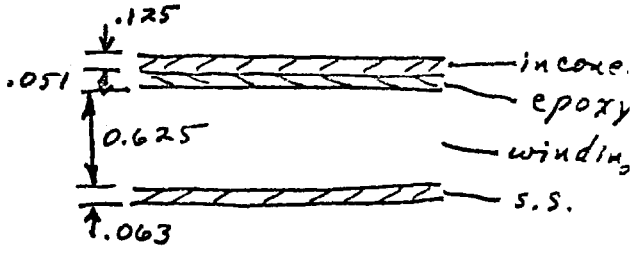

results*:

$\delta = 1.61 \times 10^{-3}$ in. (all laminates bonded)

$\tau_s = 4260$ psi (max. shear stress)

$\sigma = 22{,}500$ psi (max bending stress)

* results are based on a central field of 4.5 wb/m² with a force enhancement due to [illegible] of 1.2

Fig 8 →
Transverse Deflection Far From End Turns for P6C

Transverse section:

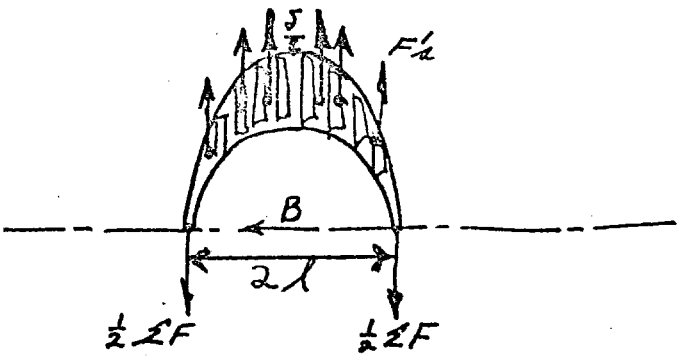

model: composite cantilever with distributed load

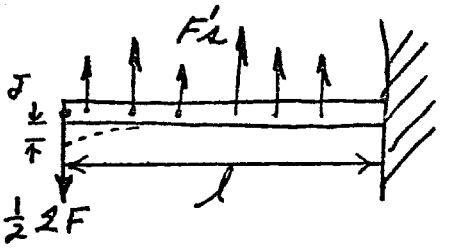

beam composition:

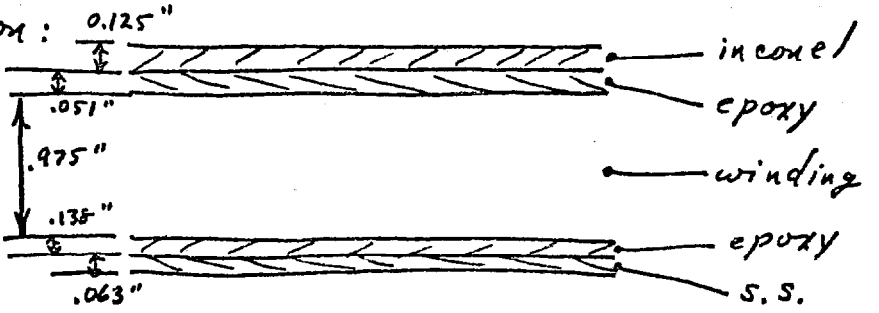

Results*:

for all laminates bonded, $\delta = 8.93 \times 10^{-4}$ in.

for all laminates unbonded, $\delta = 1.22 \times 10^{-3}$ in.

maximum shear stress = 2820 psi (in winding)

maximum bending stress = 7490 psi (in inconel strap)

* results correspond to loads for a central field of 4.5 wb/m² & to a force enhancement due to iron of 35%

Fig 9-

Transverse Deflection Near End Turns for SAB

top view:

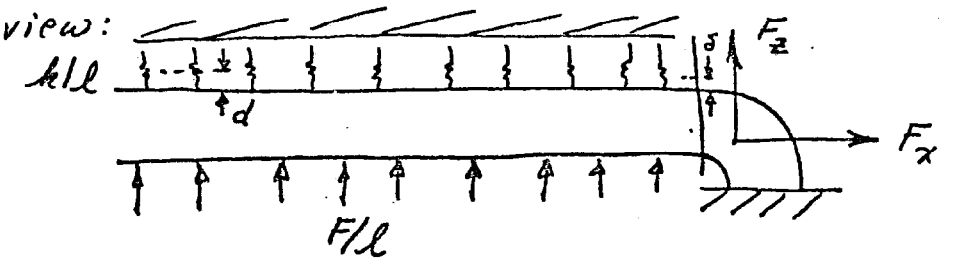

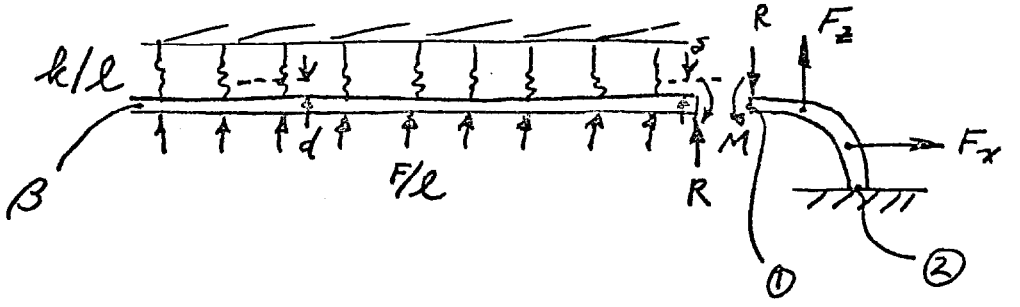

---

input: $F_x = 6700$ lb $F/\ell = 4340$ lb/in. } stick mode with 4.5 wb/m central field + 6% enhancement due to iron = 1.2

$F_z = 5270$ lb

$k/\ell = 2.69 \times 10^6$ lb/in^2 } based on deflection of sides at a section far from the end turns

$d = 1.61 \times 10^{-3}$ in.

$\beta = 0.643$ in^{-1}

$(\Sigma EI)_① = 3.93 \times 10^6$ in^2 lb. ; $(\Sigma EI)_② = 6.86 \times 10^6$ in^2 lb

note: variation of (ΣEI) assumed linear along arc length from ① to ②

---

results:

$R = -2080$ lb. $\delta = 6.68 \times 10^{-4}$ in.

$M = -171$ in lb max shear stress = 1080 psi

Fig 10
Transverse Deflection Near End Turns for P6C

top view:

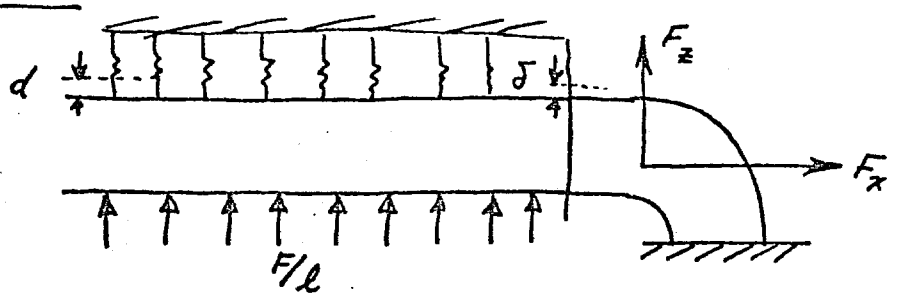

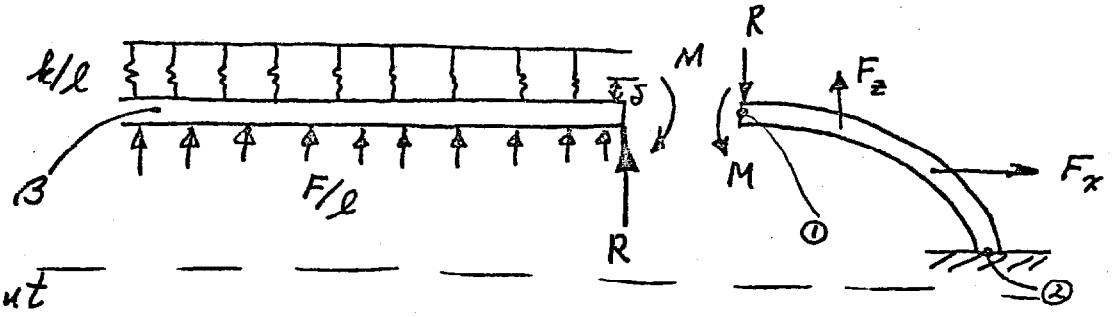

input

$F_x = 9250$ lb $F/\ell = 4830$ lb/in
$F_z = 10700$ lb

} stick model with 4.5 wb/m² central field + force enhancement due to iron = 1.35

$k/\ell = 1.29 \times 10^7$ lb/in² } based on deflection of sides at a section far from the end turns
$d = 3.74 \times 10^{-4}$ in.

$$\beta = \sqrt[4]{\frac{k/\ell}{4(\Sigma EI)}} = 0.825 \text{ in.}^{-1}$$

$(\Sigma EI)_① = 6.96 \times 10^6$ in² lb. ; $(\Sigma EI)_② = 4.57 \times 10^7$ in² lb } calculated

note: variation of ΣEI assumed linear along arc length from ① to ②

results:

$R = 1250$ lb $\delta = 3.94 \times 10^{-4}$ in.

$M = 1350$ in lb max shear stress = 605 psi

NALT 378 DIPOLE
1/6/73

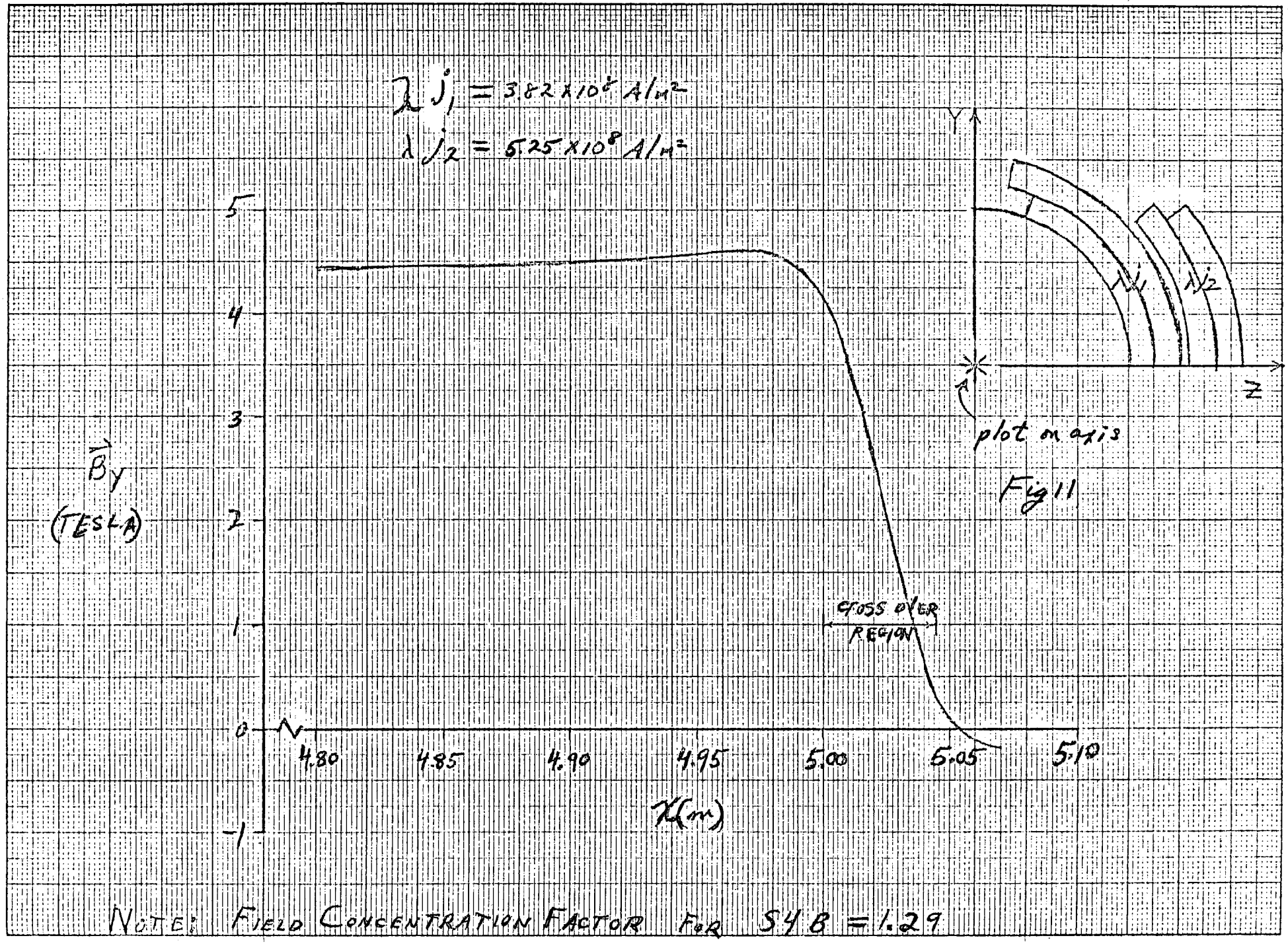

Fig 11

NOTE: FIELD CONCENTRATION FACTOR FOR SYB = 1.29

MAL-7 37D DIPOLE
1/5/73

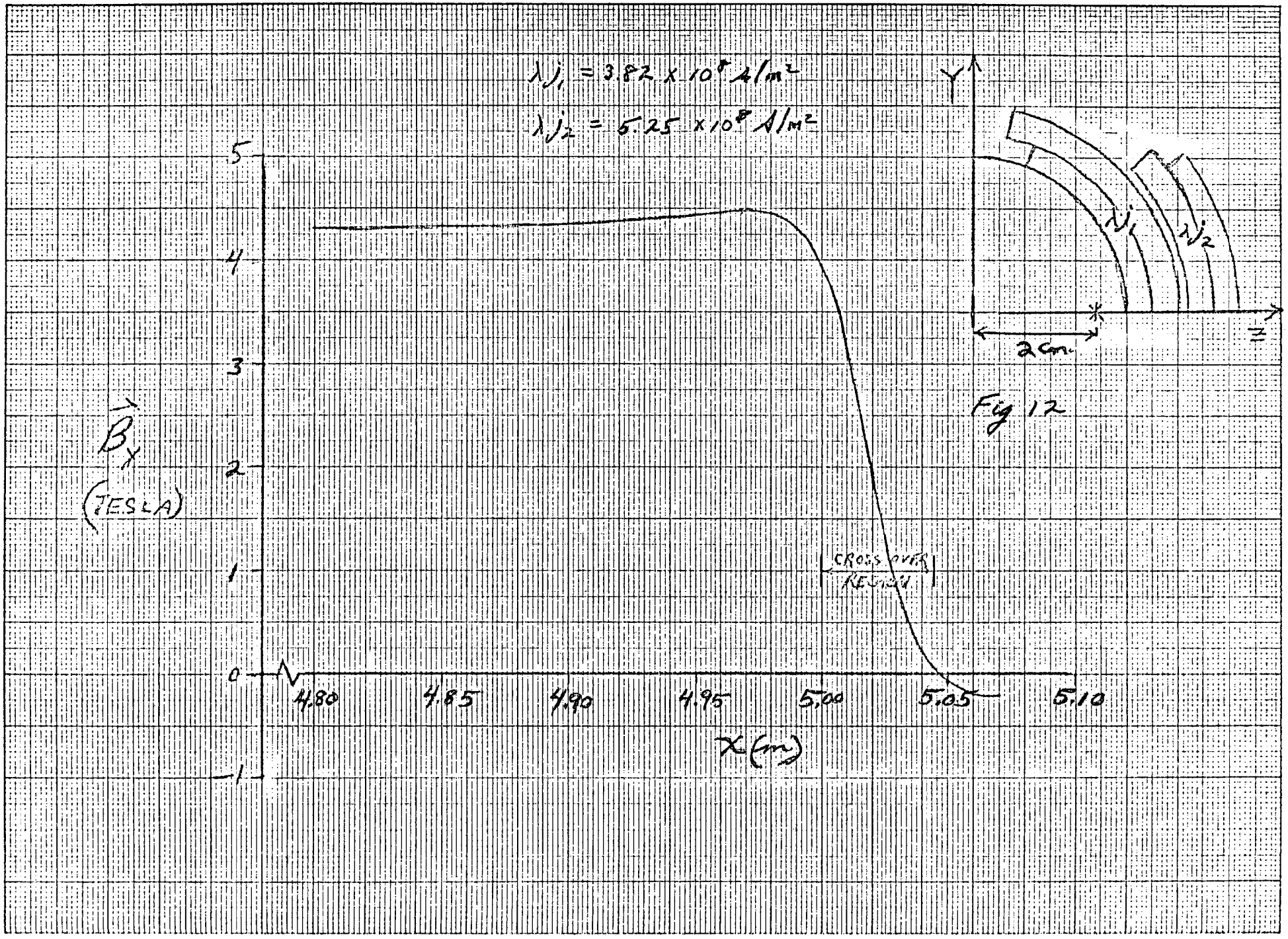

Fig 12

IV/4L-7 SAB DIPOLE
1/5/73

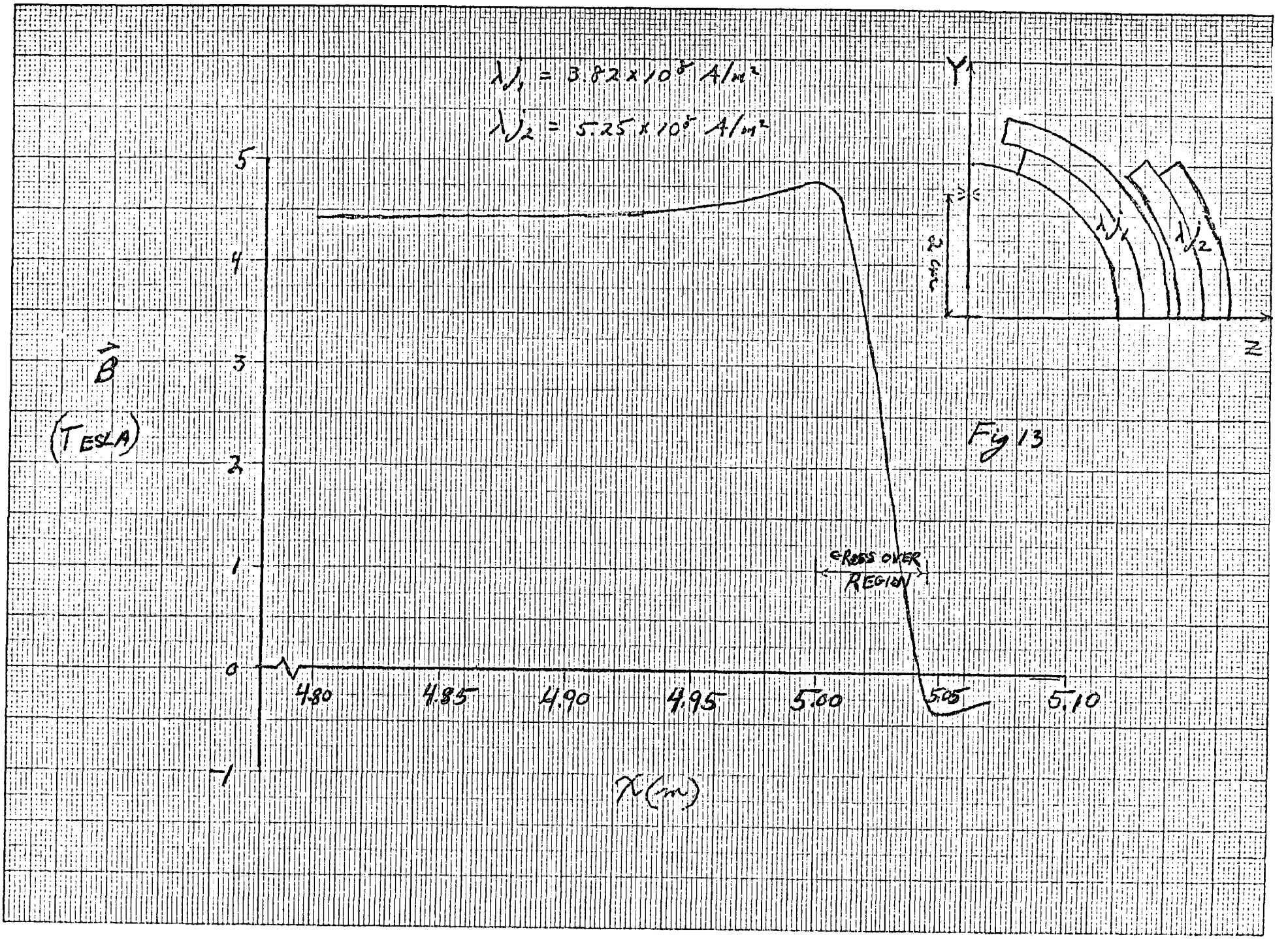

Fig 13

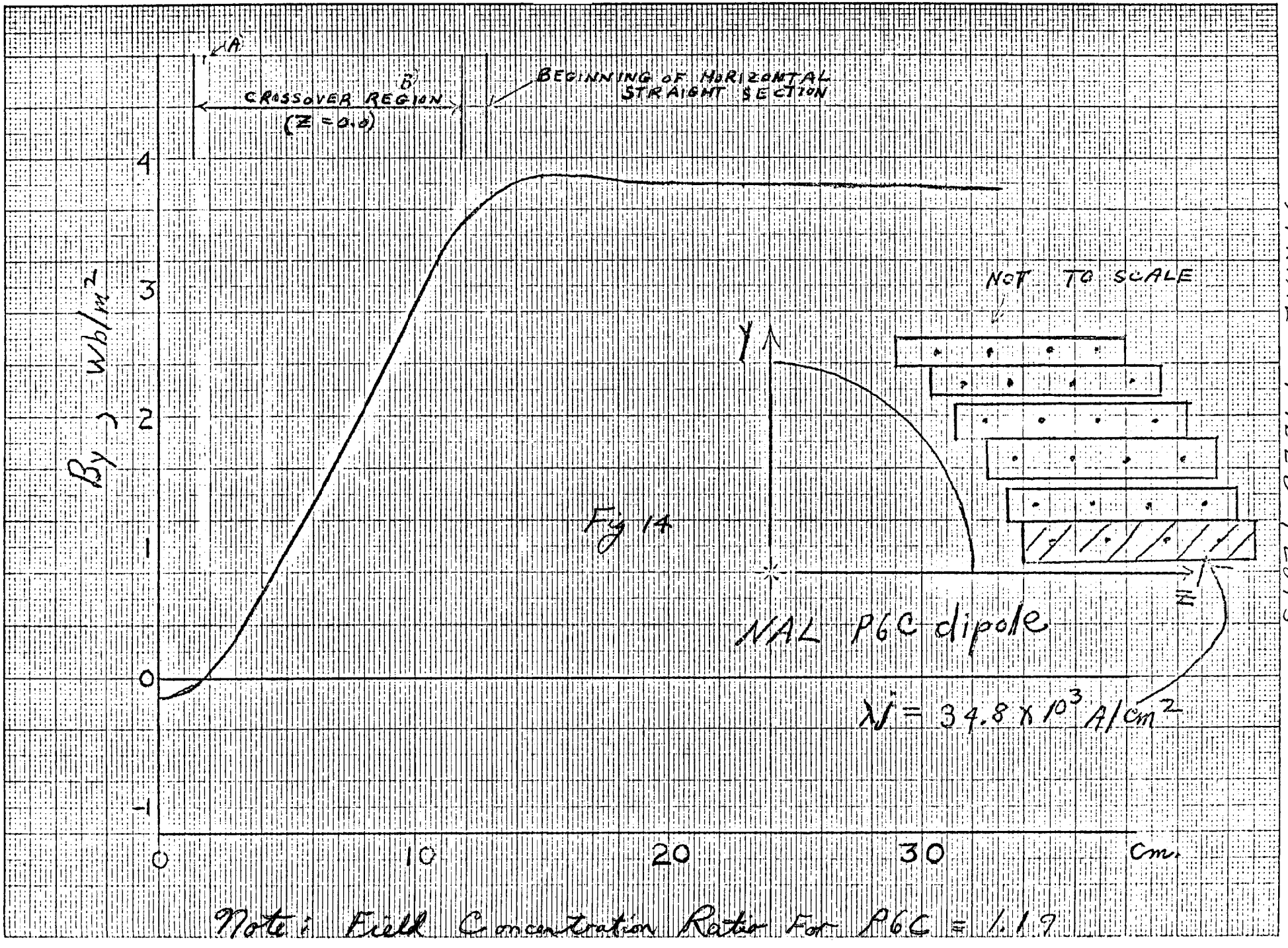
A
B
CROSSOVER REGION
(Z = 0.0)
BEGINNING OF HORIZONTAL
STRAIGHT SECTION
B_y , Wb/m^2
4
3
2
1
0
-1
0
10
20
30
cm.
NOT TO SCALE
y
z
NAL P6C dipole
$N = 34.8 \times 10^3$ A/cm^2
Fig 14
AXIAL FIELD PLOTS
Note: Field Concentration Ratio For P6C = 1.17

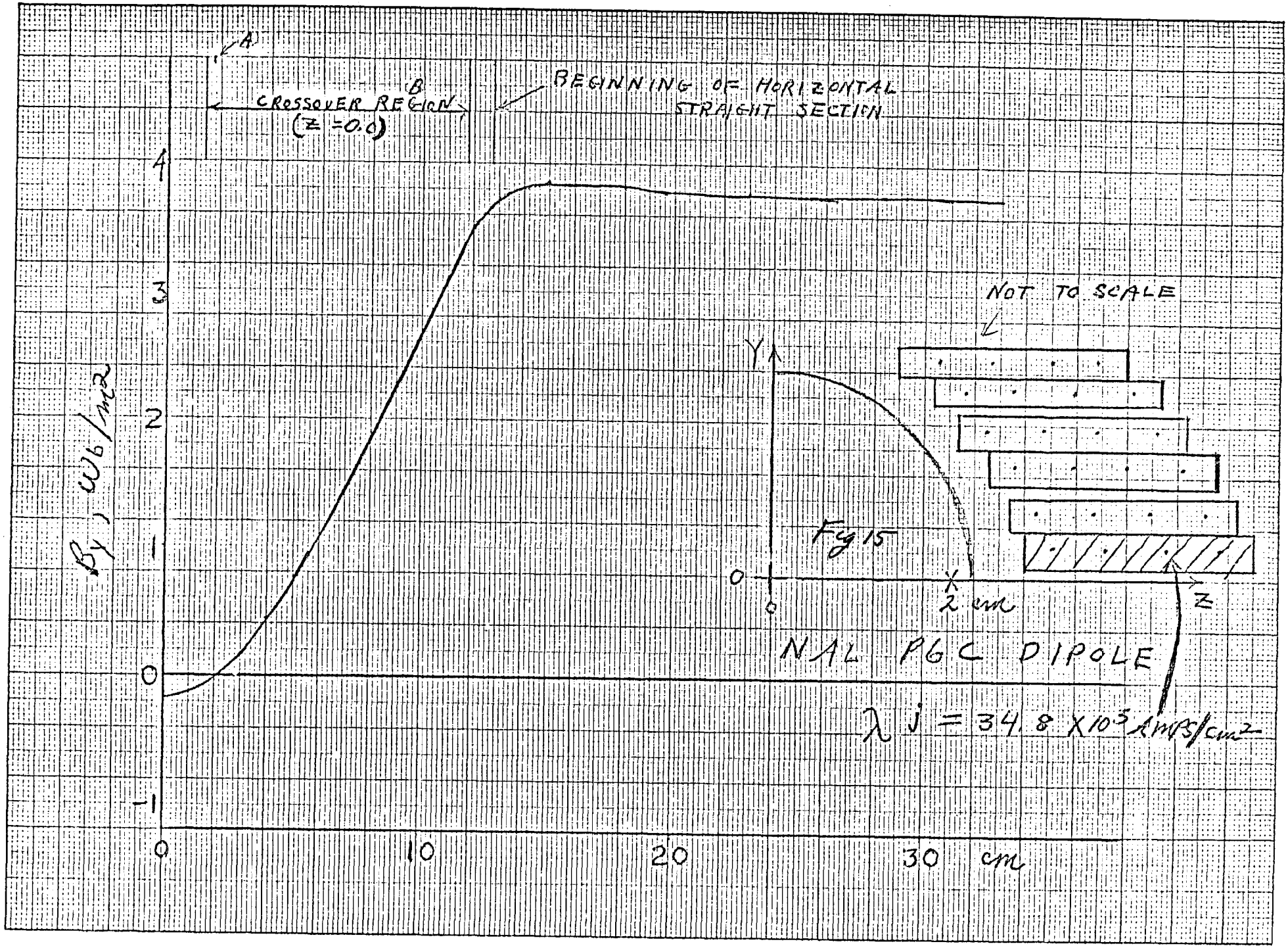
A
B
CROSSOVER REGION
(Z = 0.0)
BEGINNING OF HORIZONTAL
STRAIGHT SECTION
4
3
2
1
0
-1
B_y, Wb/m²
0
10
20
30 cm
NOT TO SCALE
Y
Z
0
2 cm
Fig 15
NAL P6C DIPOLE
λj = 34.8 X 10³ AMPS/cm²

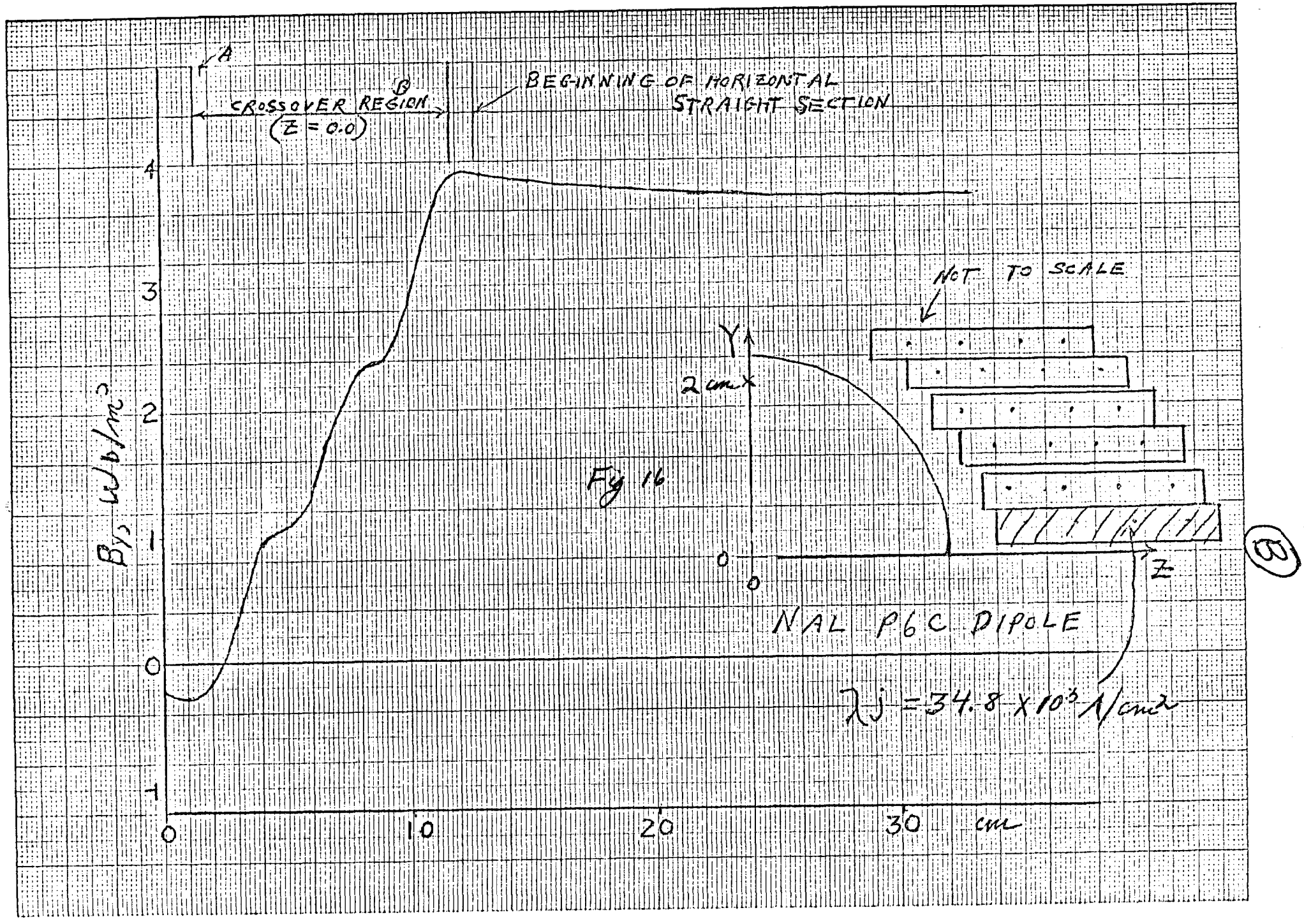
A
B
CROSSOVER REGION
(Z = 0.0)
BEGINNING OF HORIZONTAL
STRAIGHT SECTION
B_y, w/cm²
4
3
2
1
0
-1
0
10
20
30
cm
NOT TO SCALE
Y
2 cm
0
0
Z
NAL P6C DIPOLE
$\lambda j = 34.8 \times 10^{-3}$ A/cm²

Fig 16

(B)

Fig 17 —

Transverse Force Ratio

VS

Normalized dipole diameter

for constant current

for constant central field

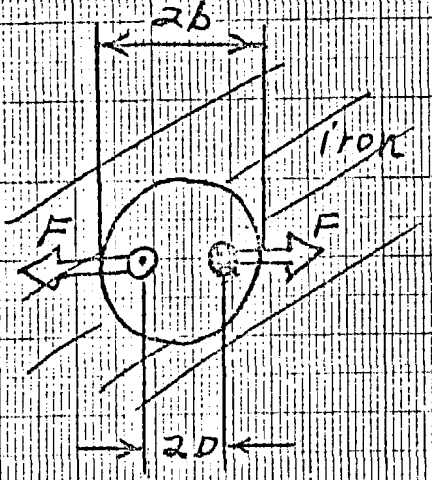

Transverse force on Winding with Iron / Transverse force on Winding without Iron

0 1 2 3 4 5 6 7 8 9 10

S4B

P6C

·1 ·2 ·3 ·4 ·5 ·6 ·7 ·8 ·9 1.0

Diameter of the dipole / Diameter of the Cavity

$\frac{2D}{2b}$

NAL DIPOLE S4B

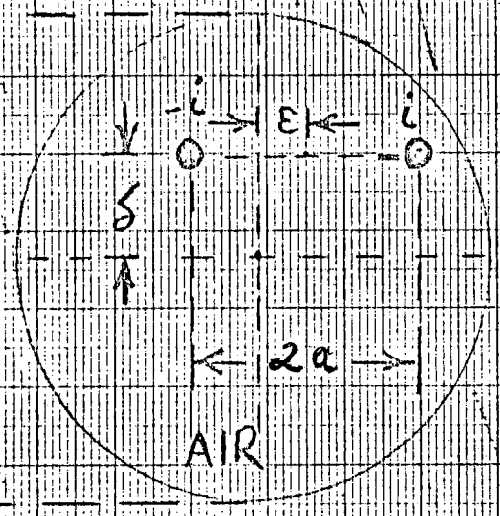

$2a = 0.667$ m.

$2b = 0.152$ m

$i = 4.04 \times 10^5$ A.

$K_v = \frac{7.8 \times 10^4 \text{ N/m}}{10 \text{ mm}} = 0.78 \times 10^4$

(VERTICAL FORCE PER UNIT LENGTH) $\frac{1}{i}$ (10^4 N/m)

48
44
40
36
32
28
24
20
16
12
8
4
0

2 4 6 8 10 12 14 16 18 20

HORIZONTAL DISPLACEMENT ε (mm.)

δ = 20 mm
δ = 18 mm
δ = 14 mm
δ = 10 mm
δ = 6 mm
δ = 2 mm

Fig. 18

NAL DIPOLE S4B

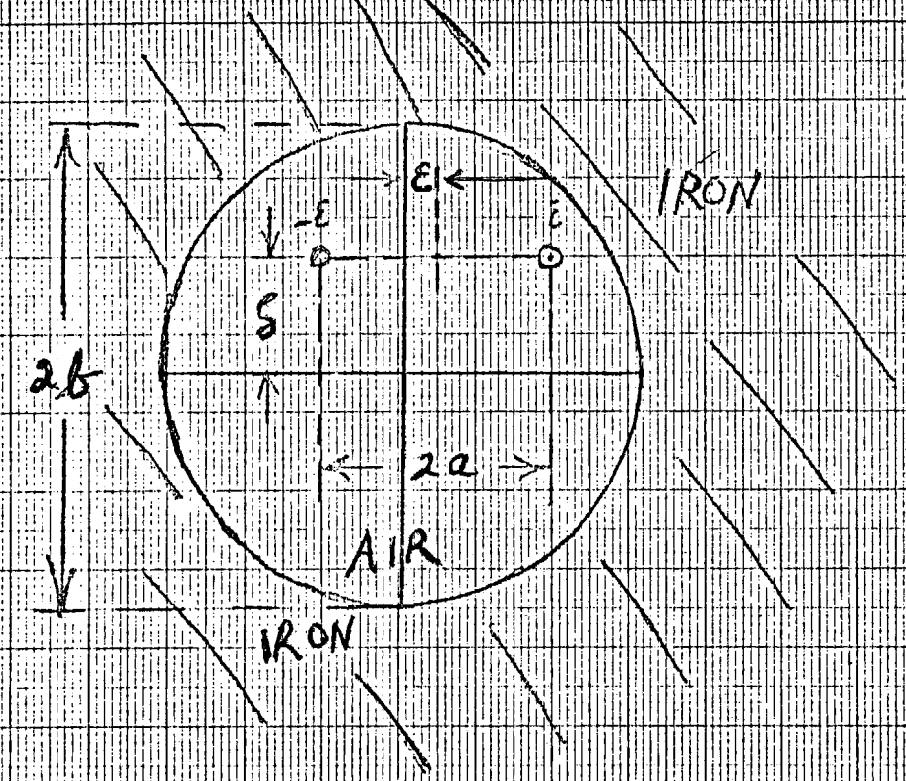

$2a = 0.0667\ m$

$2b = 0.152\ m$

$i^* = 4.04 \times 10^5\ A$

(HORIZONTAL FORCE PER UNIT LENGTH) $\frac{1}{\mu_0}$ $(10^9\ N/m)$

64 60 56 52 48 44 40 36 32 28 24 20 16 12 8 4

0 2 4 6 8 10 12 14 16 18 20

(HORIZONTAL) DISPLACEMENT (mm)

$\delta = 18\ mm$

$\delta = 0\ mm$

$k_H = \frac{12{,}000\ N/m}{10\ mm} = 1.2 \times 10^3\ \frac{N/m}{mm}$

Fig 19

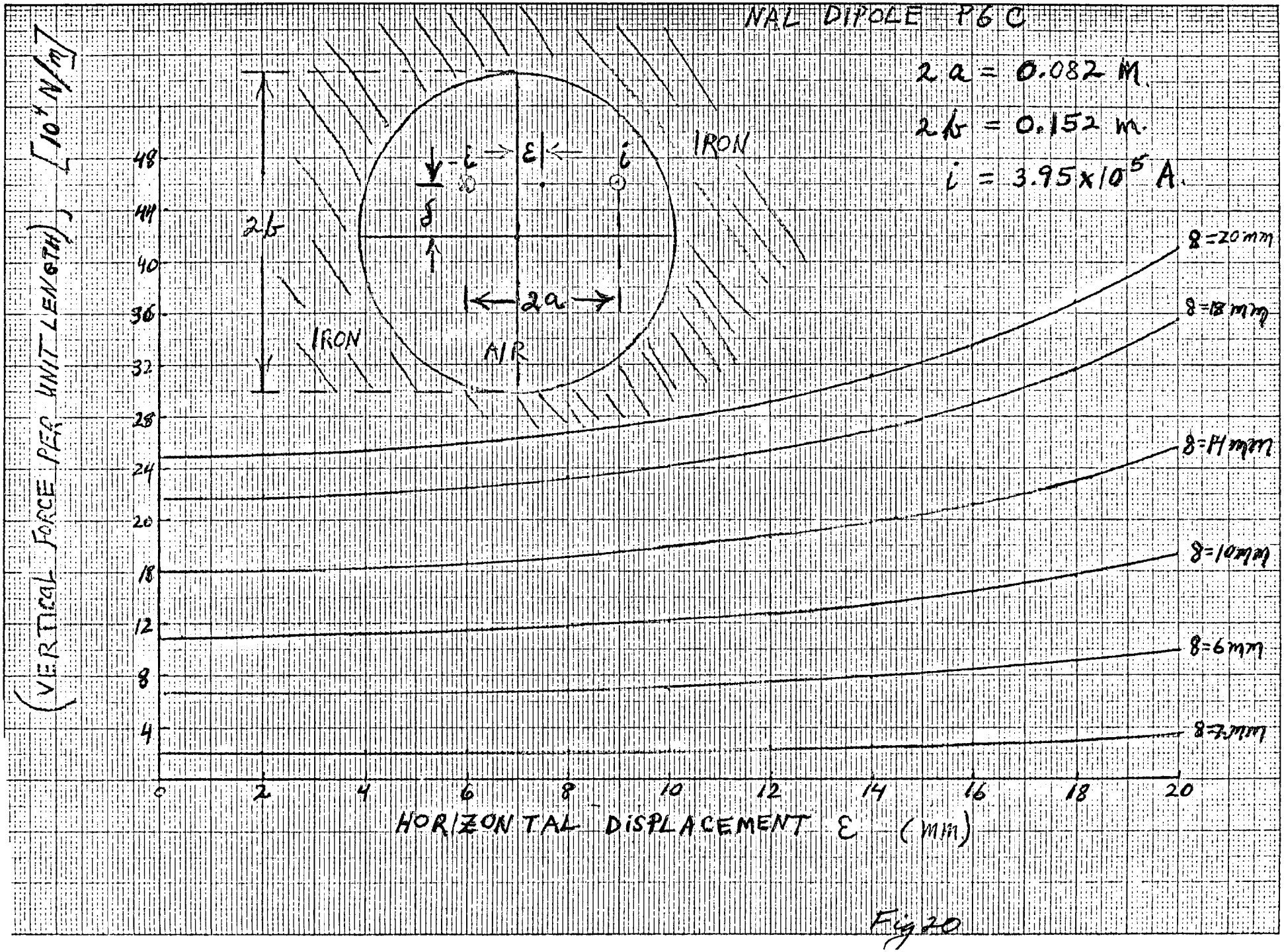
NAL DIPOLE P6C
2a = 0.082 m.
2b = 0.152 m.
i = 3.95×10⁵ A.
IRON
IRON
AIR
2b
2a
δ
ε
i
i
δ=20mm
δ=18mm
δ=14mm
δ=10mm
δ=6mm
δ=3mm
(VERTICAL FORCE PER UNIT LENGTH) [10⁴ N/m]
HORIZONTAL DISPLACEMENT ε (mm)
0
2
4
6
8
10
12
14
16
18
20
4
8
12
18
20
24
28
32
36
40
44
48

Fig 20

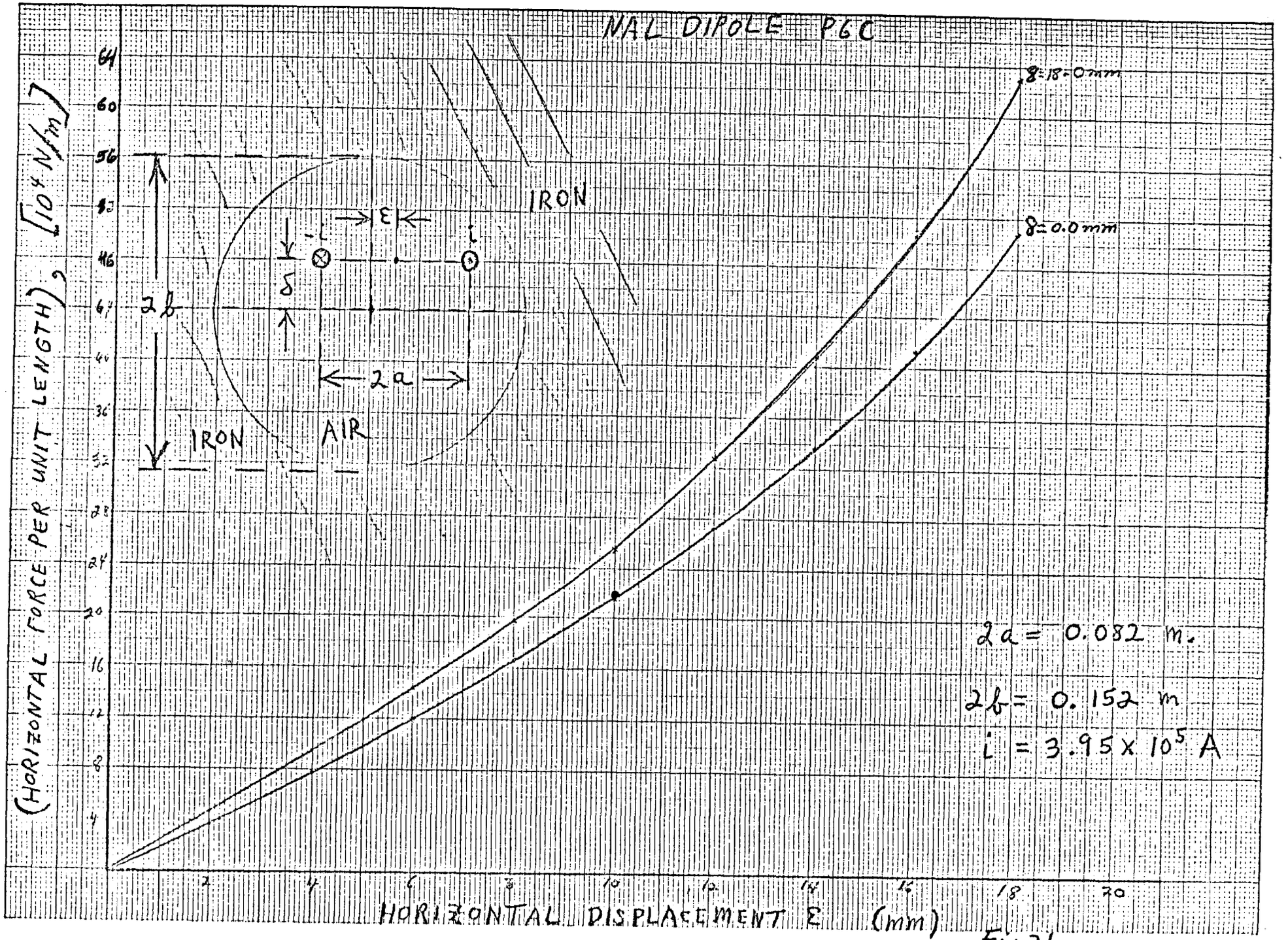
MAL DIPOLE P6C
(HORIZONTAL FORCE PER UNIT LENGTH) [10⁴ N/m]
64
60
56
52
48
44
40
36
32
28
24
20
16
12
8
4
IRON
IRON
AIR
ε
δ
2b
2a
i
i
δ=18.0mm
δ=0.0mm
2a = 0.082 m.
2b = 0.152 m
i = 3.95 x 10⁵ A
2
4
6
8
10
12
14
16
18
20
HORIZONTAL DISPLACEMENT ε (mm)

Fig 21

READY
LIST

STICKOUT 17:03EST 01/05/73

	X	Y	Z	B_X	B_Y	B_Z	TOTAL B
100	5.070	0.	0.	-0.80232E-02	-0.18335E+00	-0.84659E-03	0.18355E+00
105	5.060	0.	0.	-0.12694E-01	-0.11931E+00	-0.84508E-03	0.11993E+00
110	5.050	0.	0.	-0.15186E-01	0.11102E+00	-0.41949E-04	0.11205E+00
115	5.040	0.	0.	-0.71227E-02	0.66284E+00	0.28301E-02	0.66298E+00
120	5.030	0.	0.	0.47226E-02	0.15783E+01	0.75235E-02	0.15783E+01
125	5.020	0.	0.	0.86819E-02	0.26372E+01	0.10873E-01	0.26379E+01
130	5.010	0.	0.	0.91134E-02	0.35512E+01	0.11976E-01	0.35513E+01
135	5.000	0.	0.	0.61396E-02	0.41540E+01	0.11036E-01	0.41540E+01
140	4.990	0.	0.	0.31788E-02	0.44566E+01	0.91984E-02	0.44566E+01
145	4.980	0.	0.	0.16226E-02	0.45715E+01	0.78217E-02	0.45715E+01
150	4.970	0.	0.	0.90490E-03	0.45969E+01	0.69351E-02	0.45969E+01
155	4.960	0.	0.	0.54892E-03	0.45876E+01	0.64316E-02	0.45876E+01
160	4.950	0.	0.	0.35434E-03	0.45687E+01	0.61441E-02	0.45687E+01
165	4.930	0.	0.	0.16631E-03	0.45301E+01	0.58064E-02	0.45301E+01
170	4.900	0.	0.	0.64523E-04	0.44905E+01	0.56570E-02	0.44905E+01
175	4.850	0.	0.	0.13090E-04	0.44584E+01	0.56157E-02	0.44584E+01
180	4.800	0.	0.	0.64201E-05	0.44433E+01	0.55973E-02	0.44433E+01
185	5.070	0.	0.020	-0.53479E-02	-0.20479E+00	-0.43684E-02	0.20491E+00
190	5.060	0.	0.020	-0.87782E-02	-0.18916E+00	-0.77666E-02	0.18952E+00
195	5.050	0.	0.020	-0.13437E-01	-0.84098E-01	-0.13271E-01	0.86199E-01
200	5.040	0.	0.020	-0.17014E-01	0.22274E+00	-0.19203E-01	0.22498E+00
205	5.030	0.	0.020	-0.23368E-01	0.27875E+00	-0.16108E-01	0.27921E+00
210	5.020	0.	0.020	-0.18074E-01	0.19447E+01	0.15096E-01	0.19449E+01
215	5.010	0.	0.020	-0.87668E-02	0.30776E+01	0.58545E-01	0.30771E+01
220	5.000	0.	0.020	-0.81935E-03	0.39153E+01	0.19420E+00	0.39167E+01
225	4.990	0.	0.020	0.24770E-02	0.43910E+01	0.11713E+00	0.43926E+01
230	4.980	0.	0.020	0.17664E-02	0.44590E+01	0.11801E+00	0.44615E+01
235	4.970	0.	0.020	0.12021E-02	0.44801E+01	0.11	

340	4.960	0.	0.020	0.59240E-03	0.44667E+01	0.11795E+00	0.44683E+01
345	4.950	0.	0.020	0.37584E-03	0.44406E+01	0.11979E+00	0.44422E+01
350	4.930	0.	0.020	0.17781E-03	0.44026E+01	0.11640E+00	0.44040E+01
355	4.900	0.	0.020	0.72003E-04	0.43589E+01	0.11507E+00	0.43597E+01
360	4.850	0.	0.020	0.22961E-04	0.43263E+01	0.11306E+00	0.43278E+01
365	4.800	0.	0.020	0.92717E-05	0.43135E+01	0.11654E+00	0.43151E+01
270	5.070	0.020	0.	0.69445E-02	-0.25622E+00	0.24630E-03	0.25631E+00
275	5.060	0.020	0.	-0.13240E+00	-0.32807E+00	0.10754E-02	0.35379E+00
280	5.050	0.020	0.	-0.61158E+00	-0.38143E+00	0.36577E-02	0.72079E+00
285	5.040	0.020	0.	-0.18967E+01	0.29138E+00	0.90468E-02	0.19190E+01
290	5.030	0.020	0.	-0.24555E+01	0.18034E+01	0.72955E-02	0.31007E+01
295	5.020	0.020	0.	-0.22518E+01	0.33927E+01	0.14658E-01	0.40720E+01
300	5.010	0.020	0.	-0.14890E+01	0.45245E+01	0.55857E-03	0.47632E+01
305	5.000	0.020	0.	-0.62482E+00	0.47988E+01	-0.34306E-01	0.48394E+01
310	4.990	0.020	0.	-0.18817E+00	0.47347E+01	-0.47607E-01	0.47387E+01
315	4.980	0.020	0.	-0.24779E-01	0.46570E+01	-0.50903E-01	0.46573E+01
320	4.970	0.020	0.	0.31094E-01	0.46060E+01	-0.52236E-01	0.46064E+01
325	4.960	0.020	0.	0.45900E-01	0.45690E+01	-0.52670E-01	0.45695E+01
330	4.950	0.020	0.	0.45394E-01	0.45407E+01	-0.52938E-01	0.45413E+01
335	4.930	0.020	0.	0.33678E-01	0.45011E+01	-0.53397E-01	0.45015E+01
340	4.900	0.020	0.	0.19067E-01	0.44635E+01	-0.53586E-01	0.44639E+01
345	4.850	0.020	0.	0.81126E-02	0.44333E+01	-0.53315E-01	0.44336E+01
350	4.800	0.020	0.	0.40491E-02	0.44187E+01	-0.53377E-01	0.44190E+01
355	4.000	0.	0.	-0.24902E-07	0.44212E+01	0.55654E-02	0.44212E+01
360	3.000	0.	0.	-0.53056E-08	0.44200E+01	0.54556E-02	0.44200E+01
365	2.000	0.	0.	-0.18814E-08	0.44195E+01	0.55160E-02	0.44195E+01

CENTRAL FIELD

STADY
SYS
0044.56 CPU 0001.76 TOW 0040.58 KC

OFF AT 17:10EST 01/05/73

OLD STICKOUT

READY
LIST

P6C

STICKOUT 12:56EST 12/22/72 (1)

	X	Y	Z	B_x	B_y	B_z	B_{TOT}
100	5.130	0.	0.	-0.12535E-02	-0.15246E+00	0.54952E-04	0.15247E+00
105	5.120	0.	0.	-0.56379E-03	-0.97015E-01	0.18356E-03	0.97017E-01
110	5.110	0.	0.	0.87624E-03	0.54520E-01	0.34242E-03	0.54528E-01
115	5.100	0.	0.	0.16093E-02	0.31942E+00	0.40049E-03	0.31942E+00
120	5.090	0.	0.	0.51855E-03	0.64949E+00	0.16332E-03	0.64950E+00
125	5.080	0.	0.	-0.35389E-05	0.98438E+00	-0.25426E-03	0.98438E+00
130	5.070	0.	0.	0.10097E-02	0.13359E+01	-0.59406E-03	0.13359E+01
135	5.060	0.	0.	0.10319E-02	0.17240E+01	-0.99301E-03	0.17240E+01
140	5.050	0.	0.	-0.14679E-03	0.21103E+01	-0.15846E-02	0.21103E+01
145	5.040	0.	0.	0.21017E-03	0.24766E+01	-0.20467E-02	0.24766E+01
150	5.030	0.	0.	0.15101E-02	0.28570E+01	-0.21874E-02	0.28570E+01
155	5.020	0.	0.	0.16707E-02	0.32391E+01	-0.24508E-02	0.32391E+01
160	5.010	0.	0.	0.10491E-02	0.35487E+01	-0.30266E-02	0.35487E+01
165	5.000	0.	0.	0.66897E-03	0.37381E+01	-0.39789E-02	0.37381E+01
170	4.980	0.	0.	0.41478E-03	0.38498E+01	-0.48625E-02	0.38498E+01
175	4.950	0.	0.	0.10114E-03	0.38290E+01	-0.55652E-02	0.38290E+01
180	4.900	0.	0.	0.48341E-05	0.37886E+01	-0.54208E-02	0.37886E+01
185	4.800	0.	0.	-0.31828E-05	0.37609E+01	-0.55481E-02	0.37609E+01
190	5.130	0.	0.020	-0.14055E-02	-0.16395E+00	-0.25446E-03	0.16396E+00
195	5.120	0.	0.020	-0.10975E-02	-0.13470E+00	-0.58320E-05	0.13471E+00
200	5.110	0.	0.020	0.10290E-03	-0.33160E-01	0.71893E-03	0.33168E-01
205	5.100	0.	0.020	0.14258E-02	0.16862E+00	0.16389E-02	0.16863E+00
210	5.090	0.	0.020	0.16995E-02	0.45406E+00	0.19563E-02	0.45407E+00
215	5.080	0.	0.020	0.13269E-02	0.77573E+00	0.11579E-02	0.77574E+00
220	5.070	0.	0.020	0.19029E-02	0.11158E+01	0.73166E-04	0.11158E+01
225	5.060	0.	0.020	0.27726E-02	0.14889E+01	-0.10884E-02	0.14889E+01
230	5.050	0.	0.020	0.27808E-02	0.18858E+01	-0.32806E-02	0.18858E+01
235	5.040	0.	0.020	0.27484E-02	0.22870E+01	-0.67297E-02	0.22870E+01

240	5.030	0.	0.020	0.32943E-02	0.26979E+01	-0.10539E-01	0.26979E+01
245	5.020	0.	0.020	0.29169E-02	0.31155E+01	-0.14110E-01	0.31155E+01
250	5.010	0.	0.020	0.10102E-02	0.34918E+01	-0.16108E-01	0.34919E+01
255	5.000	0.	0.020	0.15795E-02	0.37424E+01	-0.16098E-01	0.37425E+01
260	4.990	0.	0.020	0.71227E-03	0.38525E+01	-0.18213E-01	0.38526E+01
265	4.950	0.	0.020	0.79806E-04	0.38191E+01	-0.18358E-01	0.38191E+01
270	4.900	0.	0.020	-0.99478E-07	0.37804E+01	-0.18639E-01	0.37804E+01
275	4.800	0.	0.020	-0.33265E-05	0.37525E+01	-0.17817E-01	0.37525E+01
280	5.130	0.020	0.	0.95006E-03	-0.22741E+00	0.22083E-04	0.22741E+00
285	5.120	0.020	0.	-0.14193E+00	-0.27058E+00	0.15603E-03	0.30554E+00
290	5.110	0.020	0.	-0.48332E+00	-0.13387E+00	0.39581E-03	0.50152E+00
295	5.100	0.020	0.	-0.79997E+00	0.35165E+00	0.51520E-03	0.87385E+00
300	5.090	0.020	0.	-0.71137E+00	0.99330E+00	-0.16703E-03	0.12218E+01
305	5.080	0.020	0.	-0.54062E+00	0.10787E+01	-0.51455E-03	0.12066E+01
310	5.070	0.020	0.	-0.78098E+00	0.13373E+01	0.18696E-03	0.15486E+01
315	5.060	0.020	0.	-0.94025E+00	0.19596E+01	0.39990E-03	0.21735E+01
320	5.050	0.020	0.	-0.60832E+00	0.23478E+01	-0.65252E-03	0.24253E+01
325	5.040	0.020	0.	-0.64276E+00	0.24174E+01	0.51038E-03	0.25014E+01
330	5.030	0.020	0.	-0.91001E+00	0.28427E+01	0.27574E-02	0.29848E+01
335	5.020	0.020	0.	-0.81907E+00	0.35570E+01	0.36738E-02	0.36501E+01
340	5.010	0.020	0.	-0.45855E+00	0.39013E+01	-0.70159E-02	0.39282E+01
345	5.000	0.020	0.	-0.16699E+00	0.39004E+01	-0.77363E-02	0.39040E+01
350	4.980	0.020	0.	0.75896E-02	0.38336E+01	-0.10018E-01	0.38336E+01
355	4.950	0.020	0.	0.22781E-01	0.37834E+01	-0.10238E-01	0.37835E+01
360	4.900	0.020	0.	0.10411E-01	0.37443E+01	-0.10495E-01	0.37443E+01
365	4.800	0.020	0.	0.27195E-02	0.37165E+01	-0.10104E-01	0.37165E+01

READY

Appendix III

CRYOGENIC COOLING OF SUPERCONDUCTING MAGNETS FOR THE NAL ENERGY DOUBLER SYSTEM

Peter C. Vander Arend
Henry F. Daley, Jr.
Cryogenic Consultants, Inc.
Allentown, Pennsylvania
25 January 1973

Under NAL Subcontract 80073

CONTENTS

1. INTRODUCTION

2. DESIGN PARAMETERS OF THE MAGNET SYSTEM

3. MAGNET COOLING

4. HEAT FLUX INTO THE MAGNET SYSTEM

5. MAGNET SUPPORT SYSTEM

6. REFRIGERATION SYSTEMS

7. CONCLUSIONS

LIST OF FIGURES

FIG. 1 MAGNET WINDING AND COOLING CHANNELS

FIG. 2 MAGNET ASSEMBLY CROSS SECTION

FIG. 3 MAGNET COOLING SCHEMATIC

FIG. 4 MAGNET SUPPORT SYSTEM

FIG. 5 DETAILS OF MAGNET SUPPORT SYSTEM

FIG. 6 DETAILS OF MAGNET SUPPORT SYSTEM WITHOUT SHIELD

FIG. 7 SLING SUSPENSION

FIG. 8 DISC SUSPENSION

FIG. 9 REFRIGERATION SCHEMATIC FOR SHIELDED MAGNET SYSTEM

FIG. 10 REFRIGERATION SCHEMATIC FOR UNSHIELDED MAGNET SYSTEM

1. INTRODUCTION

The NAL energy doubler will be constructed of a ring of superconducting magnets in parallel with the existing accelerator. The use of superconducting magnets imposes some difficult engineering problems, both in magnet design and the application of refrigeration. This report deals with the application of refrigeration to the magnets individuallly, the application of refrigeration to the overall system, and the preliminary design of a magnet support system with low heat leak. The preliminary definition of solutions to these problems makes it possible to define the size and number of refrigerators required. Cost of the cryogenic system can be evaluated on the basis of the chosen concepts.

2. DESIGN PARAMETERS OF THE MAGNET SYSTEM

At the very start of the program it was necessary to provide a number of criteria to start engineering. The following criteria were chosen:

2.1 Total refrigeration requirements were selected to be 5 watts per meter. This number was chosen on the basis of preliminary studies by other organizations (ref. 1 & 2). The refrigeration requirements were divided roughly as follows:

A-C Losses in the Magnets	1 W/Meter
Heat Gain Through Insulation and Supports of the Magnets	2 W/Meter
Miscellaneous	2 W/Meter

2.2 Twenty-four service buildings are available for location of equipment. For instance, the number of refrigerators may be twenty-four or twelve, if a single refrigerator can service double the distance.

2.3 The magnets will be constructed with warm iron located outside the vacuum shell of the magnet dewar.

3. MAGNET COOLING

Various methods for cooling individual magnets were investigated. In principle, cooling may be applied through the use of boiling liquid helium or supercritical helium. In the second case, one depends on the specific heat of the single phase helium for removal of heat. When boiling liquid helium is used for cooling, the temperature of the helium is a function of the local vapor pressure and it is possible to provide a uniform temperature throughout the magnet system as long as the pressure is maintained at a constant level.

The use of supercritical helium requires flow of the fluid through the magnet. The rate of temperature change is a function of the flow rate and the number of heat exchangers in which the supercritical helium is cooled. Magnet cooling needs to be studied from the macroscopic and microscopic viewpoints. The macroscopic viewpoint deals with the bulk fluid, its change in temperature or phase, and the removal of warmed fluid or vapor from the magnet system. The microscopic viewpoint deals with the heat transfer between individual windings of the magnet and the fluid directly in contact with these windings, and the transfer of this heat to the bulk fluid surrounding the magnet. It deals with the actual structure of the coils and the required porosity of the magnet assembly.

3.1 Heat transfer between windings and fluid.- The a-c losses are generated in the windings and have to be removed through heat transfer to the liquid helium surrounding the windings. In order to arrive at a high current density, the magnet windings need to be closely packed and open space for liquid helium needs to be limited. A first approach is to assume that the open spaces or channels are arranged as parallel paths and that helium is forced through by means of a pump or some other driving force. A fundamental problem of flow through a large number of parallel paths is the achievement of uniform distribution of this flow. If

distribution is to be uniform, dimensional tolerances need to be adhered to. This is difficult to do.

It is not necessary to provide many parallel paths with exactly equal distribution. Figure 1 shows the configuration of windings and channels of the magnet. The bulk fluid moves in parallel with the windings and flow as indicated by the arrows is generated through density differences in the liquid helium. The local flow rates are small relative to the bulk flow rate and only need to remove heat from the windings at a rate of 1 watt per meter of magnet length. The surface area available to heat transfer per meter length is large, and in spite of low local flow rates (and low heat transfer coefficients), it is possible to hold the temperature of the windings within .1°K of the temperature of the bulk fluid outside the windings. Outside the windings the warmed helium from the channels between windings is mixed with the bulk fluid and changes its temperature slightly.

3.2 Heat removal from the bulk fluid stream.- The bulk fluid temperature changes gradually while flowing through a series of magnets. If refrigerators are located at 800 ft intervals (one per service building), then the bulk fluid flow rate needs to be large enough to limit the temperature rise of the helium to an acceptable level in passing through this distance.

In order to eliminate the temperature rise of the bulk fluid stream, the concept shown in Figures 2 and 3 was developed. Figure 2 shows a fluid passage outside the vessel containing the magnet. Figure 3 shows schematically a complete loop of the helium flow through the magnet system. At Point 1 liquid helium is taken from a reservoir and pumped to a pressure of 10-15 psig. The heat introduced by the pump is removed and Stream 2 enters the first magnet vessel with a temperature of 4.5 - 4.6°K. The helium flows through a minimum of 400 ft of

magnet reservoir (20 magnets of 20 ft length) and exits as Stream 3. The pressure of Stream 3 is only slightly less than that of Stream 2. In flowing through the valve, the pressure of the helium is lowered and boiling is initiated. Stream 4 enters the passage between concentric tubes as shown in Figure 2 and returns through 400 ft of magnet system to the liquid reservoir of the refrigerator. In passing through the magnet system, heat transfer takes place and liquid helium vaporizes. The gas contents of the returning stream increases. The amount of heat to be transferred from the magnet reservoirs into the stream of boiling liquid helium is 1 watt per meter. The surface area available for this is approximately 3800 cm^2. Because of this large surface area, heat transfer takes place with a small temperature difference between streams.

The features of the proposed cooling system are the following:

a) The rate of helium flow is determined by the total amount of heat to be removed, divided by the heat of vaporization of helium. This rate is much lower than the one dependent on specific heat of liquid helium.

b) Heat entering the system from the environment is intercepted by boiling liquid helium before it enters the magnet system.

c) The temperature of all magnets in a loop is constant.

d) By returning the helium to the same service location, the accelerator system may be divided conveniently into a number of relatively small self-contained units.

4. HEAT FLUX INTO THE MAGNET SYSTEM

4.1 Support system.- The heat flux from the environment is closely associated with the support system necessary to accurately locate and hold the magnets relative to the iron. Section 5 deals with the mechanical aspects of the support system. This section deals with the thermal properties of the proposed support system.

Figure 4 shows the basic concept of a support and insulation system for the magnet. The insulation consists of superinsulation and support pins located as indicated. It is to be noted that a shell surrounds the magnet. The shell is equipped with high pressure helium coolant passages. The temperature of the shell is maintained at 15-20°K. This has the following advantages:

a) Thermal conductivity of materials used for the support pins (G-10) is extremely low between 4 and 20°K.

b) Radiation from a shell at 20°K to a surface of 4°K is extremely small.

c) Refrigeration provided at the 20°K temperature level is much cheaper than that provided at 4°K (by a factor 3).

Figure 5 shows details of the proposed support and insulation system. Dimensions are shown with heat fluxes through the superinsulation and supports. The numbers are those for a complete system of 800 ft (40 magnets) length. In order to evaluate the economic significance of the 20°K shield, heat flow from the environment to the 4°K temperature level was determined for an identical support system without cooled shield. Figure 6 shows details of this system.

Tables I and II summarize the heat input to the magnet system from all sources.

TABLE I

Heat Flux and Magnet Heat Input with Use of a 20°K Shield:

1) To Magnet (at 4.6°K)	Watts/Magnet
Radiation from 20°K Shield	0
Conduction through Supports	.43
A-C Losses	6.00
Connecting Tubes between Magnets	.10
TOTAL.....	6.53

2) To 20°K Shield	
Superinsulation	3.50
Conduction through Supports	9.84
Radiation through Non-Superinsulated Spaces	1.10
Connecting Tubes between Magnets	.20
TOTAL.....	14.64

TABLE II

Heat Flux and Magnet Heat Input without Use of a 20°K Shield:

1) To Magnet (at 4.6°K)	Watts/Magnet
Conduction through Supports	0
Radiation from 300°K	0
A-C Losses	6.00
Connecting Tubes between Magnets	.10
TOTAL.....	6.10

TABLE II, (Continued)

2) To Boiling Liquid Helium between 4" and 4¼" Tubes	Watts/Magnet
Superinsulation	2.86
Conduction through Supports	7.60
Radiation through Non-Superinsulated Spaces	1.10
Connecting Tubes between Magnets	.20
TOTAL.....	11.76

The significance of the numbers in Tables I and II is as follows:

Heat to be removed from the 4.6°K temperature level is 6.53 watts per magnet with shield and 18.39 watts per magnet without shield. The fluid flow rate through the magnets is proportional to the heat to be removed. Consequently, the shielded magnet system requires only 35½% of the helium flow rate through the magnets of that of the unshielded magnet system. This is quite significant from an economic standpoint, because:

a) For the same overall pressure drop the shielded magnet system will more easily tolerate the location of a refrigerator at every other service station.

b) The heat input from pump work is significantly less for the shielded magnet system as shown in Section 4.2.

c) The size of refrigerators is much smaller for the shielded magnet system.

It should be noted that at the present time the numbers quoted in Tables I and II are not necessarily optimal.

The study of the refrigerator systems may show that the shield temperature should be different from the one chosen. Also, after more detailed analysis, the magnet support system may pass less heat either into the shield at 20°K or the magnet system at 4.6°K.

4.2 Heat input from the liquid helium pump.- Figure 3 shows that a liquid helium pump is used to generate sufficient pressure for the maintenance of a single phase fluid in the magnet system. Typical operating conditions are given in Table III.

TABLE III

Helium Pump Operating Conditions:

Fluid At:	Inlet	Discharge
Pressure	1.19 atm	2.00 atm
Temperature	4.4°K	4.86°K
Enthalpy	10.96 J/g	14.96 J/g

The discharge conditions are based on a pump efficiency of 60%. In order to maintain the magnet temperature at 4.6°K, the liquid helium discharged by the pump needs to be cooled to 4.5°K through heat exchange with boiling liquid helium in the reservoir of Figure 3. The enthalpy of the liquid helium entering the magnet system is then 12.57 J/gr and is maintained at this level during its passage through the magnets.

In order to remove the heat from the 4.6°K temperature level through vaporization of helium, a minimum helium flow rate of 14.5 or 39.6 g/sec is required for the shielded or the unshielded system, respectively (based on 40 magnets of 20 ft length). This minimum flow rate is based on having vaporized all of the helium in the space between concentric tubes around the

magnets prior to entry in the vapor space of the liquid reservoir of Figure 3. In practice, to obtain sufficient heat transfer without a temperature increase in the two-phase fluid system, the flow rate needs to be twice the minimum required. Therefore, total heat inputs from the pump are 116 and 317 watts for shielded and non-shielded magnet systems, respectively.

4.3 Heat input through transfer lines between the refrigerator and magnet system.- A preliminary estimate based on length and diameter of transfer line shows that the heat leak will be of the order of 50 watts. In case a shielded magnet system is used, practically all of this heat will be removed at the 20°K level. For the non-shielded case it obviously will be removed at the 4.6°K temperature level.

4.4 Heat input through electrical leads and other connections between ambient temperature and the magnet system.- A well designed electrical lead carrying 2000 A of d-c current requires approximately 3 liters of liquid helium per hour for adequate cooling. The pulsed magnet system requires maximum current only during a fraction of the time. Without a detailed study of the lead and vent tube requirements, it has been assumed that the refrigerators, when spaced at 800 ft intervals, need to provide 25 liters of liquid helium per hour per refrigerator. This liquid is returned to the refrigerator in the form of warm gas of low pressure.

4.5 Summary of refrigeration requirements.- Tables IV and V show the total amounts of refrigeration to be supplied to 800 ft of magnets.

TABLE IV

Magnet System with 20°K Shield:

1) Refrigeration at 4.4°K	Watts
A-C Heat in Magnets	240
Heat from 20°K Environment	21
Pump Work	116
Heat Leak in Transfer Lines	0
Unknowns	61
TOTAL.....	438

2) Refrigeration at 20°K	Watts
Superinsulation	140
Conduction through Supports	393.6
Radiation through Non-superinsulated Space	44
Connecting Tubes between Magnets	8
Transfer Lines	50
TOTAL.....	636

TABLE V

Magnet System without Shield:

Refrigeration at 4.4°K	Watts
A-C Heat in Magnets	240
Superinsulation	114.4
Conduction through Supports	304
Radiation through Non-superinsulated Space	44

TABLE V, (Continued)

	Watts
Connecting Tubes between Magnets	12
Pump Work	317
Transfer Lines	50
TOTAL.....	1081

In addition to refrigeration, it is assumed that 25 liters of liquid helium need to be made to satisfy cooling requirements of electrical leads and vent tubes connecting the magnet system with the environment.

5. MAGNET SUPPORT SYSTEM

Investigations were made of various magnet support systems to be used for supporting the magnet within the vacuum containing outer jacket and the magnet iron. In examining the various potential support systems, the following factors, some of which tend to be inherently contradicting, were considered:

1) Low Thermal Heat Leak.

2) High Rigidity.

3) Reliability.

4) Low Cost.

In the investigation, the basic configuration was assumed to use ambient temperature iron and to be substantially similar to Figure 2, although applications without the shielding structure and its tubing were also considered. The magnet core was assumed to weigh 25 lb/running foot. NAL advised that misalignment of the coil in operating conditions relative to the iron would generate a force of 600 lb/running foot in the horizontal direction for .010" horizontal misalignment and 200 lb/running foot

in the vertical direction for .010" vertical misalignment. These forces were stated to be linear with misalignment.

The first step in the investigation was to determine the frequency or spacing of the supports. Beam calculations on the 4¼" O.D. tube used for containing the helium showed a practical limit of 2 ft spacing without excessive deflection provided that all loadings were uniformly spaced around the circumference of the tube. Since the continuous loading of the tube by the coil with adequate cooling channels is difficult to attain, some of the investigation was performed at 1 ft support intervals.

As a first approach to the design of support members, various arrangements consisting of double opposed slings, similar to that shown in Figure 7, were examined. The principle advantage in such an arrangement was the fact that the loading was distributed around the circumference of the helium tube, thereby reducing the distortion of the tube. The iron, which has a large cross section, can carry the localized loading. It was found that relatively long rods having reasonably low heat leak characteristics and a capability for carrying longitudinal shrinkage were quite elastic under load and would be expensive to construct. The system was then abandoned, since no reasonable compromise was available with metallic rods. High strength composite materials involving filaments would improve the total characteristics of the system, but the use of such materials generated additional problems, such as the technique for end attachments and considerable sponginess.

Composite discs of fiberglass-epoxy in a plane perpendicular to the axis of the bore tube as shown in Figure 8 were examined. Such a system showed high heat leak for a reasonable degree of stability. Other characteristics, such as cost and rigidity, were very good.

All of the above systems maintain the position of the magnet relative to the vacuum jacket and the iron in a concentric location which does not change during cooldown of the magnet from ambient to liquid helium temperatures. Such a system must anticipate misalign-

ment and consequent forces in any direction. If it can be established that misalignment would be in only one predetermined direction, then the support system can be designed so as to carry this unidirectional force with consequent elimination of redundant members.

Figures 4 and 5 show a system of posts in which the magnet drops vertically downward during cooldown because of the thermal shrinkage of the various components. This vertical movement develops a vertical downward force to be carried by the support system. The upper posts shown on Figure 4 will disengage from the wall of the jacket, thereby substantially eliminating the heat leak through these unloaded members.

In addition to reducing the heat leak by eliminating the unnecessary members, there is a further substantial structural advantage to a post system. As indicated earlier, thin-walled shells are highly susceptible to distortion under local loading. By having the post system bear directly upon the magnet coil, the intermediate shells become shims for structural purposes and the load is transmitted directly from the coil to the outer vacuum shell and thence to the close fitting iron.

Because of the uncertainty as to the beam strength of the coil, the post system was analyzed on the basis of 1 ft centers along the axis between supports. The performance of such a system will not change substantially with spacing.

In calculating the performance of the system shown in Figures 4 and 5, it was first determined that if the system of four posts is snug in the warm condition, the bore tube will drop .016" upon cooldown. This value is based on the assumption that the coil has the same thermal contraction characteristics as stainless steel. Since the thermal contraction value of the coil is the main element in the above numerical change, it is essential that the value for the coil be accurately known before final design.

A change in center line of .016" in the vertical direction will produce a vertical magnetic force of 320 lb/support. Since misalignment may produce additional force, it may be desirable to install the magnet coil above center in the warm condition by up to .010" so that on cooldown, the deviation between center lines is limited to as low as .006". If additional vertical deviation of .004" is accepted, the total vertical deviation could be .010" with the consequent generation of 200 lb per ft magnetic force and 25 lb per ft of weight to be carried by the support system. The control of the vertical is substantially within the designer's control.

Positioning of the posts at 30^{o} off the horizontal center line was determined by the need to provide horizontal stability without excessive vertical loading. As positioned, the posts can carry a horizontal variance of .0033" consistent with the .010" vertical variance described above. This can be increased by allowing additional vertical deflection on initial cooldown.

Longitudinal thermal contraction during cooldown and under fully cooled down condition is allowed by anchoring each of the spacing posts to its adjacent inner wall and allowing sliding motion against its adjacent outer wall. This motion occurs before the magnet is energized and forces on the pins are due only to the weight. One limitation involved in this technique of allowing for longitudinal motion is the requirement that the magnet temperature be lower than shield temperature. If shield temperature is lower, the shield will shrink faster than the magnet and its helium tube and the posts will experience a high radial force which may create problems when sliding is required.

The selection of size and material to be used for the pins represents a compromise among the four basic factors described earlier. Minimum heat leak is furnished by a low conductivity/stress ratio in the pins, but this low ratio tends to high strain or spring rates and fragility.

Stainless steel tubes or pins were first considered, but it was found that at a stress level of 40,000 psi for .010" vertical variance, deflection in the pins was almost .002", heat leak to the 20°K end was approximately 3 watts per meter, and typical posts might be 3/8" O.D. tube with a 0.005" wall or a 0.085" Dia. pin. These posts were considered to be very delicate for the ultimate usage.

An alternate and more desirable material is fiberglass reinforced epoxy (NEMA G-10). This material has ultimate compressive and flexural strengths in excess of 50,000 psi and a thermal conductivity only 5% of stainless steel. Using this material at a very conservative stress level of 5,000 psi under a loading of 225 lb in the configuration of Figures 4 and 5, it was determined that the pin diameter needs to be 0.24", the strain in the pin would be 0.0007", the pin heat leak to the 4°K level would be 16.8 watts for 240 meters of magnets (based upon 4 pins touching per support), and the pin heat leak to the 20°K level would be less than 400 watts for 240 meters of magnets (based upon 2 pins touching per support).

To insure that heat transferred through the outer pin was properly absorbed by the shield and not transmitted into the inner pin, a 0.020" thick copper shim is inserted under the outer pin and fastened to a shield cooling tube. The temperature difference between the base of the pin and the shield cooling fluid was less than 2°C.

The fabrication of the magnet is obviously critical since any unplanned variation of more than a few mils from concentricity may generate large forces. A suggested procedure for the assembly of the magnet illustrated in Figure 4 has been developed and will provide the necessary alignment. The procedure as described below does require that the relationship of the windings, and consequently the magnetic field, to the bore tube be known within an accuracy of 1 or 2 mils. Inability to establish this relationship will render it impossible to pre-align the supports and iron and will necessitate post-assembly adjustment of iron through the technique of partially energizing the magnet.

The general technique visualized for the assembly of the magnet consists of first establishing the outside diameter of the four bumpers mounted on the magnet windings at each support location at a known and selected position relative to the inside of the bore tube. If the magnetic field is symmetrical with the bore tube, the relationship of the field to the outside of the buttons is established. The various tubes and shims with carefully controlled lengths and thicknesses are then added. If these known pieces are added to a known diameter, the eventual outside diameter will be known within the tolerances to which parts are manufactured. Fianlly, the iron is precisely manufactured and would be installed with or without shims at the load depending upon the buildup of tolerances.

Typical specific procedures to be used for assembling the magnet are as follows:

1) Install bumpers on the coil windings by the use of epoxy.

2) Machine outside diameter of each ring of bumpers to 3.930". The vertical center of this diameter may or may not coincide with bore tube center depending upon the vertical position desired, but there must be a known relationship to the center of the bore at each support point. This is best accomplished by the use of a special tool in the bore of the coil which is used to align each support position. This tool would likely be of the optical type.

3) Press dimples into 4¼" O.D. x .035" tube at support points.

4) Slide 4¼" O.D. tube over 4" O. D. tube and spot weld at dimples. The technique for sliding longitudinally requires a pressing or squeezing of the tube at the top and bottom so that the vertical diameter reduces, the horizontal diameter increases, and the diameter at the post points increases slightly, thereby permitting telescoping. The deflection on the diameter at the support points is linear

with load and calculates, for each of these tubes, to be in the order of .034" on diameter under a continuous uniform vertical clamp-type load of 8 lb per running inch.

5) The assembly of the 4" and 4¼" tubes is then telescoped onto the coil using the squeeze technique described above.

6) The lower temperature pins are epoxied to the dimples in the 4¼" O.D. tube.

7) The cooling tubes are pre-fastened to the shield and the shield is installed over the low temperature pins. The shield may be either squeezed and telescoped on or may be wrapped and clamped.

8) After installing the copper shorting clips, the outer pins are epoxied to the shield.

9) The outer jacket is then installed over the outer pins again by squeezing. It should be noted that for this squeezing operation, the outer jacket should be as thin as possible, consistent with vacuum and structural requirements. For example, 6", Schedule 5 pipe requires 55 lb per inch to obtain the desired 1/32" diametrical deflection. Force required varies with the cube of the thickness.

10) The closely toleranced iron is then mounted to the outer jacket with solid bearing at the load points. Shims probably will be necessary for accumulated tolerances and ease of manufacturer.

11) The above procedure will be satisfactory only if proper quality control is exercised relative to the maintaining of the radial post system lengths. The accumulation of lengths, including tolerances, can be checked at any point in the course of the assembly by reference back to the inside of the bore tube. The maintaining of close tolerances is necessary to avoid looseness in the system, to control the intended forces on the support system, and to insure that unwanted forces do not appear.

6. REFRIGERATION SYSTEMS

In order to compare the cost of refrigerators for the shielded and unshielded magnet systems, some calculations were carried out to define the refrigeration cycles for each case. Figures 9 and 10 show the basic refrigeration cycles. The figures only show that part of the refrigerators which operates below 80°K.

Table VI shows the requirements for the refrigerators.

T A B L E V I

Refrigerator Requirements: Magnets:	With 20°K Shield	Without 20°K Shield
Liquid Helium Required	25 L/hr	25 L/hr
Refrigeration at 4.4°K	438 W	1081 W
Refrigeration at 20°K	636 W	-
Compressor Flow Rate	450 lb/hr	698 lb/hr
Compressor Horsepower	232	360
Vacuum Pump Horsepower	34	77

It is possible to provide refrigeration at a lower temperature level by using vacuum pumps. The vacuum pump operates at ambient temperature and only provides vacuum to the liquid bath from which the helium pump takes fluid. The heat exchangers of the refrigerators will have an extra passage to accommodate the vacuum helium stream. The last line of Table VI shows the horsepower requirements of the vacuum pump to provide a 3.55°K temperature level in the liquid bath

7. CONCLUSIONS

The work described in the report shows that the construction of a superconducting accelerator ring consisting of some 1,000 magnets is feasible from a standpoint of cryogenics. In general, the cryogenics applied is within the state of the art.

7.1 Test program.- It appears useful to carry out some experimental work in the following areas:

7.1.1 Construct a full-size dewar with all the features described in the report. Test this dewar without magnet to evaluate:

a) Heat loads.

b) Cooling of the fluid contained in the magnet space.

c) Heat transfer characteristics of the boiling liquid helium.

d) Deflections and motion of the dewar support system.

e) Problems associated with assembly.

7.1.2 Test a reciprocating pump of the required capacity under actual operating conditions. Determine its efficiency and mechanical features.

7.2 Shielded Versus Non-shielded Magnets.- It appears that the use of a shield operating at approximately $20^{\circ}K$ will lower the cost of the refrigeration system. Detailed costs are not available at this time. A rough first estimate shows that the difference in refrigerator cost for the complete system is of the order of $\$1.5 \times 10^6$ for shielded versus non-shielded magnets. This amount is not completely saved, because the installation of the shield requires additional cost.

In addition to lower cost, there are other significant advantages to the use of the cooled shield, as follows:

a) The amount of fluid pumped through the magnet system is considerably less in the case of the shielded magnets. This represents lower pressure drops, less heat input by the pump into the fluid, and the potential to locate refrigerators at every other service station.

b) The shielded magnet provides a system with larger safety factors. For instance, the refrigeration to be supplied at the 4.4°K temperature level is used mainly to take up a-c heat. If the a-c heating were larger than anticipated, a reduction in frequency of pulsing would immediately provide sufficient refrigeration.

c) If refrigeration at the 20°K level were insufficient, a change in temperature level to 25 or 30°K would provide an increase in refrigeration at this temperature level proportional to the absolute temperature of the shield. The heat flux to the 4.4°K temperature level would increase some, but a slight reduction in frequency of pulsing would balance heat load and refrigeration.

REFERENCES

(1) Superconducting Synchroton Magnets, Present Status. P. F. Smith. Page 41. Proceedings of the 8th International Conference on High Energy Accelerators. Cern, 1971.

(2) Studies and Construction of Superconducting Magnets Applied to Synchrotons of More than 1000 GeV. Bronca, etal. Page 177. Proceedings of the 8th International Conference on High Energy Accelerators. Cern, 1971.

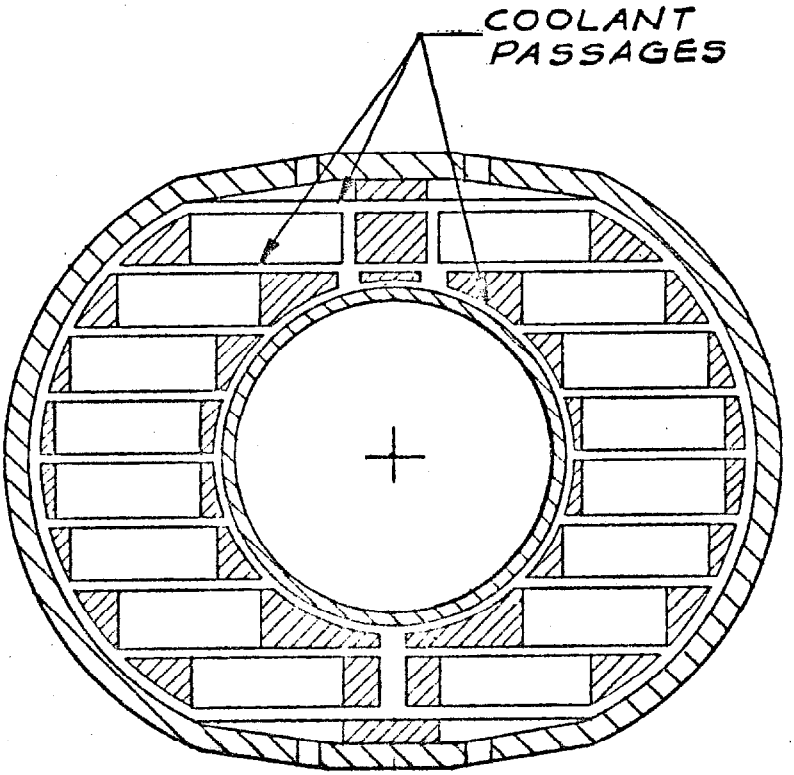

FIG. 1 - MAGNET WINDING AND COOLING CHANNELS

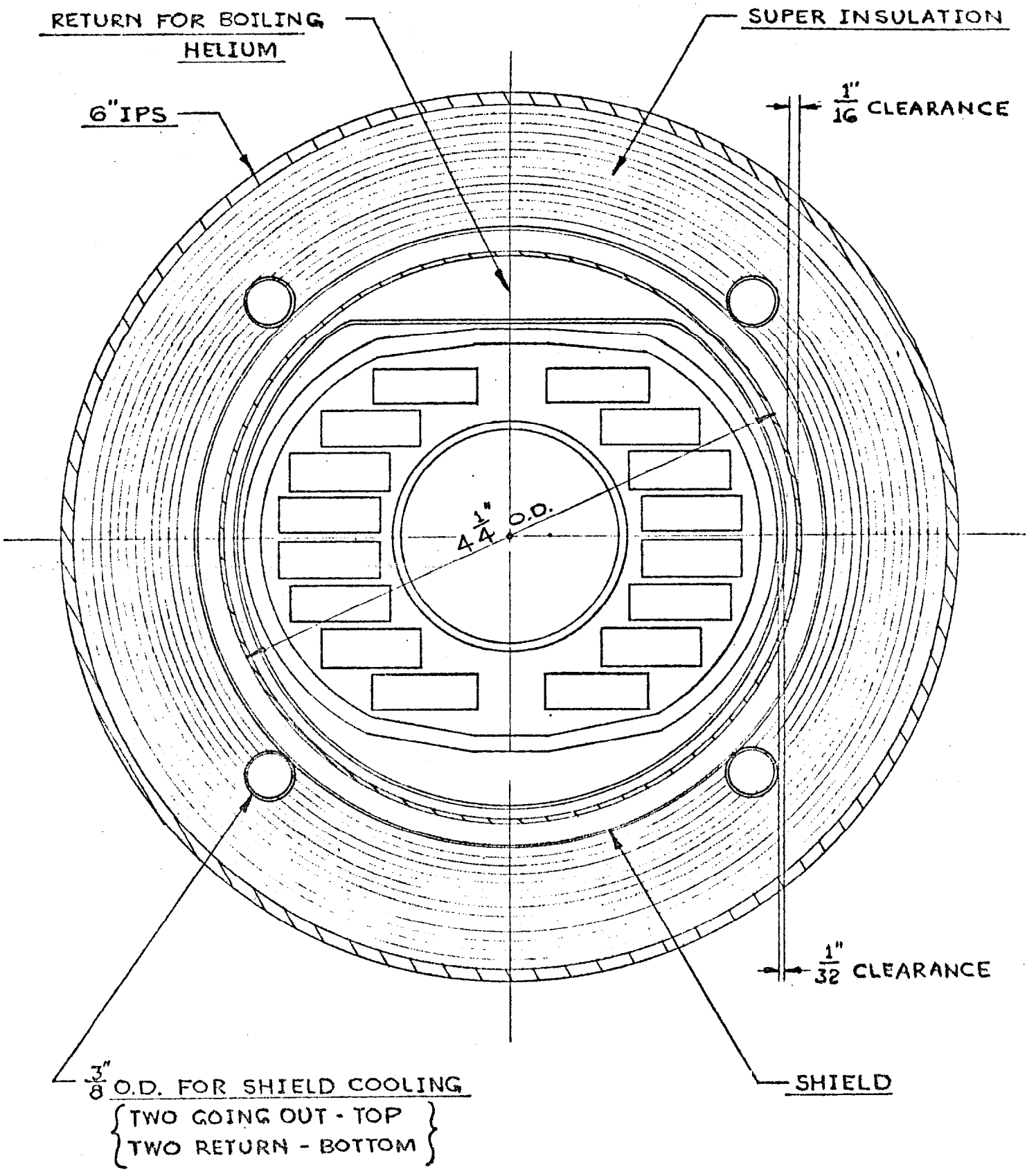

FIG. 2 - MAGNET ASSEMBLY CROSS-SECTION

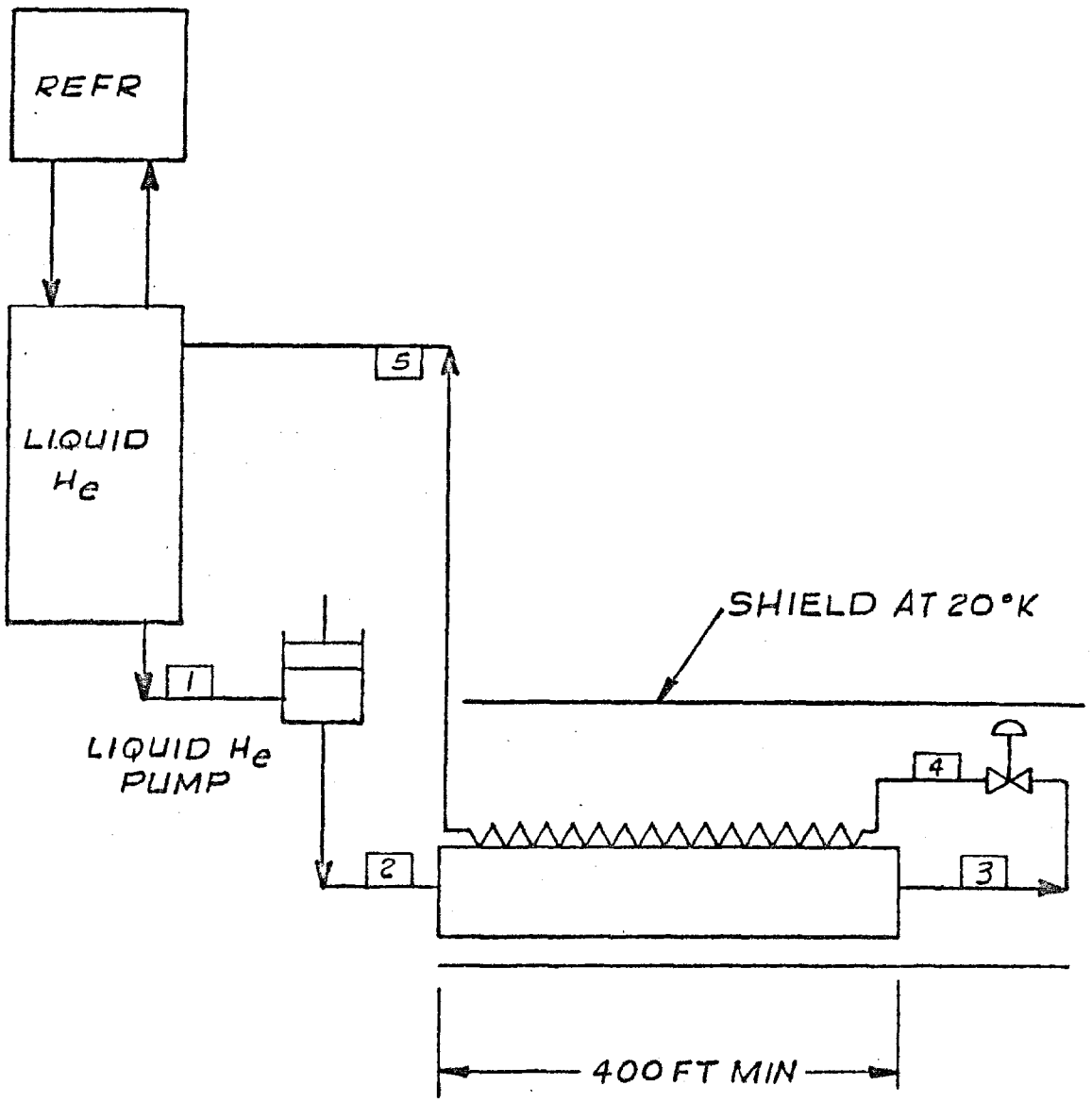

FIG. 3 - MAGNET COOLING SCHEMATIC

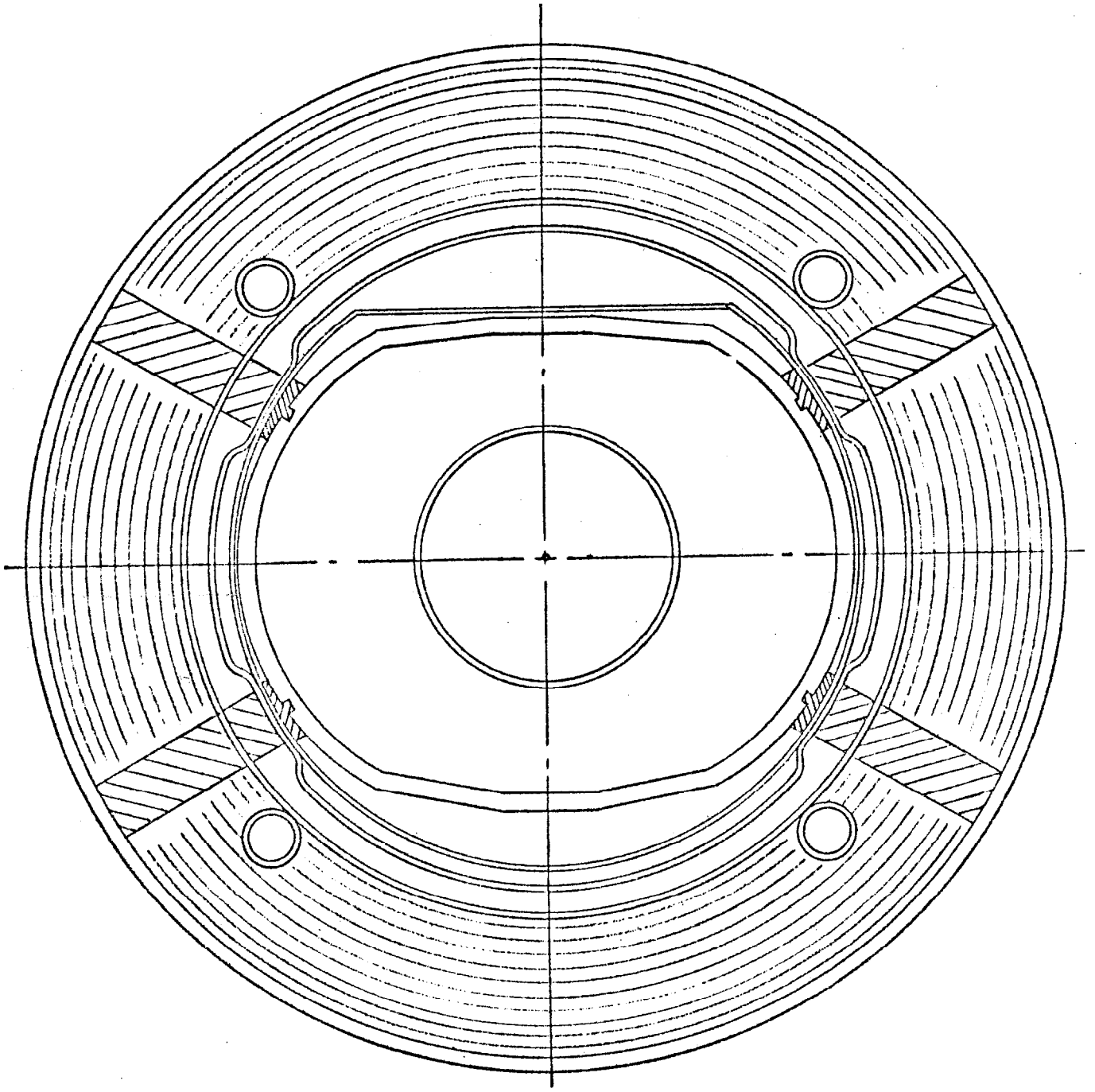

FIG.4 - MAGNET SUPPORT SYSTEM

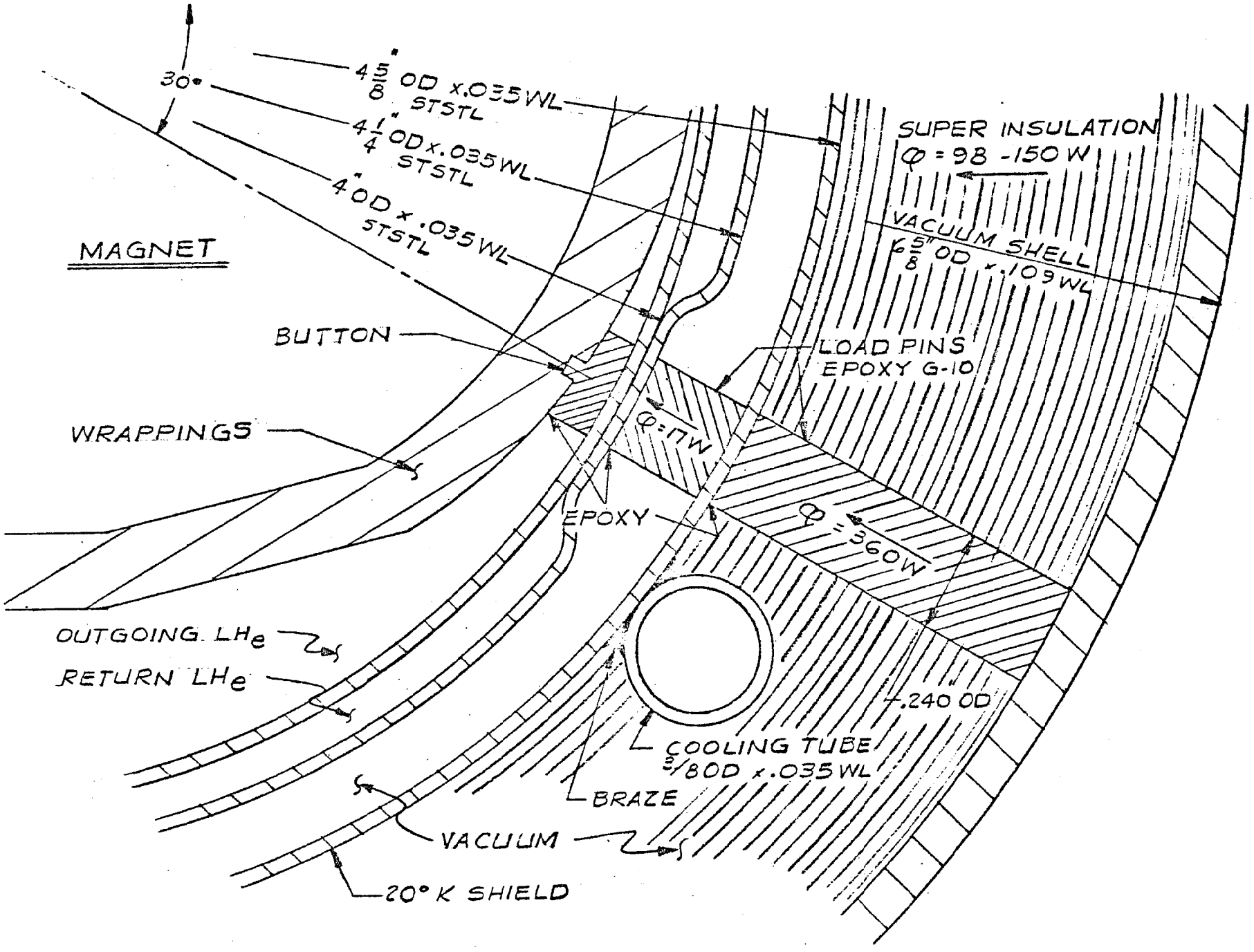

FIG. 5 - DETAILS OF MAGNET SUPPORT SYSTEM

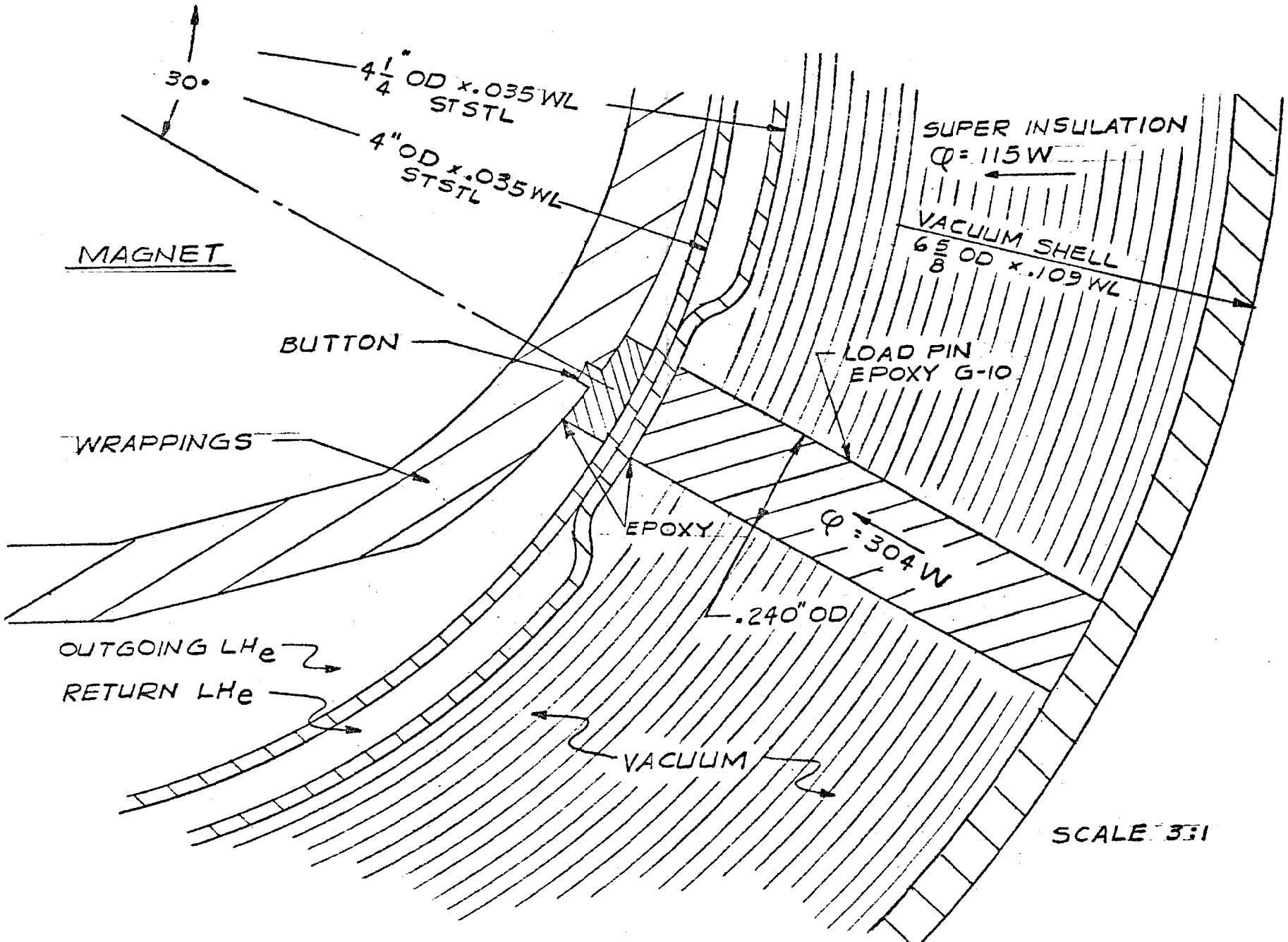

FIG. 6 - DETAILS OF MAGNET SUPPORT SYSTEM WITHOUT SHIELD

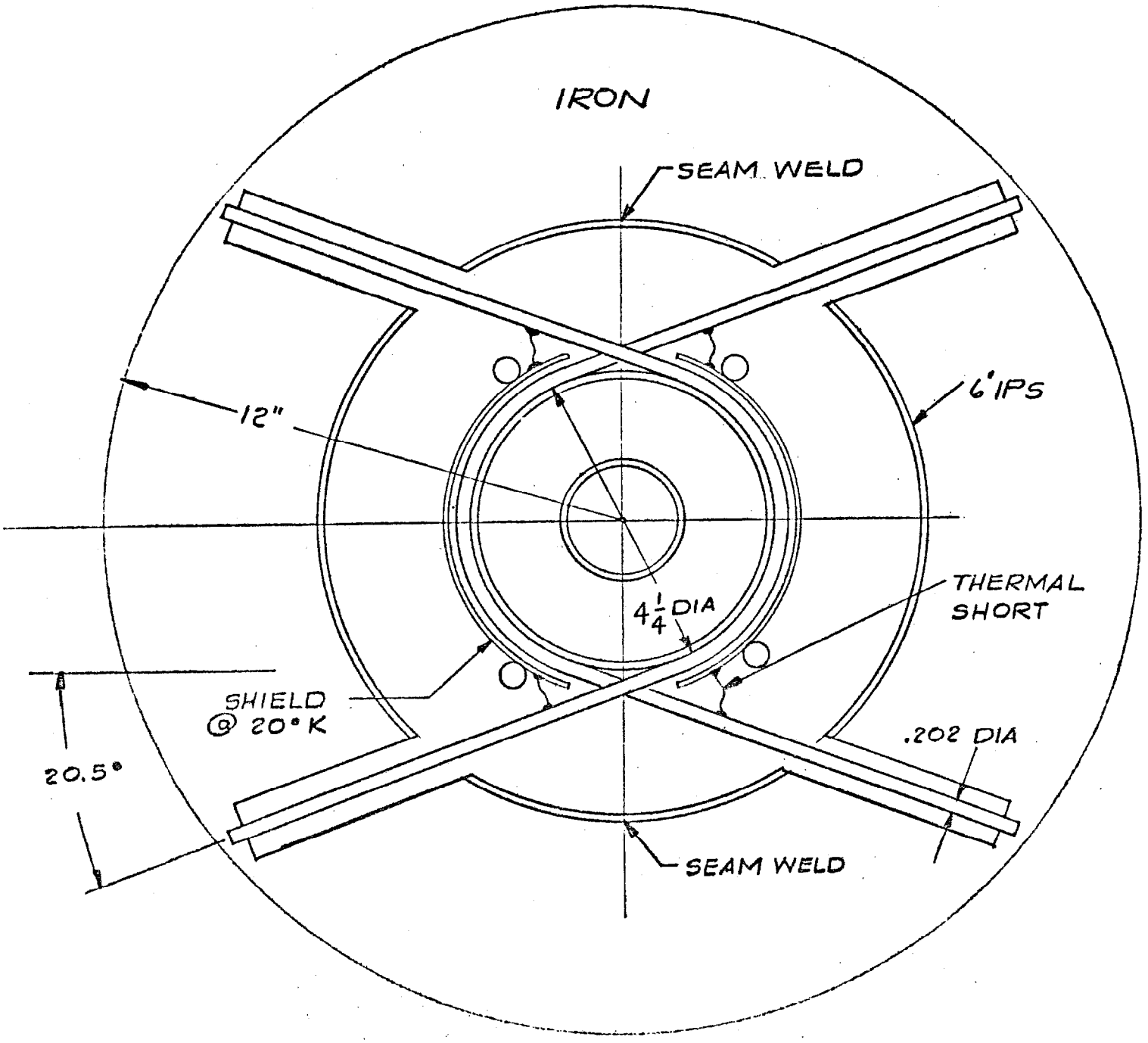

FIG.7 - SLING SUSPENSION

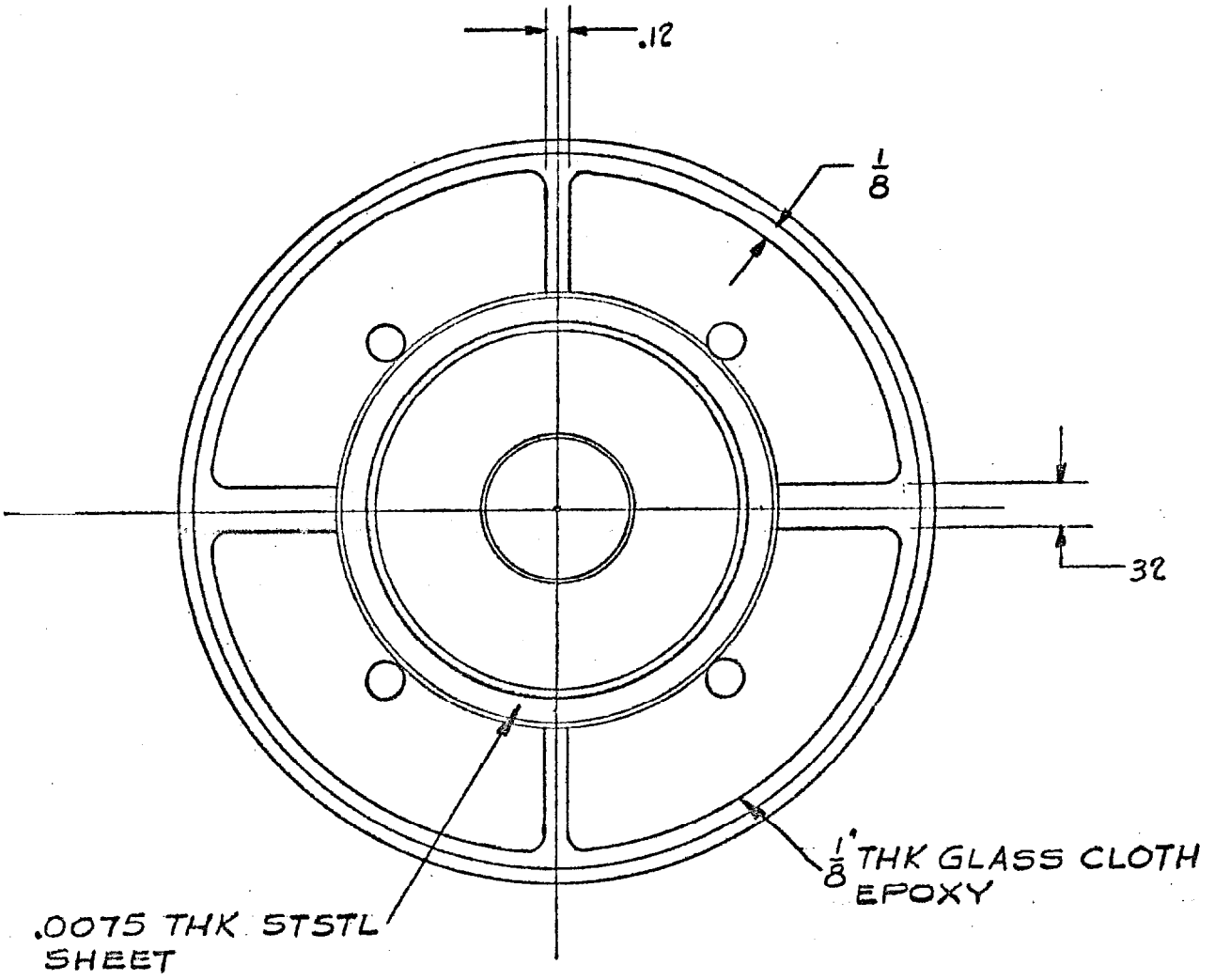

FIG. 8 - DISC SUSPENSION

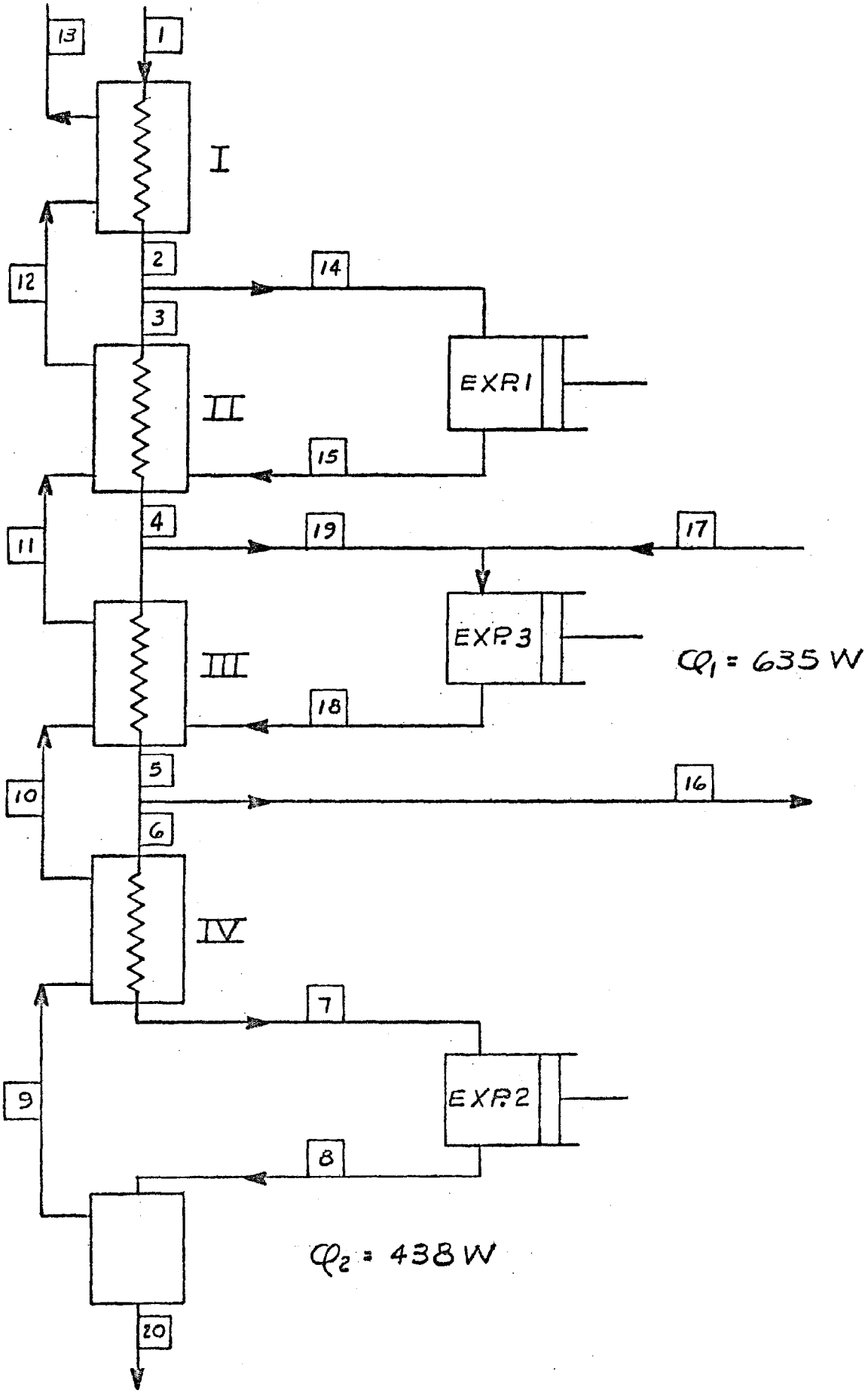

FIG.9 - REFRIGERATION SCHEMATIC FOR SHIELDED MAGNET SYSTEM

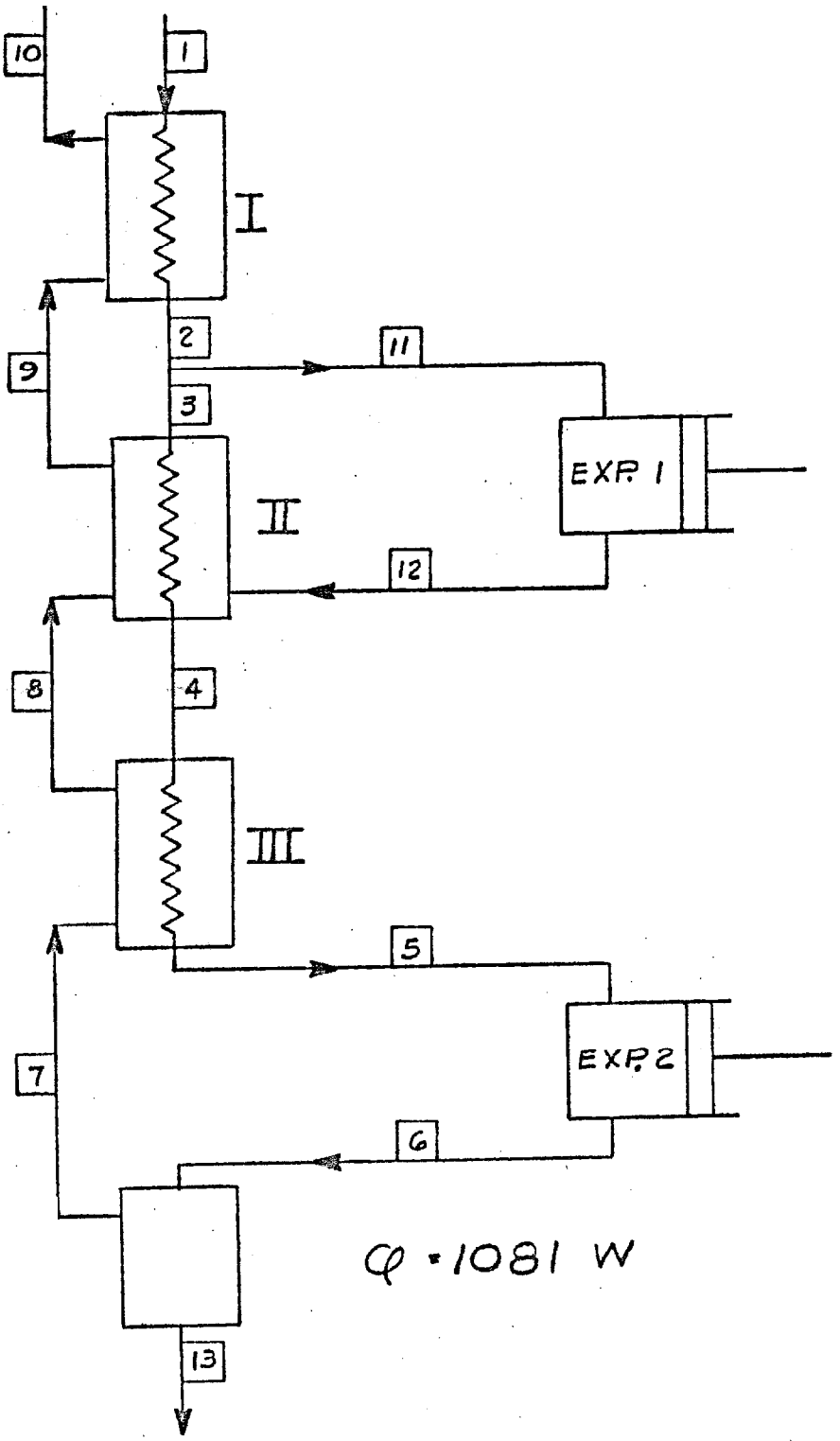

FIG. 10 - REFRIGERATION SCHEMATIC FOR UNSHIELDED MAGNET SYSTEM

CRYOGENIC CONSULTANTS, INC.
January 26, 1973

SCHEDULE

PUMP LOOP INSTALLATION

Liquefier	
Test Complete	1-10-73
Ready to Ship	1-23-73
Arrive NAL	1-25-73
Cold Box Leak Checked	2-12-73
Foundations Complete	1-19-73
All Equipment, Except Cold Box, Set and Aligned	2-12-73
Cold Box Set	2-19-73
Piping (Helium Process)	
Drawings Complete	1-18-73
B/M Complete	1-18-73
Material Complete	2-12-73
Contract Award	2-5-73
Work Complete & Tested	3-19-73
Piping (N_2 System)	
Storage Selected	2-9-73
Storage Received	3-5-73
Drawings Complete	3-2-73
Material Complete	3-2-73
Work Complete & Tested	3-16-73

SCHEDULE (Continued)
PUMP LOOP INSTALLATION

Liquefier	
Piping (Helium Gas Storage)	
Storage Selected	2-26-73
Storage Received & Installed	3-12-73
Drawings Complete	3-9-73
Work Completed & Installed	3-19-73
Piping (Cooling Water)	
Drawings Complete	2-23-73
Work Completed & Installed	3-19-73
Electrical	
Start	2-5-73
Finish	3-12-73
Performance Test	
Start	3-19-73
Finish	3-30-73
Heat Exchanger	
Received	3-30-73
Foundation Design	2-15-73
Foundation Installed	3-5-73
Installed	4-6-73
Pump	
Received	5-1-73
Installed	5-4-73

SCHEDULE (Continued)
PUMP LOOP INSTALLATION

Pump Loop	
Drawings Complete	1-29-73
Sub-assemblies Ordered	2-5-73
Sub-assemblies Received	3-12-73
All Other Material On-hand	3-5-73
Installation Drawings Complete	3-9-73
Tunnel Modification Complete	3-19-73
Piping Fabrication Complete & Tested	4-13-73
Vacuum Jacketed Interconnecting Piping	
Piping Received	3-30-73
Cold Box Modified for V.J. Line	4-13-73
V.J. Lines Installed (Except Pump)	4-20-73
V.J. Lines Installed to Pump	5-4-73
Miscellaneous Piping	
Design Complete	3-23-73
Installation Complete & Tested	4-27-73
Instrumentation	
All Purchased Items On-Hand	3-30-73
Installation Complete	4-13-73
Checkout Complete	4-20-73
Ready to Operate	5-4-73

Appendix IV

PRESSURE DROPS IN THE MAGNET SYSTEM OF THE NAL ENERGY DOUBLER SYSTEM

Peter C. Vander Arend
Henry F. Daley, Jr.
Cryogenic Consultants, Inc.
Allentown, Pennsylvania
1 February 1973

Under NAL Subcontract 80073

All of this work is supported by the USAEC

CONTENTS

1. DISCUSSION

2. CALCULATIONS

3. CONCLUSIONS

LIST OF FIGURES

FIG. 1 MAGNET ASSEMBLY CROSS SECTION

FIG. 2 MAGNET COOLING SCHEMATIC

FIG. 3 CONNECTION BETWEEN MAGNETS

FIG. 4 PRESSURE DROP IN MAGNET, HELIUM SYSTEM

1. DISCUSSION

Pressure drops will be considered for a magnet system consisting of 20 magnets in series and 2 series in parallel. Figure 1 shows the arrangement relative to the refrigerator. Magnet cross sections will be as shown in Figure 2. Without a detailed design of the winding configuration and the banding around the windings, we will assume that a clear space of 3/32" is available between the banding and the ID of the 4" OD, .035" wall tube. In reality the space will not be uniform, with smaller dimensions at the equator and larger open areas at top and bottom. This will decrease the pressure drop relative to those calculated in this report.

It is further assumed that half of the length of the magnet is banded and that the number of bands in 20 ft of length is 320 (bands of 3/8" width spaced on 3/4" centers).

The pressure drop for flow through this arrangement will consist of two contributions, as follows:

1) Pressure drop calculated with the maximum mass flow rate through the narrowest cross section over a length of 10 ft per magnet.

2) Pressure drop consisting of 320 velocity heads. The velocity head is based on the maximum velocity generated in the narrow section between band and wall.

In addition to pressure drop through the magnet reservoir, there is pressure drop in the tubes connecting individual magnets. This pressure drop consists of a velocity head based on the highest velocity in a contraction at the entrance of the pipe and the friction in the pipe itself. It is assumed that bellows required for flexibility will have a smooth bore tube for reduction of pressure drop. Figure 3 shows the arrangement of the connecting tubes between magnets.

The return path pressure drop is calculated for each magnet. The fraction of liquid changes from approximately .92 at the entrance of the first magnet to approximately .50 at the exit of the last magnet

(nearest to the refrigerator). The flow rates chosen are half of those given on Pages 8-9 of ref. (1).

2. CALCULATIONS

2.1 Pressure drop in connecting tubes between magnets.- Table I is a summary of the calculated pressure drops in smooth-walled tubes connecting the high pressure fluid spaces of the magnets. The length of a connecting tube is 1 ft. Pressure drop in a tube is calculated from:

$$\frac{\Delta P}{L} = \frac{f\,(G^1)^2}{193 \times \rho \times d_h} \quad \text{psig/ft}$$

where: $f = \frac{.046}{Re^{.2}}$

$$G^1 = \frac{G}{3600}$$

d_h in inches

ρ in lb/cft

TABLE I

Pressure Drop in Connecting Tubes Between Magnets

	MAGNET	
	With 20 °K Shield	Without 20 °K Shield
Flow Rate - g/sec	14.5	39.6
Flow Rate - lb/hr	115	314
Tube ID - Inches	.742	.92
Flow Area of Tube - Sq. Inches	.432	.665
Mass Flow Rate - lb/hr ft^2	38300	68000

Table I (Continued)

	With 20 °K Shield	Without 20 °K Shield
Viscosity - lb/ft hr	75×10^{-4}	75×10^{-4}
Hydraulic Dia. - ft	.062	.077
Re x 10^4	31.7	69.8
Density (ρ) - lb/cft	7.8	7.8
f	.0037	.0031
Δ P/L - psig/ft	3.7×10^{-4}	8.0×10^{-4}
Velocity Head - psig	4.4×10^{-3}	32.8×10^{-3}
Pres. Drop Per Connecting Tube - psig	4.77×10^{-3}	35.6×10^{-3}

2.2 Pressure drop in magnets.- Table II summarizes the calculated pressure drops in the fluid space surrounding the magnets.

T A B L E I I

Pressure Drop in Fluid Space of Magnets

	M A G N E T	
	With 20 °K Shield	Without 20 °K Shield
Flow Rate - g/sec	14.5	39.6
Flow Rate - lb/hr	115	314
Minimum Flow Area - Sq. Inches	1.13	1.13
Hydraulic Dia. - ft	.0156	.0156
Mass Flow Rate - lb/hr ft^2	14700	40000

Table II (Continued)

	With 20 ^{o}K Shield	Without 20 ^{o}K Shield
Viscosity - lb/ft hr	75×10^{-4}	75×10^{-4}
Re x 10^4	3.05	8.33
Density (ρ) - lb/cft	7.8	7.8
f	.0058	.0048
Δ P/L - psig/ft	3.43×10^{-4}	2.11×10^{-3}
Velocity Head ($\frac{1}{2}\rho v^2$) - psig	2.32×10^{-4}	1.73×10^{-3}
Pres. Drop Per Magnet - psig	7.76×10^{-2}	57.4×10^{-2}

The total pressure drop for a series of 20 magnets is as follows:

Magnet With Shield - 1.65 psig

Magnet Without Shield - 12.14 psig

It appears that pressure drop in the non-shielded case is too high. All but 5% of the pressure drop is generated by the changes in velocity which take place across the bands. It will be much better to provide a flow path either below or above the bands with a much larger d_h, or to cover the bands with a shroud of some type. To provide circulation through the windings, it will be necessary to provide holes in top and bottom of the shroud.

2.3 Pressure drop in return channels surrounding the magnets.- Two-phase flow occurs in this space. In the first magnet after the expansion valve the enthalpy of the entering fluid is 12.58 J/gr.

At 1.2 atm (4.4 ^{o}K) enthalpies of liquid and vapor are 10.96 and 30.65 J/gr, respectively.

Fraction of liquid entering the channel around the first magnet is 91.8% by mass and 71% by volume. Density of this mixture is 4.40 lb/cft.

Area for flow between 4¼" OD, .035" wall tube and 4" OD tube is 1.15 sq in. Hydraulic diameter is .179". Table III shows the summarized calculation for pressure drop in the channel surrounding the first magnet.

T A B L E I I I

	M A G N E T	
	With 20 ^{o}K Shield	Without 20 ^{o}K Shield
Flow Rate - g/sec	14.5	39.6
Flow Rate - lb/hr	115	314
Flow Area - Sq.Inches	1.15	1.15
Hydraulic Dia. - ft	.0149	.0149
Mass Flow Rate - lb/hr ft^2	14400	39200
Viscosity (liquid) - lb/hr ft	75×10^{-4}	75×10^{-4}
Re	28600	78000
f	.0059	.0048
Density - lb/cft	4.4	4.4
Δ P/L - psig/ft	6.2×10^{-4}	3.75×10^{-3}
Δ P (L = 20 ft) - psig	.012	.073

The magnet return channels are connected through sections of 3/4", Schedule 5 pipe. To provide flexibility, each connecting link between magnets contains a bellows. To reduce pressure drop, a liner consisting of 3/4" pipe inside the bellows provides a smooth path. Pressure drop in the link connecting the valve with the first magnet is of no consequence, since there is no heat transfer.

Pressure drop in the pipe connecting return paths of magnets 1 and 2 is summarized in Table IV.

TABLE IV

Pressure Drop in Connecting Link Between Magnets 1 and 2

	MAGNET	
	With 20 ^{o}K Shield	Without 20 ^{o}K Shield
Flow Rate - lb/hr	115	314
Fraction Liquid Entering Pipe - % (Mass)	89.5	89.5
Fraction Liquid Entering Pipe - % (Volume)	65	65
Flow Area of Pipe - Sq. Inches	.665	.665
Hydraulic Dia. - ft	.077	.077
Mass Flow Rate - lb/hr ft^2	24900	68000
Viscosity	75×10^{-4}	75×10^{-4}
Re	256000	698000
f	.0038	.0031
Density - lb/cft	4.15	4.15
Δ P/L - psig/ft	2.46×10^{-4}	1.5×10^{-3}

Table IV (Continued)

	With 20°K Shield	Without 20°K Shield
ΔP (L = 1 ft)	2.46×10^{-4}	1.5×10^{-3}
$\frac{1}{2}\rho v^2$ - psig	1.25×10^{-3}	9.3×10^{-3}
$\Delta P = \rho v^2$ - psig	2.5×10^{-3}	18.6×10^{-3}

The fraction of liquid in the return path changes from magnet to magnet through heat transfer into the two-phase flow system. In the case of the magnet with shield, the heat flux per magnet is 6.53 W. This heat flux vaporizes .332 g/sec (2.63 lb/hr) of liquid. This represents 2.3% of the flow through the system.

In the case of the magnet without shield, the percentage of liquid vaporized per magnet is the same. As a result of the heat transfer, the fluid flowing through the two-phase system of the magnets changes density by 6% in flowing from magnet to magnet.

The pressure drop in the system consisting of 20 magnets in series may be calculated on the basis of a geometric procession, as long as the density of the fluid is the only parameter changing. This is approximately true.

The sum of a geometric progression is:

$$S_n = a \frac{Z^n - 1}{Z - 1}$$

Where: n = number of terms

Z = common ratio

a = first term

S_n is the sum of n terms. In the case of 20 magnets:

n = 20

a = (.012 + .00275) = .01475 psig or

a = (.073 + .020) = .093 psig from Tables III and IV

Z = 1.06 as calculated from the change in density in passing through one magnet.

We find:

For magnets with 20°K shield,

$$\Delta P \text{ total} = .01475 \times \frac{1.06^{20} - 1}{.06} =$$

$$= \frac{.01475}{.06} \times (3.28 - 1) = .56 \text{ psig}$$

For magnets without 20°K shield,

$$\Delta P \text{ total} = .093 \times \frac{1.06^{20} - 1}{.06} = 3.54 \text{ psig}$$

2.4 Pressure drop in the shield tubing.- Reference 1 indicates that the tubes used for carrying high pressure helium gas are 3/8" OD. A wall thickness of .035" is sufficient to carry gas of 20 atm pressure.

The heat to be removed from 400 ft of shield is 293 W (ref. 1). Per service building, the minimum amount of heat to be removed is 586 W + 50 W in the line connecting the refrigerator and the accelerator. Figure 9 of ref. (1) shows stream 16 to be the helium flow to the accelerator and stream 17 to be the returning high pressure stream. The flow rate chosen is 11.5 g/sec and temperatures are 11.5 and 20°K, respectively for streams 16 and 17. Table V shows the calculated values for the shield flow.

TABLE V

Pressure Drop in Shield Flow System

ID of Shield Tube - Inches	.305
d_h - ft	.0254
Flow Rate - lb/hr	91.2
Mass Flow Rate G - lb/hr ft^2	90000
Viscosity at 16°K - lb/hr ft	72×10^{-4}
Re	318000
f	.00365
Density at 19 atm, 16°K - lb/cft	3.73
$\frac{\Delta P}{L}$ - psig/ft	1.04×10^{-2}

If we assume that the length of tubing between refrigerator outlet and return is 1000 ft, then the pressure drop is of the order of 10.4 psig.

3. CONCLUSIONS

Pressure drops are considerably lower for the magnet system which employs a cooled shield. Figure 4 shows the schematic arrangement with flow points for the shielded and non-shielded magnet systems. It is obvious that the chosen dimensions of the system are incorrect for the non-shielded system. Pressure drops are too high and passages need to be enlarged to reduce the pressure drops to reasonable numbers. A widening of the flow passages will result in a somewhat reduced thickness of insulation and a shorter support system. The low pressure drops in the shielded magnet system provide us with a number of options, as follows:

a) The application of a return helium path under partial vacuum is possible without generating a great increase in pressure drop (ΔP is approximately proportional to $1/\rho$).

b) It is possible to lower the discharge pressure of the helium pumps somewhat. This will result in a reduction of heat input through pump work and a smaller refrigerator. The pump work is approximately proportional to the pressure difference generated.

c) It appears possible to reduce the number of refrigerators by a factor 2. In order to accomplish this with an increase in pressure drop by a factor of only 2, the flow paths need to be doubled in cross section or a distribution system allowing partial bypassing of the flow from high pressure to low pressure circuits needs to be provided.

The non-shielded system needs either increased flow passages or a much lower heat leak in the support system. The best possible system would have zero heat leak in the support system. Ref. (1) shows that the refrigeration required at the 4.4°K temperature level is then 10.26 W per magnet. This amount is approximately one and a half times that of the shielded system. Since refrigeration at the 20°K level is approximately three times cheaper than that at 4.4°K, the cost of the refrigerator in this case would be about the same as that for the shielded magnet system.

Ref. (1) Cryogenic Cooling of Superconducting Magnets for the NAL Energy Doubler System. Cryogenic Consultants, Inc., Jan. 25, 1973. Progress Report to NAL.

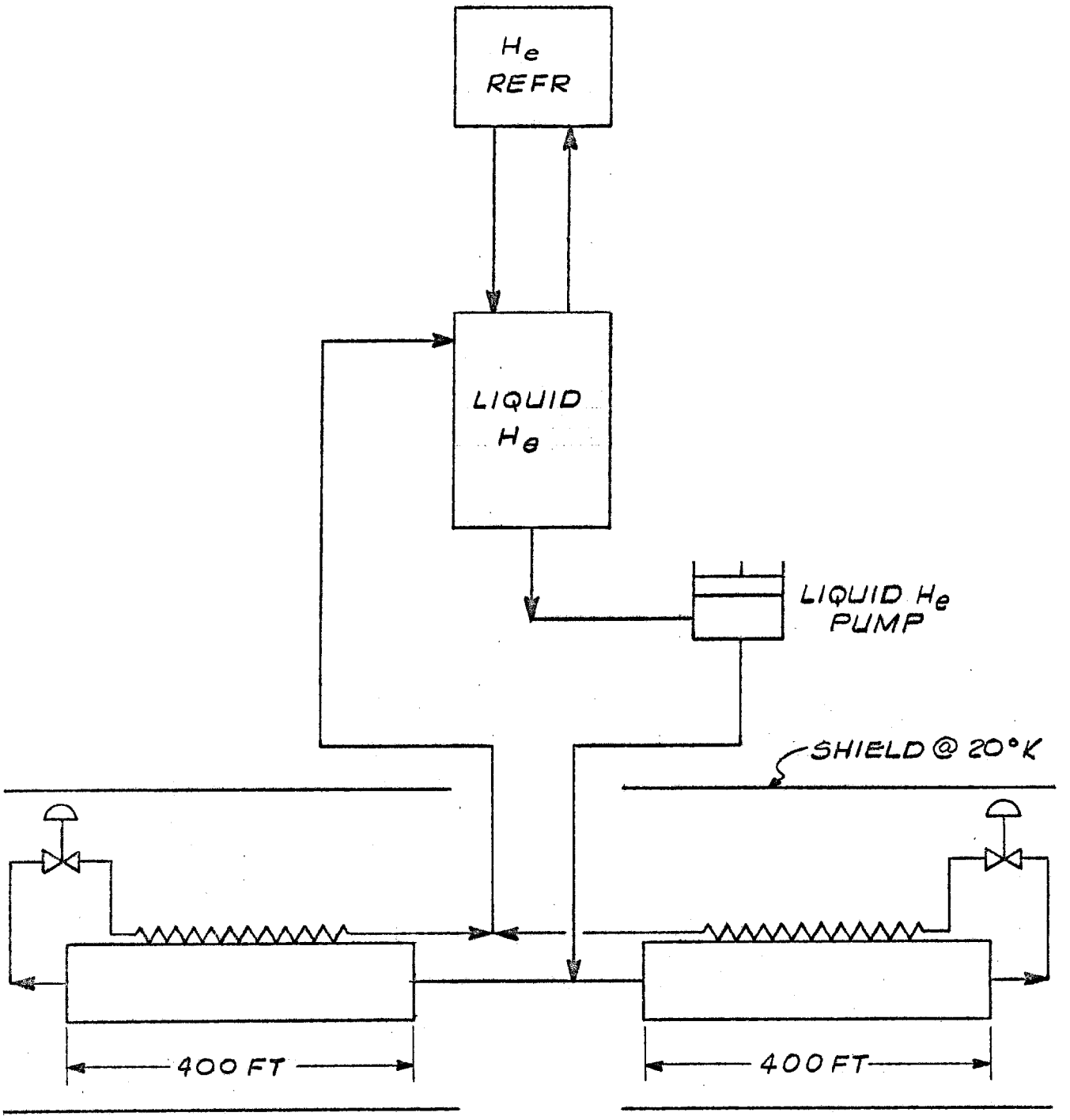

FIG. 1 - MAGNET COOLING SCHEMATIC

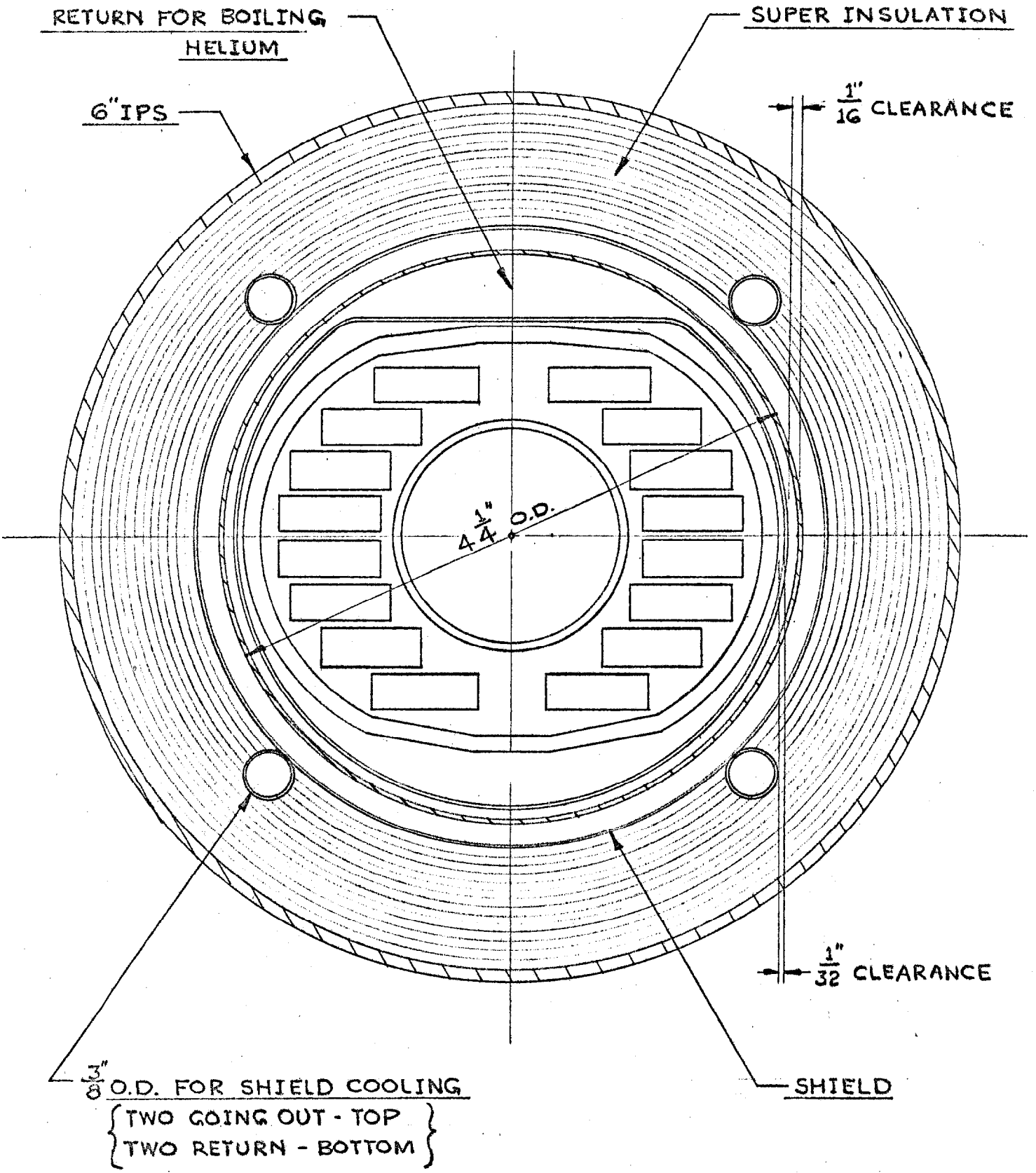

FIG. 2 - MAGNET ASSEMBLY CROSS-SECTION

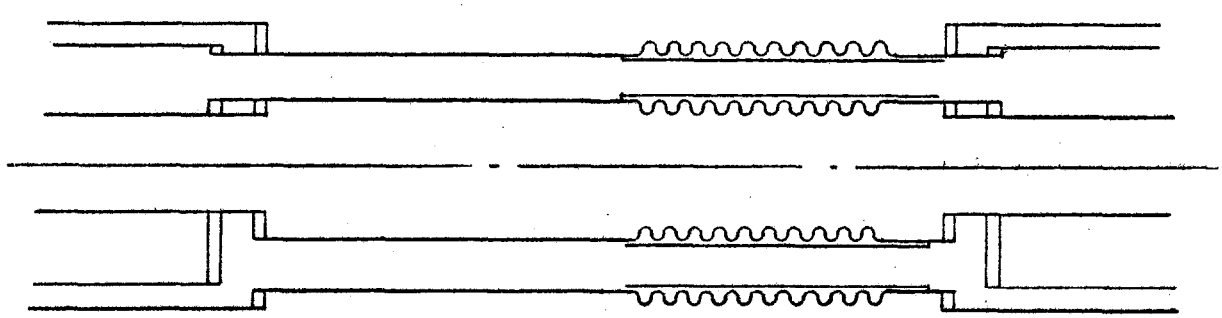

FIG. 3 - CONNECTION BETWEEN MAGNETS

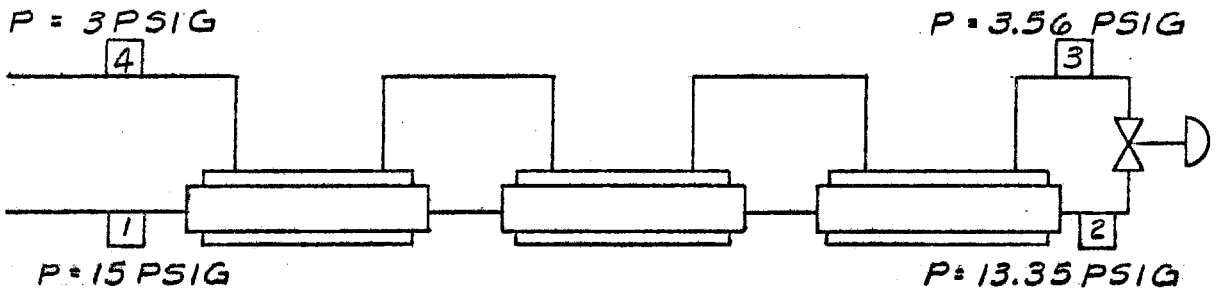

20 MAGNETS OF 20 FT IN SERIES, SHIELDED

(4a)

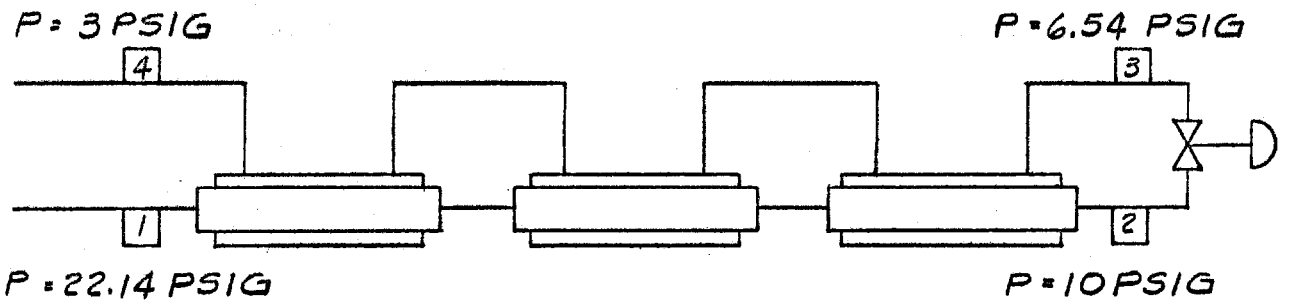

20 MAGNETS OF 20 FT IN SERIES, NON-SHIELDED

(4b)

FIG.4 - PRESSURE DROP IN MAGNET He SYSTEM

Appendix V

HEAT TRANSFER BETWEEN HIGH PRESSURE AND LOW PRESSURE BOILING HELIUM STREAMS OF THE NAL ENERGY DOUBLER SYSTEM

Peter C. Vander Arend
Henry F. Daley, Jr.
Cryogenics Consultants, Inc.
Allentown, Pennsylvania
6 February 1973

Under NAL Subcontract 80073

CONTENTS

1. INTRODUCTION

2. CALCULATIONS

3. TYPE OF TWO-PHASE FLOW IN RETURN CHANNEL

LIST OF FIGURES

FIG. 1 MAGNET ASSEMBLY CROSS SECTION

FIG. 2 FLOW REGIMES IN A CHANNEL

1. INTRODUCTION

The present magnet concept is shown in Figure 1. Liquid helium at a pressure of approximately 2 atm transfers heat through the wall of the 4" OD, .035" wall tube to the stream of boiling liquid helium flowing between the 4¼" OD and 4" OD tubes. There are potential problems in the transfer of heat to a boiling fluid, when this fluid is flowing in a tube. The volume moving through the tube is a mixture of gas and liquid. The density of the gas is much lower than the density of the liquid. In the case of a mixture of 50-50, liquid and gaseous helium (by mass) at a pressure of 1.19 atm, the volumes of liquid and gas are 14.3% and 85.7%, respectively. Because most of the volume is taken up by gas, heat transfer takes place primarily between wall and gas. The gas temperature increases and liquid droplets will vaporize in the gas stream. The process of vaporization is slow since the liquid droplet is surrounded by gas with a temperature gradient. Only when this layer of gas insulation is distributed through turbulent flow and mixing will vaporization take place at a reasonable rate.

2. CALCULATIONS

2.1 Heat Transfer Coefficient Between Wall and Liquid Helium Flowing in the Magnet:

The coefficient may be calculated from standard correlations applicable to fluid flow through channels. A conservative heat transfer coefficient may be calculated on the basis of uninterrupted flow through the narrow passage between magnet bands and wall. Table I gives a summary of the calculations to determine the heat transfer coefficient in the magnet vessel.

T A B L E I

Heat Transfer Coefficients Inside Magnet Vessel:

Magnet -	Without Shield	With Shield
Flow Rate - lb/hr	115	314
Minimum Flow Area - sq. in.	1.13	1.13

TABLE I (Continued)

Magnet -	Without Shield	With Shield
Mass Flow Rate - lb/hr ft^2	14700	40000
Hydraulic Dia. - ft	.0156	.0156
Viscosity - lb/ft hr	75×10^{-4}	75×10^{-4}
Re x 10^4	3.05	8.33
j	.0029	.0024
C_p - Btu/lb ^oF	1.59	1.59
Pr $\frac{(C_p/\mu)}{(K)}$ at 4.5^oK	.82	.82
h - Btu/hr ft^2 ^oF	77.5	174.5
h - W/cm^2 ^oK	.044	.099

2.2 Conduction Through Wall of 4" OD Tube:

We assume that the heat flux through the wall of the tube is distributed evenly. The surface area participating in the heat transfer is then:

$$20 \times 30.5 \times 4 \times \pi \times 2.54 = 19500 \text{ cm}^2$$

At 4.5^oK, the thermal conductivity of stainless steel is: $K = 3 \times 10^{-3}$ W/cm ^oK. Temperature drop through the wall of the vessel is determined from:

$$Q = \frac{K A \Delta T}{d}$$

$$= \frac{3 \times 10^{-3} \times 19500 \times \Delta T}{.035 \times 2.54} = 657 \Delta T$$

For Q = 6 watts, $\Delta T = .00915^oK$

2.3 Heat Transfer to Boiling Liquid Helium:

The helium entering the first magnet after the expansion valve has an enthalpy of 12.57 J/gr (liquid at 4.5°K and 2 atm). In expanding through the valve the enthalpy remains the same, but the fluid becomes a gas and liquid mixture. Fractions of gas and liquid are determined from the enthalpies for helium gas and liquid at the local pressure. If we assume the pressure to be 1.19 atm, then the liquid and gas fractions are 89 and 11%, respectively (by mass). The liquid volume is 57% of the total volume.

Table II shows the calculated heat transfer coefficient in the space between 4" and 4¼" OD tubes, using the standard correlation for heat transfer.

T A B L E I I

Heat Transfer to Boiling Liquid Helium:

Magnet -	With Shield	Without Shield
Flow Rate - lb/hr	115	314
Area for Flow - sq.in.	1.15	1.15
Hydraulic Dia. - ft	.0149	.0149
Mass Flow Rate - lb/hr ft^2	14400	39200
Viscosity - gas	32×10^{-4}	32×10^{-4}
Viscosity - liquid	75×10^{-4}	75×10^{-4}
Re - gas	67000	184000
Re - liquid	28600	78000
j - gas	.0025	.0020
j - liquid	.0030	.0024
C_p - gas - Btu/lb °F	1.63	1.63
C_p - liquid Btu/lb°F	1.24	1.24

TABLE II (Continued)

Magnet -	With Shield	Without Shield
Pr - gas	.89	.89
Pr - liquid	.56	.56
h_1 - gas - Btu/hr ft^2 ^oF	63	137
h_2 - liquid -Btu/hr ft^2 ^oF	79	171
h_1 - W/cm^2 ^oK	35×10^{-3}	76×10^{-3}
h_2 - W/cm^2 ^oK	44×10^{-3}	95×10^{-3}

The overall coefficient can be determined from the calculated values in 2.1, 2.2, and 2.3. To be conservative, the lowest value calculated in Table II will be used. The overall coefficient is determined from:

$$Q = h_1 A \Delta T_1 \qquad (1)$$

$$Q = \frac{K A \Delta T_2}{d} \qquad (2)$$

$$Q = h_2 A \Delta T_3 \qquad (3)$$

From (1), (2), and (3) we obtain:

$$Q = \frac{A}{1/h_1 + 1/h_2 + d/K} \Delta T \qquad \text{in consistent units}$$

$$= U A \Delta T$$

The values of U for the shielded and non-shielded cases are 12.4 MW/cm^2 ^oK and 19.0 MW/cm^2 ^oK, respectively. From these numbers it is possible to determine the temperature difference between the two streams necessary to transfer the heat generated in the windings. The surface area of the 4" OD tube

is 19500 cm^2 (20 ft magnet). We find:

$$\Delta T = \frac{6}{19500 \times 12.4 \times 10^{-3}} = .025^{o}K \quad \text{or}$$

$$\Delta T = \frac{6}{19500 \times 19.0 \times 10^{-3}} = .016^{o}K$$

for shielded and non-shielded magnets, respectively.

3. TYPE OF TWO-PHASE FLOW IN RETURN CHANNEL

The calculations show that a very small temperature difference is required to transfer the heat generated in the windings through the wall of the tube. In order to realize the lowest possible temperature for the liquid helium stream surrounding the magnets, it is necessary to transfer heat from the gas to the boiling liquid with the lowest possible temperature difference. This only can be done by providing a large liquid-gas interface and turbulent motion of the gas and liquid streams. The type of flow of the gas-liquid mixture is important. If the liquid remains intimately mixed with the gas in the form of small droplets, the mixture will be essentially at the temperature of the boiling liquid associated with the pressure.

Baker (ref. 1) has studied two-phase flow in oil-gas mixtures and has found a correlation between gas and liquid mass flow rates which makes possible a prediction of the type of two-phase flow to be expected. The correlation is presented in Figure 2 which shows various types of flows occurring as a function of two fundamental parameters. Baker's study was based on non-cryogenic mixtures and did not include the case of boiling liquids. Work done at Los Alamos Scientific Laboratory (ref. 2) suggests that the correlation is applicable to boiling cryogenic liquids. The parameters of Figure 2 are as follows:

G gas mass flow rate - lb/ft^2 hr

L liquid mass flow rate - lb/ft^2 hr

$$\lambda = \left[\left(\frac{\rho_g}{(7.5 \times 10^{-2})} \right) \left(\frac{\rho_L}{(6.23 \times 10)} \right) \right]^{1/2}$$

ρ_g gas density - lb/cft

ρ_L liquid density = lb/cft

$$\psi = \frac{(7.3 \times 10)}{(j)} \left[\mu_L \left(\frac{(6.23 \times 10)}{(\rho_L)} \right)^2 \right]^{1/3}$$

j surface tension - dynes/cm

μ_L liquid viscosity - centi poise

In the case of two-phase helium flow at 1.19 ata and 4.4°K:

ρ_g = 1.25 lb/cft

ρ_L = 7.60 lb/cft

μ_L = 30 x 10^{-4} centi poise

j = .07 dynes/cm

From this we obtain:

Ψ = 615

λ = 1.43

Table III shows calculated values of the parameters $\frac{L\lambda\Psi}{G}$ and $\frac{G}{\lambda}$ as a function of liquid-gas ratios for the shielded and non-shielded magnet system.

T A B L E I I I

Magnet -	With 20° Shield	Without 20° Shield
Total Mass Flow Rate - lb/hr	115	314
L at First Magnet - lb/hr ft^2	13100	35800
G at First Magnet - lb/hr ft^2	1180	3220
L/G	11.1	11.1
$\frac{L\lambda\Psi}{G}$	9750	9750
$\frac{G}{\lambda}$	825	2250
L at Last Magnet - lb/hr ft^2	7200	19700
G at Last Magnet - lb/hr ft^2	7200	19700

TABLE III (Continued)

Magnet -	With 20° Shield	Without 20° Shield
L/G	1.0	1.0
$\frac{L\lambda\Psi}{G}$	880	880
$G/\lambda\Psi$	5000	13700

Figure 2 shows the points calculated in Table III. It appears that the type of flow through the complete magnet system is bubble or froth flow. This is the most advantageous type of flow from a standpoint of heat transfer. The plotted points also imply that the total flow rate might be reduced some without leaving the bubble or froth type flow regime. A reduction of flow rate has the following very significant advantages:

a) Reduced pressure drop with the potential of covering a greater distance than 400 or 800 ft with one refrigerator.

b) Reduced pump work resulting in a smaller refrigerator.

Ref. (1) O. Baker. Design of Pipe Lines for Simultaneous Flow of Oil and Gas. The Oil and Gas Journal, July 26, 1954.

Ref. (2) J. C. Bronson, et al. Problems in Cooldown of Cryogenic Systems. Advances in Cryogenic Engineering, Vol. 7, Page 198. Plenum Press, 1961.

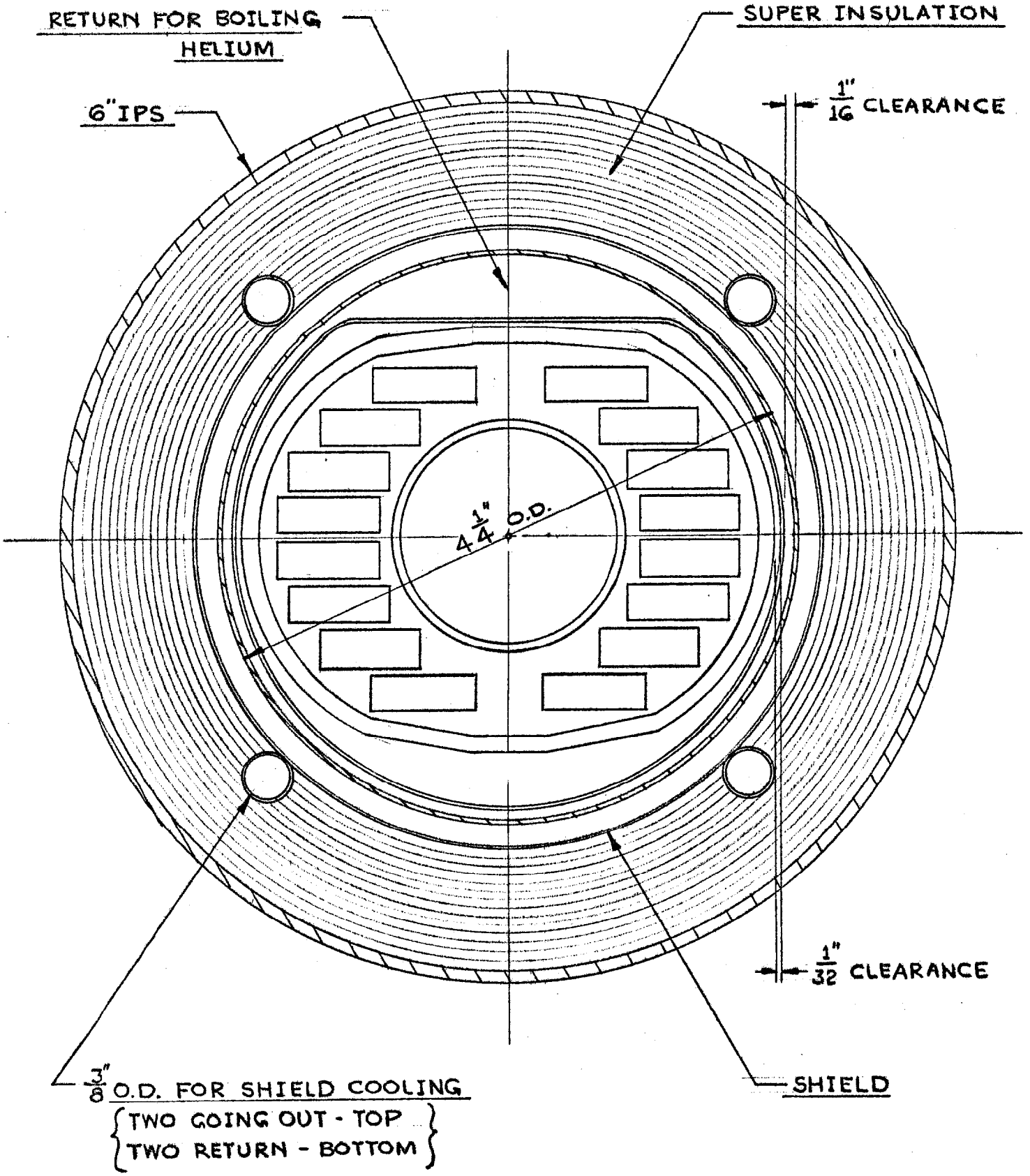

FIG. 1 - MAGNET ASSEMBLY CROSS-SECTION

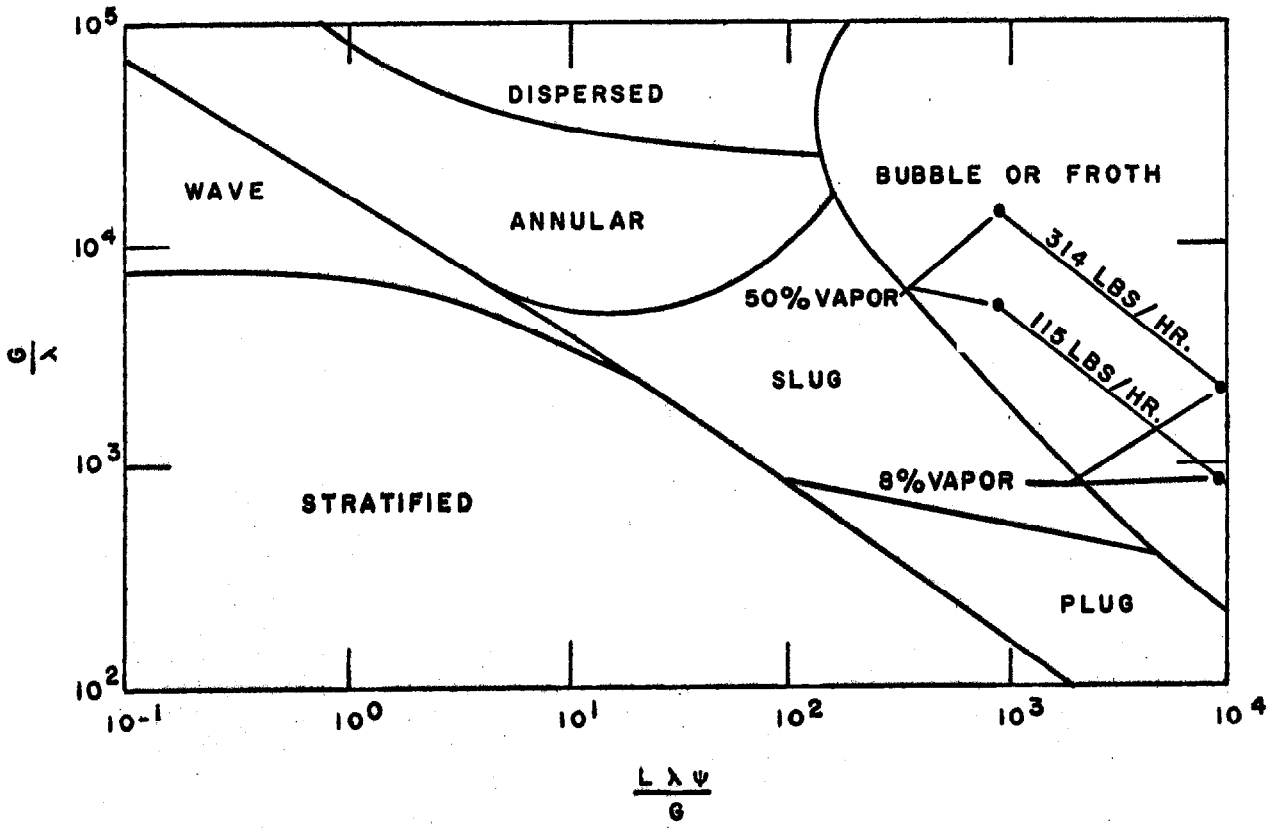

FIG. 2. FLOW REGIMES IN A CHANNEL

BIBLIOGRAPHY

FN-233
0121.000, Can An Energy Doubler Be Used to Implement A Simple 350 GeV Storage Ring System At NAL?, by R. A. Carrigan, Jr., National Accelerator Laboratory, July 1971

FN-235
0424.000, 0.5 Meter Prototype Energy Doubler Quadrupole Magnet, by R. Sheldon and B. Strauss, National Accelerator Laboratory, July 1971

Unpublished, Prototype Superconducting Magnets, by L. C. Teng, National Accelerator Laboratory, February 10, 1972

Unpublished, Preliminary Suggestions For Starting The Construction Of Prototype Magnets And Refrigeration Systems For The Proposed Energy Doubler, by W. B. Fowler and P. J. Reardon, National Accelerator Laboratory, February 24, 1972

Unpublished, Superconducting Magnet Parameters, by L. C. Teng, National Accelerator Laboratory, May 19, 1972

TM-400
0428, Magnetic Field Of Uniform Density Current Confined Within An Elliptical Boundary, by S. C. Snowden, National Accelerator Laboratory, November 21, 1972